

**EFFECT OF WEATHERING ON JOINT SHEAR
STRENGTH OF SOME WEAK ROCKS**

Teepawit Sri-in

**A Thesis Submitted in Partial Fulfillment of the Requirements for
the Degree of Master of Engineering in Geotechnology**

Suranaree University of Technology

Academic Year 2007

ผลกระทบของการผูกมัดต่อกำลังซื้อของรอยแตกในหินเนื้ออ่อนบางชนิด

นายทีปวิทย์ ศรีอินทร์

วิทยานิพนธ์เป็นส่วนหนึ่งของการศึกษาตามหลักสูตรปริญญาวิศวกรรมศาสตรมหาบัณฑิต

สาขาวิชาเทคโนโลยีธรณี

มหาวิทยาลัยเทคโนโลยีสุรนารี

ปีการศึกษา 2550

EFFECT OF WEATHERING ON JOINT SHEAR STRENGTH OF SOME WEAK ROCKS

Suranaree University of Technology has approved this thesis submitted in partial fulfillment of the requirements for a Master's Degree.

Thesis Examining Committee

(Asst. Prof. Thara Lekuthai)

Chairperson

(Assoc. Prof. Dr. Kittitep Fuenkajorn)

Member (Thesis Advisor)

(Prof. Dr. Jaak J.K. Daemen)

Member

(Assoc. Prof. Dr. Saowanee Rattanaphani) (Assoc. Prof. Dr. Vorapot Khompis)

Vice Rector for Academic Affairs

Dean of Institute of Engineering

ที่ปวิทย์ ศรีอินทร์ : ผลกระทบของการผุกร่อนต่อกำลังเฉือนของรอยแตกในหินเนื้ออ่อนบางชนิด (EFFECT OF WEATHERING ON JOINT SHEAR STRENGTH OF SOME WEAK ROCKS) อาจารย์ที่ปรึกษา : รองศาสตราจารย์ ดร.กิตติเทพ เฟื่องขจร, 119 หน้า.

วัตถุประสงค์ของงานวิจัยนี้คือเพื่อศึกษาผลกระทบของการผุกร่อนต่อกำลังรับแรงเฉือนของรอยแตกในหินเนื้ออ่อนบางชนิดด้วยวิธีการทดสอบในห้องปฏิบัติการ กิจกรรมหลักประกอบด้วย การจำลองการผุกร่อนของตัวอย่างหิน การศึกษาคุณสมบัติเชิงกายภาพและเชิงกลศาสตร์ของหินภายใต้สภาวะการผุกร่อนที่ต่างกัน และเกณฑ์กำลังเฉือนของรอยแตกในหินที่สามารถนำไปใช้พิจารณาการผุกร่อนเข้ามาพิจารณาได้ การทดสอบค่าดัชนีความคงทนต่อการผุกร่อน การทดสอบดัชนีจุดกด การทดสอบการเคลื่อนไหล และการวิเคราะห์แสง X-ray ได้ถูกกำหนดโดยใช้ตัวอย่างหิน 13 ชนิด ที่พบมากในภาคเหนือและตะวันออกเฉียงเหนือของประเทศไทย โดยมีวัตถุประสงค์เพื่อหาความสัมพันธ์ระหว่างค่าความคงทนของหินกับค่าความแข็ง และแรงองค์ประกอบ โดยได้เสนอแนวคิดเพื่ออธิบายคุณลักษณะการผุกร่อนของหินภายใต้การทดสอบค่าดัชนีความคงทน รวมทั้งได้เสนอระบบจำแนกความคงทนของหินแบบใหม่เพื่อคาดคะเนความแข็งของหินที่มีผลกระทบต่อกระบวนการการผุกร่อน ผลที่ได้ระบุว่าหินพัมมิชกรวดเหลี่ยม หินทรายแป้งชุดพระวิหาร หินทรายสีชาชุดภูกระดึง หินทรายชุดโคกกรวด และหินควอตซ์ไมกาชีสต์ในกลุ่มของหินในสัชลบุรียุคจำแนกเป็นหินที่มีความคงทนต่ำถึงต่ำมาก เนื่องจากในเนื้อหินมีแร่ kaolinite เป็นแร่องค์ประกอบ ส่วนหินดินดานถึงหินชนวนชุดน้ำตกจะมีความคงทนสูงไม่อ่อนไหวต่อปริมาณน้ำแต่จะแตกได้ง่ายภายใต้วัฏจักรการเปลี่ยนแปลงของอุณหภูมิโดยรอบ ค่าดัชนีจุดกดของหินจะลดลงในขณะที่ผลต่างระหว่างค่าดัชนีความคงทนที่มากขึ้น มุมเสียดทานพื้นฐานของรอยแตกในหินที่จำลองโดยการตัดด้วยเลื่อยจะมีค่าลดลงในขณะที่วัฏจักรของสภาวะร้อน-เย็นที่จำลองในห้องปฏิบัติการมีค่าเพิ่มขึ้น งานวิจัยนี้ได้มีการปรับเปลี่ยนเกณฑ์กำลังเฉือนรอยแตกของ Barton's เพื่อให้สามารถนำไปใช้ของการผุกร่อนมาพิจารณาในตัวแปรของความแข็งของหิน ผลจากการจำลองการผุกร่อนในห้องปฏิบัติการได้นำมาสัมพันธ์กับสภาวะจริงในภาคสนาม โดยการเทียบค่าพลังงานความร้อนที่หินได้ดูดซับในระหว่างการจำลองต่อค่าพลังงานความร้อนที่หินได้ดูดซับจริงในภาคสนาม การลดลงของค่ากำลังเฉือนสูงสุดรอยแตกของหินในภาคสนามจึงสามารถคาดคะเนได้ตามกาลเวลา

สาขาวิชา เทคโนโลยีธรณี
ปีการศึกษา 2550

ลายมือชื่อนักศึกษา _____
ลายมือชื่ออาจารย์ที่ปรึกษา _____

TEEPAWIT SRI-IN : EFFECT OF WEATHEIRNG ON JOINT SHEAR
STRENGTH OF SOME WEAK ROCKS. THESIS ADVISOR : ASSOC.
PROF. KITITEP FUENKAJORN, Ph.D., P.E. 119 PP.

SHEARSTRENGTH/WEATHERING/DEGRADATION/JOINT/ROCK/SLAKING

The main objective of this research is to investigate experimentally the effect of weathering processes on the joint shear strength of some weak rocks. The effort primarily involves simulation of the weathering-induced degradation of rock specimens, determination of the physical and mechanical properties of the rocks at various stages of degradation, and development of a rock joint shear strength criterion that can incorporate the weathering-related parameters. Slake durability tests, point load strength index tests, tilt tests and x-ray diffraction analyses were carried out on thirteen rock types that are commonly encountered in the north and northeast of Thailand, in an attempt at correlating the rock durability with its strength and mineral compositions. A concept is proposed to describe the rock degradation characteristics under the slake durability test cycles. A new classification system is also introduced for rock durability, which allows predicting the rock strength as affected by weathering. Results indicate that Pichit pumice breccia, Phra Wihan siltstone, Phu Kradung white sandstone, Khok Kruat sandstone and Chonburi quartz mica schist are classified as low to very low durability rocks, primarily due to their kaolinite content. Nam Duk slaty-shale is considered high durability, not sensitive to water, but easily disintegrated by cyclic change of surrounding temperatures. The point load strength index decreases as the difference in slake durability indices obtained from adjacent

cycles (Δ SDI) increases. Basic friction angles of the smooth (saw-cut) surfaces of the rocks decrease as the rapid heating-cooling cycles increase. Barton's joint shear strength criterion is modified here to incorporate the weathering-related parameters into the rock wall strength variable. The results of the rock degradation simulation are related to the actual in-situ conditions by comparing the heat energy absorbed by rock specimens during the simulation with those measured in the field. This allows predicting the decrease of joint shear strength as a function of time.

School of Geotechnology

Academic Year 2007

Student's Signature _____

Advisor's Signature _____

ACKNOWLEDGMENTS

I wish to express my sincere appreciation to my thesis advisor, Associate Professor Dr. Kittitep Fuenkajorn, for his continuous guidance, a critical review and encouragement throughout the preparation of this thesis. Further appreciation is extended to Assoc. Prof. Thara Lekuthai and Professor Dr. Jaak J.K. Daemen who are member of my examination committee. The author also would like to thank Akara mining Co. Ltd. to provide the rock samples.

This research is funded by the Institute of Engineering, Suranaree University of Technology.

Teepawit Sri-in

TABLE OF CONTENTS

	Page
ABSTRACT (THAI)	I
ABSTRACT (ENGLISH).....	II
ACKNOWLEDGMENTS	IV
TABLE OF CONTENTS.....	V
LIST OF TABLES.....	VIII
LIST OF FIGURES	IX
LIST OF SYMBOLS AND ABBREVIATIONS	XIII
CHAPTER	
I INTRODUCTION	1
1.1 Background of problems and significance of the study.....	1
1.2 Research objective	2
1.3 Research methodology.....	2
1.4 Scope and limitations of the study.....	5
1.5 Thesis contents.....	6
II LITERATURE REVIEW	7
2.1 Introduction.....	7
2.2 Weathering process.....	7
2.2.1 Physical weathering	8
2.2.3 Weathering resistance	11

TABLE OF CONTENTS (Continued)

	Page
2.3 Factors affecting strength and durability of some weak rocks	.12
2.4 Tests that can be correlated to strength.....	19
2.5 Joint shear strength criteria	22
III ROCK SAMPLES.....	25
3.1 Introduction.....	25
3.2 Sample collection.....	25
3.3 Mineral compositions.....	32
IV LABORATORY EXPERIMENTS.....	35
4.1 Introduction.....	35
4.2 Slake durability index test.....	35
4.2.1 Test results	37
4.2.2 Implications of SDI for long-term durability.....	43
4.2.3 Projection of rock durability	45
4.2.4 Classification of rock durability.....	46
4.3 Simulation of rock degradation.....	49
4.3.1 Simulation methods	49
4.3.2 Slake durability index	49
4.3.3 Point load strength index	52
4.3.4 Weight loss monitoring.....	59
4.3.5 Basic friction angle (Tilt test)	59

TABLE OF CONTENTS (Continued)

	Page
4.3.6 Dynamic wave velocity.....	59
V CORRELATION BETWEEN ROCK DURABILITY AND JOINT SHEAR STRENGTH	64
5.1 Introduction.....	64
5.2 Relationship between rock strength and Δ SDI	64
5.3 Correlation between simulation and actual in-situ condition ...	67
5.4 Modified Barton's joint shear strength criterion.....	72
VI DISCUSSIONS CONCLUSIONS AND RECOMMENDATIONS FOR FUTURE STUDIES.....	84
6.1 Discussions	84
6.2 Conclusions.....	86
6.3 Recommendations for future studies	88
REFERENCES.....	90
APPENDIX LABORATORY TEST RESULTS	104
BIOGRAPHY	119

LIST OF TABLES

Table	Page
2.1 Mean lifetime of one millimeter of fresh rock.....	13
3.1 Rock samples used in this study	26
3.2 Mineral compositions of rock specimens in volcanic rock group	33
3.3 Mineral compositions of rock specimens in metamorphic rock group	33
3.4 Mineral compositions of rock specimens in sedimentary rock group	34
4.1 Slake durability index test results with water in trough.....	39
4.2 Slake durability index test results without water in trough.....	40
4.3 Slake durability index of rock samples base on Gamble's classification	41
4.4 Empirical constants for an exponential relationship between Δ SDI and N^*	48
4.5 Proposed classification system for durability of intact rocks	48
4.6 Results of SDI test for all rock types obtained after 140 cycles of heating and cooling simulation	53
4.7 Results of point load strength index test	58
4.8 Empirical constants form power equation relating ϕ_B and n.....	62
5.1 Point load strength index results and their corresponding Δ SDI at $N^*=6$ (or $N=1$).....	66
5.2 Parameters used to predict the joint shear strength of each rock type	76

LIST OF FIGURES

Figure	Page
1.1 Research plan and related activity	3
2.1 Stability of some primary minerals	13
3.1 The locations where rock samples have been collected	28
3.2 Pichite crystal tuff and Pichit pumice breccia collected from Tawan pit of the Chatree gold mine in Phichit province.....	30
3.3 White quartz sandstone collected from the embankment of Thep Sathit-Chaiyaphum highway at km 287. The slope was excavated in 2003	30
3.4 Red sandstone collected from the embankment of Thep Sathit-Chaiyaphum highway at km 288. The slope was excavated in 2003	31
3.5 Micaceous siltstone collected from the embankment of Khao Chuk reservoir in Rayong province	31
4.1 Slake durability test apparatus.....	36
4.2 Slake durability index for 6 cycles with water in trough.....	38
4.3 Slake durability index for 6 cycles without water in trough	38
4.4 Comparison between SDI wet and dry test results at the first cycle	42
4.5 Comparison between SDI wet and dry test results at the sixth cycle.....	42
4.6 Proposed concept of rock degradation during SDI testing. Samples A, B and C (left) have uniform texture. Samples D, E and F (right) have rock matrix that is weaker outside and stronger inside	44

LIST OF FIGURES (Continued)

Figure	Page
4.7 Δ SDI as a function of N^* . Rock conditions as collected are plotted at cycle no. 6.....	47
4.8 Example of rock fragments of Phra Wihan sandstone prepared for slake durability index test.....	50
4.9 Example of rock disks of Phra Wihan sandstone and siltstone prepared for tilt test and point load strength index tests.....	50
4.10 Specimens of rock disks and fragments submerged under water tank at 25°C.....	51
4.11 Comparison of SDI values of sedimentary rocks before (solid lines) and after (dash lines) 140 heating-cooling cycles	54
4.12 Comparison of SDI values of metamorphic rocks before (solid lines) and after (dash lines) 140 heating-cooling cycles	55
4.13 Comparison of SDI values of volcanic rocks before (solid lines) and after (dash lines) 140 heating-cooling cycles	56
4.14 Test arrangement and apparatus for point load strength index test.....	57
4.15 Weigh loss of rock specimens monitored every 14 cycles of heating and cooling test.....	61
4.16 Basic friction angles of smooth (saw-cut) surface of rock specimens tested at various heating-cooling cycles (n)	62
4.17 Sonic Viewer 170 Model 5228 used to measure P-wave velocity	63
5.1 Point load strength index as a function of Δ SDI for all rock types tested.....	65

LIST OF FIGURES (Continued)

Figure	Page
5.1	Variation of temperatures for one cycle of heating and cooling simulation in laboratory.....68
5.2	Variation of temperatures for one day in the Nakhon Ratchasima province (Thai Meteorological Department, 2004). The line indicates average during temperature change in the year 2004.....69
5.3	Comparison of coefficients of heat capacity of various rock types (Modified from Department Angewandte Geowissenschaften und Geophysik, 2006)71
5.5	Δ SDI as a function of time under in-situ condition.....73
5.6	Normalized joint shear strength prediction for volcanic rocks. Dashed lines indicate the lower bound of normalized joint shear strength which is defined by the tangent of basic friction angle of each rock type77
5.7	Normalized joint shear strength prediction for metamorphic rocks. Dashed lines indicate the lower bound of normalized joint shear strength which is defined by the tangent of basic friction angle of each rock type78
5.8	Normalized joint shear strength prediction for sedimentary rocks. Dashed lines indicate the lower bound of normalized joint shear strength which is defined by the tangent of basic friction angle of each rock type79
5.9	Normalized joint shear strength as a function of time for Khok Kruat sandstone for various assumed ϕ_B values81

LIST OF FIGURES (Continued)

Figure	Page
5.10 Normalized joint shear strength as a function of time for Khok Kruat sandstone for various normal stress (σ_n)	82
5.11 Normalized joint shear strength as a function of time for Khok Kruat sandstone for various assumed JRC values	83

LIST OF SYMBOLS AND ABBREVIATIONS

α	=	Coefficient of Rate Weathering
β	=	Coefficient of Time Weathering
λ	=	Time Coefficient of Basic Friction Angle
δ	=	Empirical Constant
η	=	Exponent of Strength Decrease
ϕ_B	=	Basic Friction Angle
σ_c	=	Uniaxial Compressive Strength
σ_j	=	Joint Wall Compressive Strength
σ_n	=	Normal Stress
τ	=	Shear Stress
a	=	Multiplie Factor
C	=	Variable Coefficient of Basic Friction Angle
C_p	=	Specific Heat Capacity
D	=	Day
F.S.	=	Factor Safety of Slope
I_d	=	Slake durability Index Test Values
I_s	=	Conventional Point Load Strength Index
$I_{s(50)}$	=	Size Corrected Point Load Strength Index
JRC	=	Joint Roughness Coefficient
m	=	Weight of Rock Specimen

LIST OF SYMBOLS AND ABBREVIATIONS (Continued)

n	=	Cycle of Heating and Cooling Simulation
N	=	Cycle of Number Slake Durability Index Test
N*	=	Backward Cycle of Number Slake Durability Index Test
Q	=	Absorped Energy of Rock Specimen
t	=	Time of Interval of Energy absorption
ΔT	=	Difference of Temperature

CHAPTER I

INTRODUCTION

1.1 Background of problems and significance of the study

In geotechnical investigations involved with surface and subsurface structures, the evaluation of strength and deformability of rock and rock mass is frequently needed. These measurements become more difficult if the rocks encountered are influenced by weathering. The study of strength and deformational behavior of rock under uniaxial compression is of vital importance, and not only provides basic material characteristics or design indices but also serves as useful data in analysis where the rocks are at a shallow depth. Most engineering works are confined to shallow depths where weathering has a dominant role to play and affects almost all the properties of rocks (Gupta and Seshagiri, 2000).

Considerable research efforts have been carried out in an attempt at identifying the impacts of weathering processes (both physical and chemical) on the physical, hydraulic and mechanical properties of weak to medium strong rocks, including siltstone, shale, claystone and some volcanic rocks (Chigira and Oyama, 1999; Gupta and Seshagiri, 2000; Kasim and Shakoor, 1996; Tugrul, 2004). The key mineral compositions and petrographic features of these rocks are also studied in relation to the environment and duration to which these rocks have been subjected. Several forms of mathematical relationship between these factors have been derived. Significant understanding on the impact of weathering on the rock has been gained

from the research. These findings are however not directly applicable to the engineering practices, specifically to the stability analysis and design of geo-engineering structures. Rare attempt has been made at determining the mathematical relation between the weathering processes and the parameters used in the failure or strength criteria of rock mass. In addition a shear strength criterion that can incorporate the weathering parameters or rock mass aging parameters has not been derived. Such criterion would be useful to predict the stability of geological structures as a function of time, and hence allows implementing an appropriate support system (if needed) to ensure their long-term stability.

1.2 Research objectives

The main objective of this research is to investigate experimentally the effect of weathering processes on the joint shear strength of some rocks commonly encountered in Thailand. The effort primarily involves mechanical testing of rock samples in the laboratory and determination of relationship between rock durability, compressive strength, water absorption and bulk density under various degrees of rock degradation. The results will lead to the derivation of a new joint shear strength criterion that can be used to predict the mechanical stability of geo-engineering structured (e.g. rock foundation, slope and tunnel) as a function of time.

1.3 Research methodology

This research is divided into 5 main tasks, as follows (Figure 1.1).

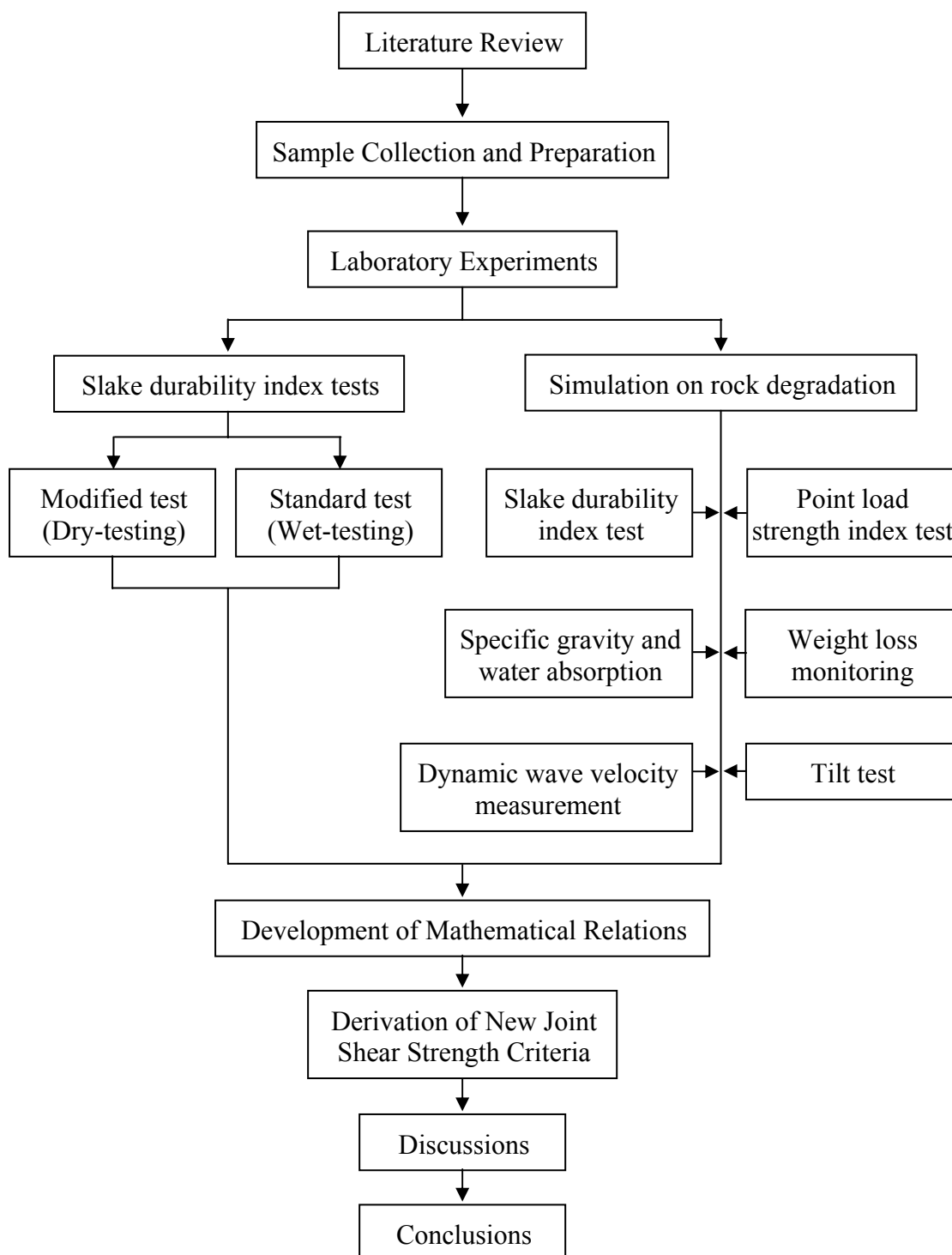


Figure 1.1 Research plan and related tasks.

Task 1: Literature review Literature review have been carried out to gain an understanding of the weathering process and the factors affecting strength and durability of rocks. The reviewed topics include slake durability index testing, point load strength index testing, specific gravity and water absorption measurements, and joint shear strength criteria. The sources of information are from journals, technical reports and conference papers.

Task 2: Sample collection and preparation Thirteen rock types has been collected from the field. Sample preparation is carried out in the laboratory at the Suranaree University of Technology. Preparation of these samples follows the relevant ASTM standard as much as practical.

Task 3: Laboratory experiments The laboratory testing is divided into five main groups: slake durability tests, point load tests, dynamic tests, tilt test and measurements of the rock specific gravity and water absorption. The slake durability test method follows the ASTM (D4644) standard practice. The tests are intended to assess the effect of water on the rate of rock weathering. The point load strength test method follows the ASTM (D5731) standard practice. The tests have been performed to understand the rock degradation under cycles of heating and cooling. The dynamic wave velocity testing and tilt testing follow the suggested method given by the International Society for Rock Mechanics (Brown, 1981). The methods of specific gravity and water absorption measurements follow the ASTM (C127).

Task 4: Development of mathematical relations The results from task 3 are used to develop mathematical relations between the weathering parameters and rock properties. These include correlation between point load strength index and slake durability, and between the dynamic wave velocity, specific gravity and water

absorption and degree of rock weathering. This task also includes the derivation of a new joint shear strength criterion that can incorporate the effect of rock weathering.

Task 5: Thesis writing and presentation All research activities, methods, and results are documented and compiled in the thesis. The research findings will be published in conference proceedings or journals.

1.4 Scope and limitations of the study

a. A minimum of 10 rock types that are commonly found in Thailand are collected from the field for the laboratory testing. These rocks include sandstone, siltstone, shale, claystone, and some volcanic rocks as they are likely to deteriorate quickly after exposed to atmosphere.

b. The laboratory testing includes slake durability index test, point load strength index test, and measurements of rock specific gravity and water absorption, dynamic wave velocity, and basic friction angle using relevant ASTM and ISRM standard.

c. No in-situ measurement or field testing is carried out.

d. The Barton's joint shear strength criterion is primarily used as an initial equation because it is capable of linking the joint strength and the intact rock strength.

e. During physical simulation test, the maximum testing temperature is 110°C

f. The X-ray diffraction method is used to determine the mineral composition of the rock samples.

g. Petrographic analyses determine the rock texture.

1.5 Thesis contents

The first Chapter introduces the thesis by briefly describing the background of problems and significance of the study, and identifying the research objectives, methodology, scope and limitations. The second Chapter summarizes results of the literature review. Chapter three describes the rock sample collection and results of mineralogical analysis. Slake durability index testing and rock degradation simulation are presented in Chapter four. Chapter five shows the mathematical relations between the weathering parameters and mechanical rock properties, as well as the prediction scheme of rock degradation. Chapter six provides the discussion, conclusions, and recommendations for future studies. Details of the laboratory experimental results are given in Appendix A.

CHAPTER II

LITERATURE REVIEW

2.1 Introduction

This chapter summarizes the results of literature review carried out to improve an understanding of rock degradation by weathering. The topics reviewed here include the factors influencing the rock weathering, laboratory test methods that can be correlated to rock strength, and the joint shear strength criteria.

2.2 Weathering processes

Abramson et al. (1995) state that weathering in general is a group of processes by which surface rock disintegrates into smaller particles or dissolves into water due to the impact of the atmosphere and hydrosphere. The weathering processes often are slow (hundreds to thousands of years). The amount of time that rocks and minerals have been exposed at the earth's surface will influence the degree to which they have weathered. Weathered material may be removed leaving a porous framework of individual grains, or new material may be precipitated in the pores, at grain boundaries or along fractures. Weathering processes can be divided into two types, chemical weathering due to chemical changes and physical or mechanical weathering as results of wind, temperature changes, freeze-thaw cycles, and erosion by streams and rivers. Chemical weathering is the breakdown of minerals into new compounds by the action of chemical agents, acid in air, in rain and in river water. Mechanical

weathering is a process by which rock is broken into small fragments as a result of energy developed by physical forces. Examples are freeze-thaw cycles and temperature changes.

2.2.1 Physical weathering

Primary minerals and rocks are splitted in fragments due to physical weathering. This leads to environmental conditions that favor chemical weathering. There are several forms of physical weathering (Robison and Williams, 1994), as follows.

Abrasion: Water carrying suspended rock fragments has a scouring action on surfaces. Examples are the grinding action of glaciers, gravel, pebbles and boulders moved along and constantly abraded by fast-flowing streams. Particles carried by wind have a sand-blasting effect.

Wetting and drying: Water penetrates into rocks and reacts with their constituent minerals.

Freezing and thawing: When water is trapped in rock and reacts with constituent minerals.

Thermal expansion and contraction of minerals: Rocks are composed of different kinds of minerals. When heated up by solar radiation each different mineral will expand and contract at a different rate with surface-temperature fluctuations. With time, the stresses produced are sufficient to weaken the bonds along grain boundaries, and thus flaking of fragments.

Pressure unloading or pressure-release jointing: There is a reduction in pressure on a rock due to removal of overlying material. This allows rocks to split along planes of weakness or joints.

Crystallization: In arid environments, water evaporates at the surface of rocks and crystals form from dissolved minerals. Over time, the crystals grow and exert a force great enough to separate mineral grains and break up rocks.

Action of organisms: They aid in the physical disintegration of rocks. Pressures exerted by roots during growth are able to rupture rocks.

2.2.2 Chemical weathering

The process of chemical weathering generally occurs in rock where water and minerals are in constant contact. Agents of weathering are oxygen, air pollution, water, carbonic acid, and strong acids. They combine with the minerals in rocks to form clays, iron oxides, and salts, which are the endpoints of chemical weathering. A brief description of the most important chemical weathering processes is as follows:

Hydration: Hydration is the chemical addition of water molecules to a mineral. Ions have the tendency to hydrate when H₂O is present and dissociate. In general, ions with the same charge but smaller ion radius have a larger layer of H₂O ions and therefore do not tend to adsorb. The small Li⁺ ion tends to remain hydrated at the surface, whereas the large Al³⁺ ion tends to dehydrate and becomes tightly adsorbed. The strength of adsorption increases in the following sequence, Li⁺ < Na⁺ < K⁺ < Mg²⁺ < Ca²⁺ < Al³⁺.

Hydrolysis: Water molecules at the mineral surface dissociated into H^+ and OH^- penetrate the crystal lattice, creating a charge imbalance, which causes cations such as Ca^{2+} , Mg^{2+} , K^+ and Na^+ to diffuse out.

Oxidation and Reduction: Oxidation is accelerated by moisture and high temperatures. It is an important process in the alteration of iron and magnesium rich minerals. Several primary minerals contain Fe^{2+} and Mn^{2+} . If there are oxidizing environmental conditions the Fe^{2+} is oxidized to Fe^{3+} and Mn^{2+} to Mn^{3+} or Mn^{4+} partly inside the minerals, which results in a positive charge and the mineral becomes unstable.

Moon and Jayawardane (2004) studied the geomechanical and geochemical weathering of Karamu basalt in New Zealand. They concluded that the early stages of weathering as initial fracturing of the rock were physical processes, followed by the progressive development of secondary minerals that reduced the strength of the rocks. From these results, it is apparent that an early loss of alkaline earth elements (magnesium, calcium and ferrous) can be measured geochemically before any significant mineralogical change occurs, and is closely linked to a dramatic drop in the intact strength of slightly weathered basalt. This drop in intact strength in turn allows for fracture development in response to residual stresses, after which secondary mineral development occurs following well-established patterns.

Yokota and Iwamatsu (1999) studied the weathering process of soft pyroclastic rocks in a steep slope. The pyroclastic rocks composing the slopes contain many weakly interlocked volcanic glass and pumice fragments. Their physical properties depend on the degree of welding. A pyroclastic rock is generally similar to sandstone with regard to its engineering properties. In general, the weathering and

softening of rocks are attributable to changes not only in the physical and mechanical characteristics, but also in the chemical properties of the rocks. Mechanical changes in these rocks include that the surface tends to loosen easily and disintegrates at an early stage. The unlocking mechanism of volcanic glass may also be considered as a mechanical change. The dissolution of chemical components, such as ferric oxide and silica, which serve as intergranular cement, and volcanic glass may also commence at an early stage. Although the processes involved in both chemical dissolution and mechanical disintegration are difficult to measure, they may be the dominant weathering processes in these rocks, especially within the shallow portion of slopes affected by changes in the groundwater table. As a result of a water-glass reaction, some of the volcanic glass changes to clay minerals such as allophone and halloysite. The chemical changes mentioned above also accelerate the physical and mechanical changes that occur as results of small volumetric changes in intergranular structures. Rock porosity increases and both dry density and strength decrease with time.

2.2.3 Weathering resistance

The resistance to weathering of rock depends on types of mineral present, surface area of rock exposed and porosity of rocks. Weathering is not only dependent on the mineral composition but also on the porosity of the rock (Robinson and Williams, 1994). Rocks consisting of coarse fragments such as granite easily weather physically but do not weather chemically fast. In contrast, in rock consisting of fine fragments, such as basalt, chemical weathering is quicker than physical weathering. The weathering of stratified sedimentary rocks is dependent on the orientation of the stratification and cementation. The ranking of some primary

minerals in order of increasing stability is shown in Figure 2.1. Olivine weathers rapidly because the silicon tetrahedral is only held together by oxygen and the metal cat-ions which form weak bonds. In contrast, quartz is very resistant, because it consists entirely of linked silicon tetrahedral. The rate of weathering is influenced by temperature, rate of water percolation and oxidation status of the weathering zone. Weathering depends on climate such as temperature and the mean annual precipitation rates. The mean lifetime of one millimeter of different rocks into a kaolinitic saprolite is shown in Table 2.1. These numbers suggest that in cold or tropical humid zone, the climate controls the rate of weathering.

2.3 Factors affecting strength and durability of some weak rocks

The mineralogy and the geometric arrangement (microfabric) of particles affect slaking and strength of weak rocks (Engin et al., 1999). For shales, their microfabric includes features of both argillaceous rocks (e.g. mudstones and clay rocks) and fragmental rocks (composed of grains, e. g. sandstones). Therefore, the geomechanical characteristics of shales cannot be determined as easily as for other types of rocks. In order to predict the behavior of shales, one has to understand the effect of both grains and clay minerals on geomechanical properties of rocks (Koncagul and Santi, 1999). These factors are briefly discussed as follows.

Finer grained sediments are more susceptible to breakdown and at higher rates than coarse grained sedimentary materials (D'Appolonia Consulting Engineers, 1980). Conversely, although there are conflicting findings, fine grained samples can withstand higher uniaxial compressive loads (Brace, 1961; Fahy and Guccions, 1979). The probable reason for this is the number of grain to grain contacts is higher for fine

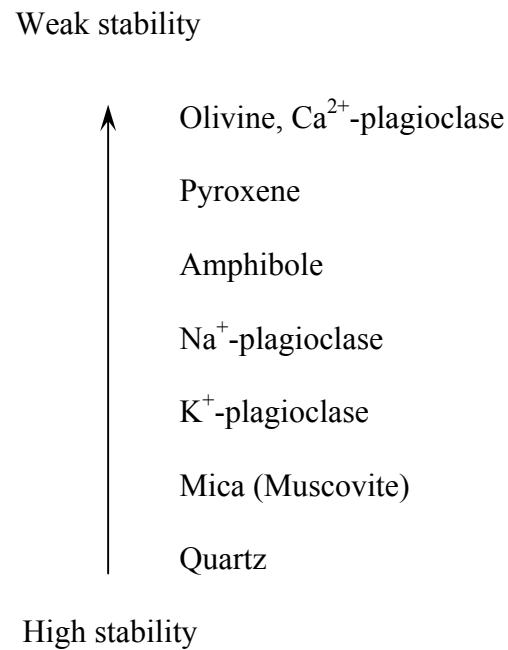


Figure 2.1 Stability of some primary minerals (Robinson and Williams, 1994).

Table 2.1 Mean lifetime of one millimeter of fresh rock (Nahon, 1991).

Rock Type	Climate	Lifetime (years)
Acid rocks	Tropical semi-arid	65 to 200
	Tropical humid	20 to 70
	Temperate humid	41 to 250
	Cold humid	35
Metamorphic rocks	Temperate humid	33
Basic rocks	Temperate humid	68
	Tropical humid	40

grained samples. Therefore the applied external force is distributed over a larger contact surface.

Rocks made of rounded grains are more durable (D'Appolonia Consulting Engineers, 1980) because crystals or grains with sharp edges are exposed to a greater degree of abrasion during the slake durability test, resulting in lower slake durability indices. Similarly, stresses will concentrate along grain edges in the uniaxial compression test. However, depending on the degree of bonding between the grains, such angular shaped particles may provide a great deal of interlocking thus increasing the compressive strength. Several researchers (Fahy and Guccions, 1979; Ulusay, et al., 1994; Shakoor and Bonelli, 1991) reported positive correlation between the uniaxial compressive strength and percentage of angular grains. Assuming properties such as mineralogy of grains and cement and degree of bonding are the same, a rock made of angular grains should be stronger and harder (due to better interlocking of grains) but less durable (due to higher degree of erosion) than a rock composed of rounded grains. Grain boundaries and type of grain contacts are likely to affect the strength of rock material (Ulusay et al., 1994; Shakoor and Bonelli, 1991). These researchers found a significant positive correlation between these variables and uniaxial compressive strength of sandstone samples. Since sutured contacts provide better interlocking of grains, these types of contacts should increase the hardness and durability of specimens also.

Due to its abundance as a rock forming mineral, most of the correlations established by previous researchers (Fahy and Guccions, 1979; Shakoor and Bonelli, 1991; Gunsallus and Kulhawy, 1984) found a negative relationship between quartz content and uniaxial compressive strength of the investigated sandstones. Handlin

and Hager (1957), Bell (1978), and Barbour et al. (1979) did not find any significant correlation and suggested that the structural interlocking of the quartz grains and not the quartz content itself influences uniaxial compressive strength. Also, while not clearly stated in the literature, it is believed that rocks composed of quartz grains should have a higher durability due to the higher resistance of this mineral to mechanical abrasion.

Bonding determines the ease with which macrofractures can propagate through the specimen by disrupting the structure and breaking the bonds within the groundmass. Mineralogy of bonding or cementing material is an important property that controls strength, hardness and durability. Quartz provides the strongest binding followed by calcite and ferrous minerals. Clay binding material is the weakest (Vutukuri et al., 1974). There is not much literature about the relationship between the mechanical properties of a rock and the cement and matrix content. Among published material, Bell (1978) reported that the strength increases proportionally with the amount of cement. Fahy and Guccione (1979) and Shakoor and Bonelli (1991) state that the correlations they had found between cement and strength were insignificant.

Bell (1978) correlated packing density, which is the space occupied by grains in a given area, with the uniaxial compressive and tensile strengths of Fell sandstone. He showed that strength increased with increasing packing density. Hoek (1965) suggests that severe interlocking of grains could occur in sedimentary rocks in which grains have been tightly packed and well cemented. This would result in a considerable increase in the amount of applied stress required to propagate grain boundary cracks. Shakoor and Bonelli (1991) did not find any significant relationship between packing density and strength.

Shale rocks may contain various amounts of clay and non-clay minerals, organic matter, and precipitated salts. Mineralogy is the primary factor controlling the physical and chemical properties of such rocks (Mitchell, 1993). For engineering applications, as a size term, clay refers to all material smaller than 0.002 mm. As a mineral term, it refers to specific clay minerals (e.g. talc, mica, chlorite or smectite). These clay minerals occur in small particle sizes and their unit cells ordinarily have a residual negative charge that is balanced by the adsorption of cations from solution (Mitchell, 1993). The type of clay minerals and availability of cations affect the properties of argillaceous rocks.

Different clay minerals have varying degrees of swelling capability. The order in which swelling potential decreases is : montmorillonite > illite > halloysite > kaolinite. Types of ions existing as dissolved solids in the wetting fluid also strongly affect the degree of swelling. For instance, swelling of montmorillonite decreases as other univalent or divalent ions in following order substitute for sodium (Na) : lithium (Li) > potassium (K) > calcium (Ca) > magnesium (Mg) > hydrogen (H) (Mitchell, 1993). Swelling potential is expected to decrease durability but to have little effect on hardness or strength.

Slaking is the most common physical degradation mechanism affecting clays, clay soils and clay rich rocks. Moriwaki and Mitchell (1977) study various types of slaking and the factors behind them in detail. The investigated variables were clay mineralogy, adsorbed-cation ratios, water content and consolidation-fluid electrolyte concentrations. It is concluded that the type of slaking is strongly controlled by clay mineralogy and the concentration of exchangeable Na-ions. The four common types of slaking in pure clays are dispersion slaking (Na-kaolinite), swelling slaking (Na-

montmorillonite), body slaking (Ca-kaolinite and Ca-illite) and surface slaking (Ca-montmorillonite). Since clay minerals constitute the dominant portion of shales, the intrinsic rock-slaking behavior will differ based on the amount and type of the constituent clay minerals in shale. Mixtures of various clay minerals will lead to combinations of slaking modes. Some clay minerals may exhibit two different slaking modes following one another (Santi and Koncagul, 1996). Increase of hydration and double layer repulsion force and negative pore pressure are slaking mechanisms common in smectites (D'Appolonia Consulting Engineers, 1980). Their open structure allows the entry of water carrying dissolved ions and leads to great expansion and destruction of the crystal lattice. Dispersed structures are less susceptible to these mechanisms due to their lower permeability. Pore air compression could be a significant slaking mechanism for materials composed of non-swelling clay minerals. None of these mechanisms are directly related to strength or hardness of argillaceous rocks.

In general, experimental literature shows that the greater the water content (w_c), the lower the compressive strength of a specimen. Water can soften the bonds or interact with mineral surfaces and alter their surface properties (Horn and Deere, 1962). With the aid of pore water pressure, it may cause instability along weakness planes. Water may also decrease frictional shearing resistance or change the characteristics of gouge or clay mineral constituents of the rock (Touloukian et al., 1981). Reduction in compressive strength due to water has been reported by numerous investigators including Kjaernsli and Sande (1966) and lately by Moon (1993). High water content also decreases durability and hardness of rock specimens. Rocks containing non-swelling clay minerals, such as kaolinite, slake faster upon

submersion in water when they are completely dry beforehand (due to pore air compression) (Moriwaki and Mitchell, 1977).

While porosity determines the total surface area open to physical or chemical interaction, hydraulic conductivity determines the ease with which fluids can seep through these pores. A high value of hydraulic conductivity indicates a well interconnected pore network. The factors that affect hydraulic conductivity are mineral composition, texture, particle size distribution, characteristics of the wetting fluid, exchangeable cation composition, void ratio and degree of saturation of rock mass (Domenico and Schwartz, 1990). Clay rocks have a very high porosity but their permeability is in the order of 10^{-8} to 10^{-10} m/s. Clay minerals with granular or fibrous shape (Kaolinite and Illite) are permeable to a greater degree than those that are flake shaped (Montmorillonite). Strength, hardness and durability decrease with increasing water content. Therefore, it is not unreasonable to expect lower strength, hardness and durability values from specimens with relatively high hydraulic conductivity values, which should also have higher water content.

Shales with larger pores are more resistant to slaking (Vallejo et al., 1994). This is specifically true for shales composed of kaolinite, which slake as a result of pore air compression breaking up the hydrogen bonds that connect individual plates to one another. Conversely, the larger the pores, the lower the compressive strength (Deere and Miller, 1966), hardness and crushing strength of shale samples under point load (Vallejo et al., 1994). Porosity has a significant effect on mechanical performance. Price (1960) and Dube and Singh (1972) report that in sedimentary rocks all strength properties decrease with increasing porosity. The physical explanation of this is that high porosity assists the networking (propagation) of stress-

induced microfractures (Howarth and Rowlands, 1986). The slake durability index of highly porous argillaceous rocks should also be lower (except those containing kaolinite) due to higher degree of slaking because higher porosity (combined with high permeability) provides a larger surface area open to water interaction. Although much research has focused on measurement of strength and durability, the number of studies that compared strength and durability predictive tests to microscopic properties is very limited, with almost no studies focusing on weak rocks and especially shales. Moon (1993) concludes that groundmass microstructure is probably the most important factor controlling the geomechanical behavior of ignimbrites. Both strength and slake durability are controlled by closeness of packing of the groundmass (packing density), degree of bonding between individual grains and average crystal size.

2.4 Tests that can be correlated to strength

Simple laboratory tests that can be correlated to compressive strength of intact rocks include point load strength testing, slake durability testing, dynamic wave velocity measurement and specific gravity and water absorption testing. The slake durability tests are intended to assess the resistance to weathering of shale or other weak or soft rocks samples after being subjected to two standard cycles of drying and wetting (ASTM D4644). In this test dried fragments of rock with known weight are placed in drum fabricated with 2.0 mm square wire mesh. The drum is rotated in horizontal position along its longitudinal axis while partially submerged in distilled water to promote wetting of the sample. The specimens and the drum are dried at the end of the rotation cycle (10 minutes at 20 rpm) and weighed. After two cycles of

rotating and drying the weight loss and the shape and size of the remaining rock fragments are recorded and the slake durability index is calculated. Koncagul and Santi (1999) establish a correlation between the uniaxial compressive strength, the slake durability and shore hardness using mineralogical and intrinsic properties of 31 shale samples (varying degrees of silt and sand contents in Kentucky, USA) to explain the differences between the measured and the predicted results. The results of slake durability index after two cycles range from 30 to 97%. The correlation can be represented by the following equation:

$$\text{UCS} = 658(I_{d2}) + 9081 \quad ; \quad r = 0.63 \quad (2.1)$$

where UCS is uniaxial compressive strength (kPa). I_{d2} is the second cycle of slake durability index (%).

Gokceoglu et al. (2000) study the factors affecting the rock durability with an emphasis on the influence of number of drying and wetting cycles of 141 weak rock samples, including schist and sandstone. The samples were subjected to slake durability test and uniaxial compressive test. A relationship between the uniaxial compressive strength and the fourth cycle slake durability index is found only for the marls.

$$\text{UCS} = 2.54I_{d4} - 202 \quad ; \quad r = 0.76 \quad (2.2)$$

where UCS is the uniaxial compressive strength (MPa). I_{d4} is the fourth cycle of slake durability index (%).

Point load strength index tests have often been reported as an indirect measure of the compressive or tensile strength of intact rock (ASTM D5731). It has been used widely in practice due to its simplicity of testing and specimen preparation, and field application. Conventional point load testing is intended as an index test for the strength classification of rock material. It has long been practiced to obtain an indicator of the uniaxial compressive strength of intact rock. Broch and Franklin (1972) state that the compressive strength is approximately equal to 24 times the point load index (I_s), referred to a standard size of 50 mm. Bieniawski (1975) experimentally showed that the compressive strength is nearly 23 times I_s . Greminger (1982) stated that the compression factor of 24 cannot be validly applied to anisotropic rocks. It is stated by ISRM (1985) that on average the compressive strength is 20-25 times I_s . Tsiambaos and Sabatakakis (2004) study the soft to strong rocks under different conversion factors relating uniaxial compressive and point loading strength. The samples were mainly sedimentary carbonate rocks (limestones, marly limestones, sandstone and marlstone), since this type of sedimentary rocks is the most common one in Greece. The results show the conversion factor between point load and uniaxial compressive strength varies from 13 for soft sedimentary rocks exhibiting a value of $I_{s(50)} < 2$ MPa, 20 for medium rocks exhibiting a value of $2 < I_{s(50)} < 5$ MPa and 28 for hard rocks with value of $I_{s(50)} > 5$ MPa.

Dynamic wave velocity test determines the pulse velocities of compression and shear waves in intact rock and the ultraseismic elastic constants of isotropic rock. The ultraseismic elastic constants are calculated from the measured travel time and distance of compression and shear waves in a rock specimen. Sousa et al. (2005) study the influence of microfractures and porosity on the physico-mechanical

properties and weathering of nine granites (coarse grain size and porphyritic texture). They conclude that the primary wave velocity appears to increase linearly with uniaxial compressive strength:

$$\text{UCS} = 0.004V_p^{1.247} : r = 0.72 \quad (2.3)$$

where V_p is primary wave velocity (m/s).

Specific gravity and water absorption tests determine the bulk specific gravity, apparent specific gravity, and absorption of coarse aggregate (ASTM C127). Tugrul (2004) studied the weathering on four different types of rock, sandstone, limestone, basalt and granodiorite. The results suggest that the rock dry unit weight decreases and water absorption increases as grade of weathering increases. Water absorption is a useful property in evaluating the durability of different rocks as building materials (Shakoor and Bonelli, 1991). Begonha and Braga (2002) study the weathering degrees of Oporta granite as affecting geotechnical and physical properties (porosity, dry bulk density, ultrasonic velocity, uniaxial compressive strength and modulus of elastic). They conclude that dry bulk density, ultrasonic velocity, uniaxial compressive strength and modulus of elastic appear to decrease with increasing degree of weathering.

2.5 Joint shear strength criteria

The shearing resistance of rock joints is one of the important parameters that are used in the analysis and design of engineering structures in rock mass. Several criteria have been proposed in the past to identify the strength of a rough rock joint. These criteria delineate the state of stress that separates pre-sliding and post-sliding of

the joint. The simplest peak-shear strength model for rock joints is perhaps Patton's model (Patton, 1966). Based on the Coulomb friction law, this model characterizes the joint behavior by a single surface parameter that is the average roughness angle. More complicated joint models appeared later, such as Ladanyi's empirical model (Ladanyi and Archambault, 1970) and Barton's empirical model (Barton, 1973).

Coulomb criterion represents the relationship between the peak shear strength and normal stress by

$$\tau = c + \sigma_n \tan \phi \quad (2.4)$$

where τ is joint shear strength, σ_n is normal stress, c is the cohesive strength, and ϕ is angle of friction.

Patton (1966) performed a series of constant load stress direct shear tests with regular teeth inclination (i) at varying normal stresses. From these tests, he established a bilinear failure envelope-failure from an asperity sliding and asperity shearing mode.

$$\tau = \sigma_n \tan (\phi_B + i) \quad (2.5)$$

where ϕ_B is basic friction angle, and i is regular teeth inclination.

Ladanyi and Archambault (1970) develop a model for the shear strength of rock joints.

$$\tau = \frac{\sigma_n (1 - a_s) (V + \tan \phi_B) + a_s \tau_r}{1 - (1 - a_s) V \tan \phi_B} \quad (2.6)$$

where a_s is the proportion of the discontinuity surface which is sheared through projections of intact material, V is the dilation rate (dv/du) at peak shear strength, and τ_r is the shear strength of the intact material.

Barton (1973) studies the behavior of natural rock joints and proposes a criterion that is modified from Patton. It can be written as:

$$\tau = \sigma_n \tan \left[\phi_B + JRC \log_{10} \left(\frac{\sigma_j}{\sigma_n} \right) \right] \quad (2.7)$$

where JRC is the joint roughness coefficient (ranging from 0 to 20), and σ_j is the joint wall compressive strength.

There are some advantages to the use of the Barton's criterion, as follows:

- 1) The model provides easy and practical means to predict the shear strength of a joint by its roughness and wall strength.
- 2) Barton's criterion is more realistic than the Coulomb criterion because Barton considers the joint roughness.
- 3) Barton's criterion is more conservative than Ladanyi and Archambault's at higher normal stress levels.

For unfilled joints, the roughness and compressive strength of the wall are important, whereas in the case of filled joints the physical properties of the material separating the joints wall are of the primary concern. Barton criterion is only valid where joint wall is in rock-to-rock contact and the maximum allowable shear strength given by $\arctan(\tau/\sigma_n) = 70^\circ$. Hoek and Bray (1981) report that the criterion is valid for the normal stress range, $0.01 < (\sigma_n/JCS) < 0.3$.

CHAPTER III

ROCK SAMPLES

3.1 Introduction

Thirteen rock types were selected for this research. They were divided into three main groups: two volcanic rocks, three metamorphic rocks and eight sedimentary rocks. These rocks represent the exposed outcrops that are commonly found in the east and northeast of Thailand. They also have significant impacts on long-term stability of many engineering structures constructed in the regions (e.g., embankments and foundations of highways, railways and reservoirs, dam abutments, and tunnels). The key criterion of sample selection is that the rock matrix should be as homogeneous as possible. This is to minimize the intrinsic variability of the test results. This chapter describes the mineral compositions of the rock samples and the locations from which they have been obtained.

3.2 Sample collection

Table 3.1 gives rock names, locations from which they have been collected, and formations to which they belong. A map shown in Figure 3.1 gives the locations where the rock samples have been collected. For each location, a minimum of 6 kg of 1-1.5 inch fragments and two 1×1×1 ft³ blocks have been collected. The rock fragments are planned for the slake durability tests and the rock blocks for the mechanical tests.

Table 3.1 Rock samples used in this study.

Rock Names	Code	UTM	Location	Rock Formation	Age
Volcanic Rocks					
1. Pichit crystal tuff	PCT	47Q0676363/1802064	Chatree Gold Mine Phichit province	Loei - Petchabun Volcanic belt	Permo - Triassic
2. Pichit pumice breccia	PPB	47Q0676002/1802024	Chatree Gold Mine Phichit province	Loei - Petchabun Volcanic belt	Permo – Triassic
Metamorphic Rocks					
3. Kanchanaburi green schist	KSch	47P0801984/1422888	Khao Chuk reservoir, Rayong province	Kanchanaburi	Silurian - Devonian
4. Chonburi quartz mica schist	CSch	47P0768172/1403836	Ban Mab Chan, Klaeng district, Rayong province	Chonburi Gneiss Group	Precambrian
5. Nam Duk slaty shale	NDSch	47Q0752546/1850965	Chum Phae-Lom Sak highway, Phetchabun province	Nam Duk	Middle – Permian
Sedimentary Rocks					
6. Maha Sarakham mudstone (Lower Clastic)	MSMD	47P0821065/1687136	Amphur Non Thai, Nakhon Ratchasima province	Maha Sarakham	Lower Tertiary - Upper Cretaceous

Table 3.1 Rock samples used in this study (Continue).

Rock Names	Code	UTM	Location	Rock Formation	Age
Sedimentary Rocks					
7. Phra Wihan siltstone	PWST	47P0812777/1600138	Amphur Wang Nam Khieo, Nakhon Ratchasima province	Phra Wihan	Lower - Jurassic
8. Nam Phong sandstone	NPST	47Q755660/1852758	Chum Phae-Lom Sak highway, Phetchabun province	Nam Phong	Upper – Triassic
9. Kaeng Krachan micaceous siltstone	KKST	47P0800265/1422680	Khao Chuk reservoir, Rayong province	Kaeng Krachan	Carboniferous
10. Khok Kruat sandstone	KkSS	47P0820992/1646362	Khok Kruat district, Nakhon Ratchasima province	Khok Kruat	Upper - Lower Cretaceous
11. Phu Kradung white sandstone	PKSS1	47P0759070/1701842	Amphur Thep Sathit, Chaiyaphum province	Phu Kradung	Lower – Jurassic
12. Phu Kradung red sandstone	PKSS2	47P0758292/1701367	Amphur Thep Sathit, Chaiyaphum province	Phu Kradung	Lower-Jurassic
13. Phra Wihan sandstone	PWSS	47P0812102/1598902	Amphur Wang Nam Khieo, Nakhon Ratchasima province	Phra Wihan	Lower - Jurassic

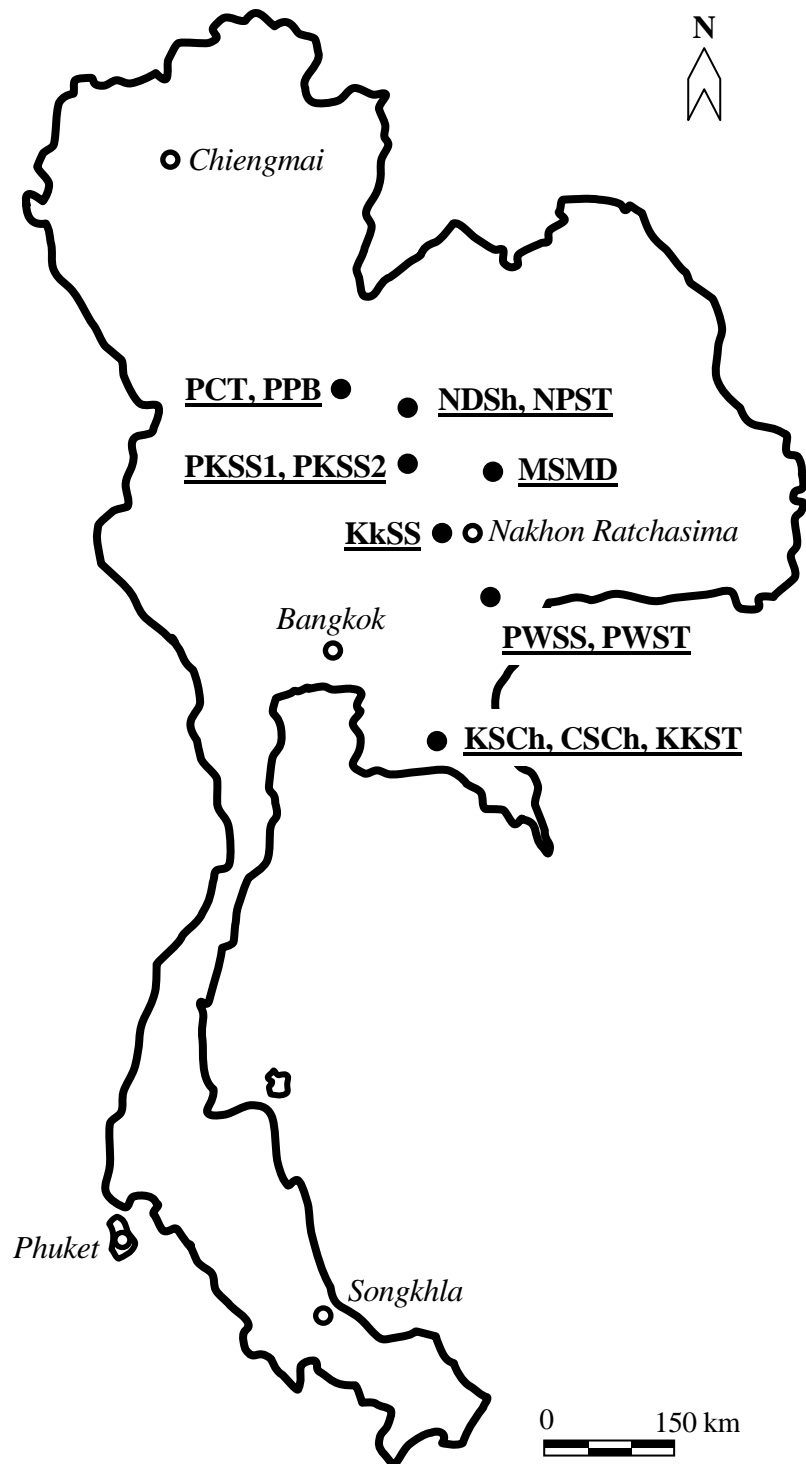


Figure 3.1 The locations where rock samples have been collected.

Pichit crystal tuff (PCT) and pumice breccia (PPB) are obtained from the Chatree gold mine in Phichit province (Figure 3.2). The rocks belong to Loei-Petchabun volcanic belt and are of Permo-Triassic age.

Phu kradung white and red sandstones (PKSS1 and PKSS2) are obtained from the embankment of Thep Sathit-Chaiyaphum highway at km 287 to 288 (Figures 3.3 and 3.4). The rocks are of Lower-Jurassic age.

Kaeng Krachan micaceous siltstone (KKST) and Kanchanaburi green schist (KSch) are obtained from the Khao Chuk reservoir in Rayong province (Figure 3.5). The rocks are of Silurian-Devonian age.

Phra Winhan yellow sandstone (PWSS) and red siltstone (PWST) are obtained from the embankment of Wang Nam Khieo-Tap Lan highway at km 69. The rocks are classified as the Phra Wihan formation and are of Lower-Jurassic age.

Nam Duk slaty shale (NDSH) and Nam Phong sandstone (NPST) are obtained from the embankment of Chum Phae-Lom Sak highway at km 19 and 23 in Pechabun provinces. Nam Duk slaty shale is of Middle-Permian age. Nam Phong sandstone (NPST) is of Upper-Triassic age.

Khok Kruat sandstone (KkSS) is obtained from Ban Phong Marangwan reservoir in Nakhon Ratchasima province. The rock is of Upper-Lower Cretaceous age.

Maha Sarakham mudstone (MSMD) is obtained from borehole coring of Siam Submanee Cooperation Limited in Amphur Non Thai at Nakhon Ratchasima province. The rock is classified as the Maha Sarakham formation and is of Tertiary-Upper Cretaceous age.

Chonburi quartz mica schist is obtained from a quarry in Klaeng district at Rayong province. The rock is classified as the Chonburi Gneiss group and is of Precambrian age.



Figure 3.2 Pichite crystal tuff and Pichit pumice breccia collected from Tawan pit of the Chatree gold mine in Phichit province.



Figure 3.3 White quartz sandstone collected from the embankment of Thep Sathit-Chaiyaphum highway at km 287. The slope was excavated in 2003.



Figure 3.4 Red sandstone collected from the embankment of Thep Sathit-Chaiyaphum highway at km 288. The slope was excavated in 2003.



Figure 3.5 Micaceous siltstone collected from the embankment of Khao Chuk reservoir in Rayong province.

3.3 Mineralogical Study

The mineral compositions of the rock samples are determined by using X-ray diffraction method and petrographic analysis. Tables 3.2 through 3.4 give the results for volcanic, metamorphic and sedimentary rock groups, respectively. The mineral compositions determined will be used as data basis to correlate and explain the degrees and characteristics of rock degradation which will be discussed in the following chapters.

Table 3.2 Mineral compositions of rock specimens in volcanic rock group.

Volcanic Rocks	Density (g/cc)	Quartz (%)	Pyrite (%)	Kaolinite (%)	Calcite (%)	Laumontite (%)	Color
1. Pichit crystal tuff	2.57	70.8	8.4	3.1	17.7	-	dark gray
2. Pichit pumice breccia	2.28	82.0	1.9	9.3	-	6.8	white, pink and gray

Table 3.3 Mineral compositions of rock specimens in metamorphic rock group.

Metamorphic Rocks	Density (g/cc)	Quartz (%)	Muscovite (%)	Biotite (%)	Feldspar (%)	Kaolinite (%)	Chlorite (%)	Albite (%)	Chamosite (%)	Fluorony boite (%)	Color
1. Kanchanaburi green schist	2.46	43.49	6.43	-	12.85	-	22.76	13.43	14.47	-	grayish green
2. Chonburi quartz mica schist	2.18	24.80	4.94	26.86	-	17.57	-	-	-	-	yellowish brown
3. Nam Duk slaty shale	2.24	50.85	15.36	25.42	-	-	-	-	-	8.37	brownish gray

Table 3.4 Mineral compositions of rock specimens in sedimentary rock group.

Sedimentary Rocks	Density (g/cc)	Quartz (%)	Mica (%)	Hematite (%)	Kaolinite (%)	Calcite (%)	Chlorite (%)	Other (%)	Cementing	Contact	Grain size (mm)	Grain Shape	Sorting	Color
1. Maha Sarakham mudstone (Lower Clastic)	2.66	39.65	13.19	-	30.91	-	-	16.15 (Halite)	Halite and iron oxide	grain contact	<0.004	-	-	reddish brown
2. Phra Wihan siltstone	2.35	72.00	3.00	5.00	-	-	-	20.00	Hematite	Matrix support	0.06-0.004	-	-	brownish red
3. Nam Phong sandstone	2.59	59.10	-	2.1	-	22.4	3.9	12.50 (Albite)	Hematite	grain contact	0.1-1.0	angular	poorly	brownish red
4. Kaeng Krachan siltstone	2.62	58.41	22.85	-	6.50	-	-	12.24 (Feldspar)	Hematite	grain contact	0.06-0.004	-	-	yellowish brown
5. Khok Kruat sandstone	2.45	54.70	1.10	-	-	8.0	-	33.50 (Albite)	Calcite	grain contact	0.1-1.5	angular	poorly	brownish red
6. Phu Kradung white sandstone	2.29	99.30	-	-	0.70	-	-	-	Silica	grain contact	1.5-2.0	angular	well	white
7. Phu Kradung red sandstone	2.59	80.90	-	-	1.40	12.1	-	5.60 (Albite)	Hematite	grain contact	0.1-1.0	angular	moderate	brownish red
8. Phra Wihan sandstone	2.35	97.00	-	-	-	-	-	3.00	Silica	grain contact	2.00	angular	well	yellow

CHAPTER IV

LABORATORY EXPERIMENTS

4.1 Introduction

The laboratory experiments performed can be divided into two main types: slake durability index testing and simulation of rock degradation. During the simulation of rock degradation, series of point load strength index tests, tilt tests and measurements of dynamic wave velocity, specific gravity and water absorption of the rock specimens are performed. The results are used as indicators of the degrees of rock weathering.

4.2 Slake durability index test

The primary objectives of the slake durability index test (hereafter called SDI test) are to determine long-term durability of the rock specimens, to establish weathering and degradation characteristics of each rock type, and to assess the impact of water on the rock degradation. Two series of SDI test were performed on two separate sets of rock specimens with similar and comparable characteristics. For the first series, the test procedure, apparatus (Figure 4.1) and data reduction were similar to that of the standard practice (ASTM D4644), except that the tests were performed up to six cycles, instead of two cycles as specified by the standard. The second test series was identical to the first one except that no water was in the trough during rotating the drum, i.e., slaking under dry condition. The second test series (hereafter called



Figure 4.1 Slake durability test apparatus.

SDI dry-testing) was carried out to assess the impact of water on the weathering process for each rock type.

4.2.1 Test Results

The SDI values for all rock types are plotted as a function of number of cycles (N) for testing with water in the trough in Figure 4.2, and without water in the trough (dry condition) in Figure 4.3. Tables 4.1 and 4.2 list the SDI values obtained for each test cycle. The results are given in details in Appendix A. For wet testing, Phra Wihan siltstone, Phu Kradung white sandstone and Chonburi quartz mica schist tend to degrade much quicker than do other rock types probably because they contain high percentages of kaolinite in the rock matrix. The most durable rocks seem to be Pichit crystal tuff, Nam Phong sandstone, Nam Duk slaty-shale, and Kanchanaburi green schist. The thirteen rock types are classified based on Gamble (1971) classification, as shown in Table 4.3. The SDI values obtained for Phu Kradung red sandstone and Phra Wihan siltstone agree with those obtained by Phienwej and Singh (2005) who tested the same rock types.

Comparison between wet and dry testing suggests that the impacts of water on rate of rock degradation varied among different rock types. Figures 4.4 and 4.5 compare SDI obtained from wet and dry testing after the first and the sixth cycles. Phra Wihan siltstone, Phu Kradung white sandstone, Pichit pumice breccia and Chonburi quartz mica schist are highly sensitive to water in terms of their durability. In another words, without subjecting to water these rocks are still considered moderately durable. For some highly durable rocks (e.g. Pichit crystal tuff, Nam Phong sandy-siltstone, Nam Duk slaty-shale, and Kanchanaburi green schist), the SDI values obtained from

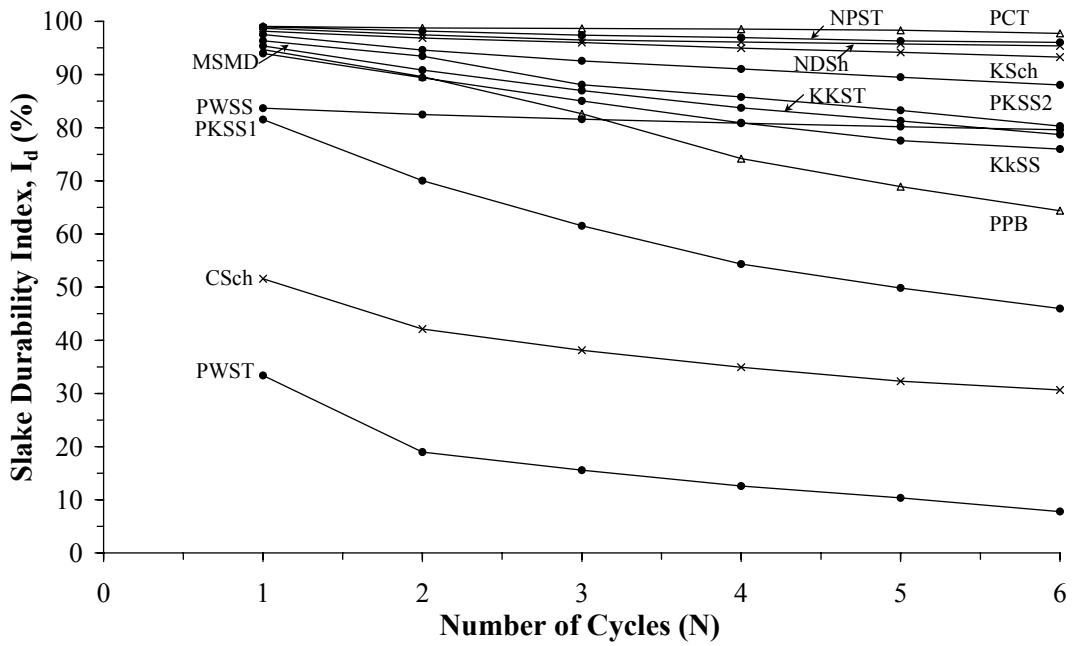


Figure 4.2 Slake durability index for 6 cycles with water in trough.

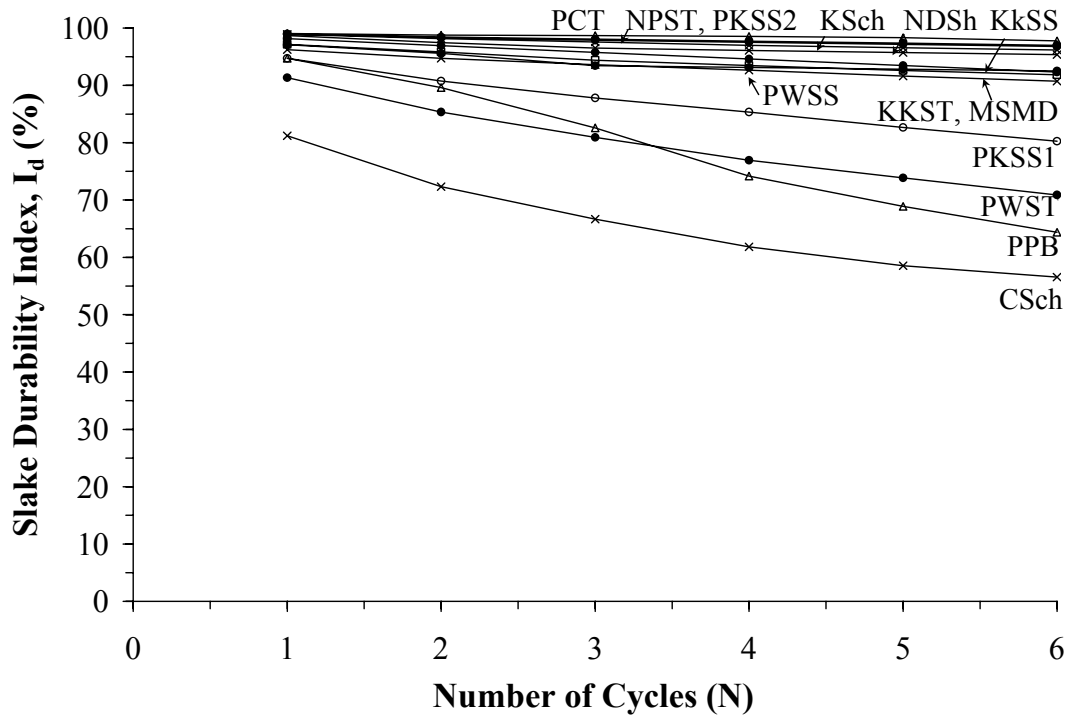


Figure 4.3 Slake durability index for 6 cycles without water in trough.

Table 4.1 Slake durability index test results with water in trough.

Rock Types	Code	Slake Durability Index, I_d (%)					
		Number of Cycles					
		1	2	3	4	5	6
Volcanic Rocks	PCT	99.06	98.77	98.67	98.55	98.32	97.75
	PPB	94.71	89.61	82.60	74.17	68.91	64.37
Metamorphic Rocks	KSch	98.15	96.87	96.01	94.95	94.18	93.28
	CSch	51.57	42.13	38.13	34.94	32.31	30.66
	NDSch	98.69	97.45	96.49	96.10	95.75	95.37
Sedimentary Rocks	PKSS1	81.52	70.02	61.54	54.33	49.85	45.98
	PKSS2	97.52	94.60	92.57	91.04	89.50	88.05
	KKST	95.37	90.83	86.99	83.73	81.28	78.71
	PWSS	83.67	82.47	81.58	80.85	80.19	79.60
	PWST	33.40	18.96	15.57	12.58	10.35	7.80
	NPST	98.98	98.17	97.41	96.97	96.30	96.02
	KkSS	93.96	89.39	85.04	80.91	77.55	75.98
	MSMD	96.35	93.47	88.05	85.77	83.25	80.30

Table 4.2 Slake durability index test results without water in trough.

Rock Types	Code	Slake Durability Index, I_d (%)					
		Number of Cycles					
		1	2	3	4	5	6
Volcanic Rocks	PCT	99.63	99.29	98.99	98.89	98.61	98.43
	PPB	99.02	98.38	97.80	97.40	96.96	96.49
Metamorphic Rocks	KSch	98.89	98.16	97.57	97.00	96.57	96.15
	CSch	81.20	72.34	66.65	61.84	58.56	56.55
	NDSch	98.99	97.84	96.93	96.32	95.80	95.48
Sedimentary Rocks	PKSS1	94.72	90.76	87.82	85.35	82.64	80.25
	PKSS2	98.95	98.45	98.07	97.70	97.36	96.99
	KKST	97.16	95.82	94.38	93.46	92.60	91.83
	PWSS	96.22	94.72	93.63	92.68	91.60	90.71
	PWST	91.35	85.36	80.94	76.94	73.86	70.88
	NPST	98.94	98.30	97.87	97.51	97.15	96.77
	KkSS	98.16	96.94	95.76	94.59	93.45	92.32
	MSMD	97.07	95.59	93.43	93.12	92.80	92.51

Table 4.3 Slake durability index of rock samples based on Gamble's classification
(ISRM, 1981).

Rock Types	Code	I_{d(1)} (%)	I_{d(2)} (%)
Volcanic Rocks	PCT	very high durability	very high durability
	PPB	medium durability	medium high durability
Metamorphic Rocks	KSch	high durability	high durability
	CSch	very low durability	low durability
	NDSch	high durability	high durability
Sedimentary Rocks	PKSS1	low durability	medium durability
	PKSS2	medium high durability	medium high durability
	KKST	medium high durability	medium high durability
	PWSS	low durability	medium durability
	PWST	very low durability	very low durability
	NPST	high durability	very high durability
	KkSS	medium durability	medium high durability
	MSMD	medium high durability	medium high durability

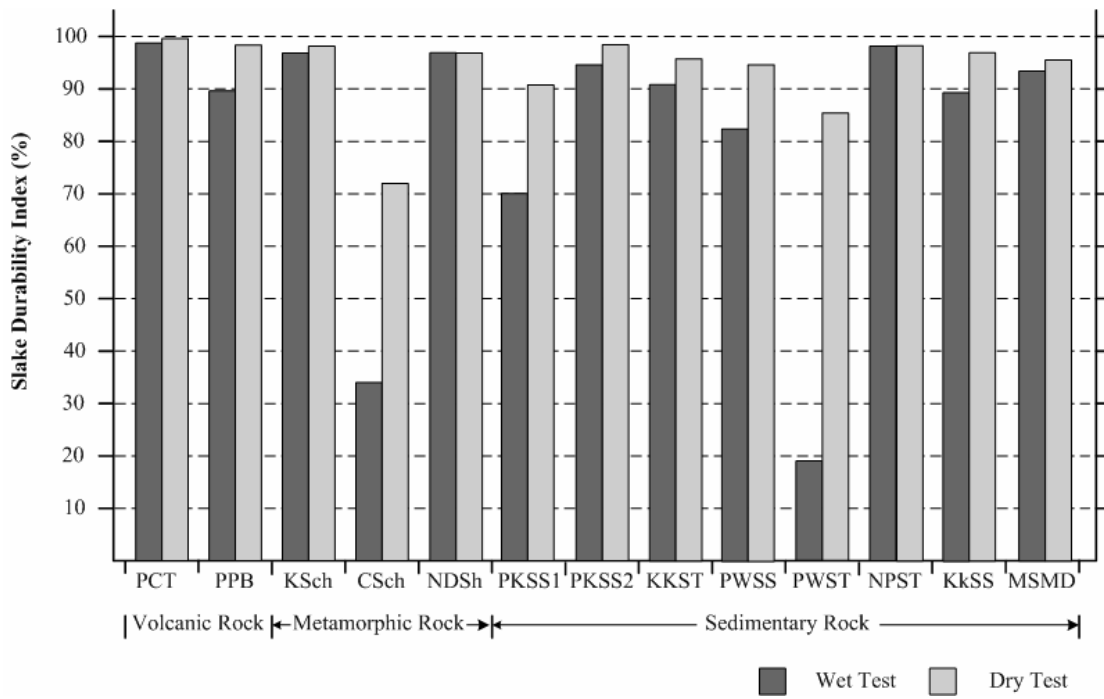


Figure 4.4 Comparison between SDI wet and dry test results at the first cycle.

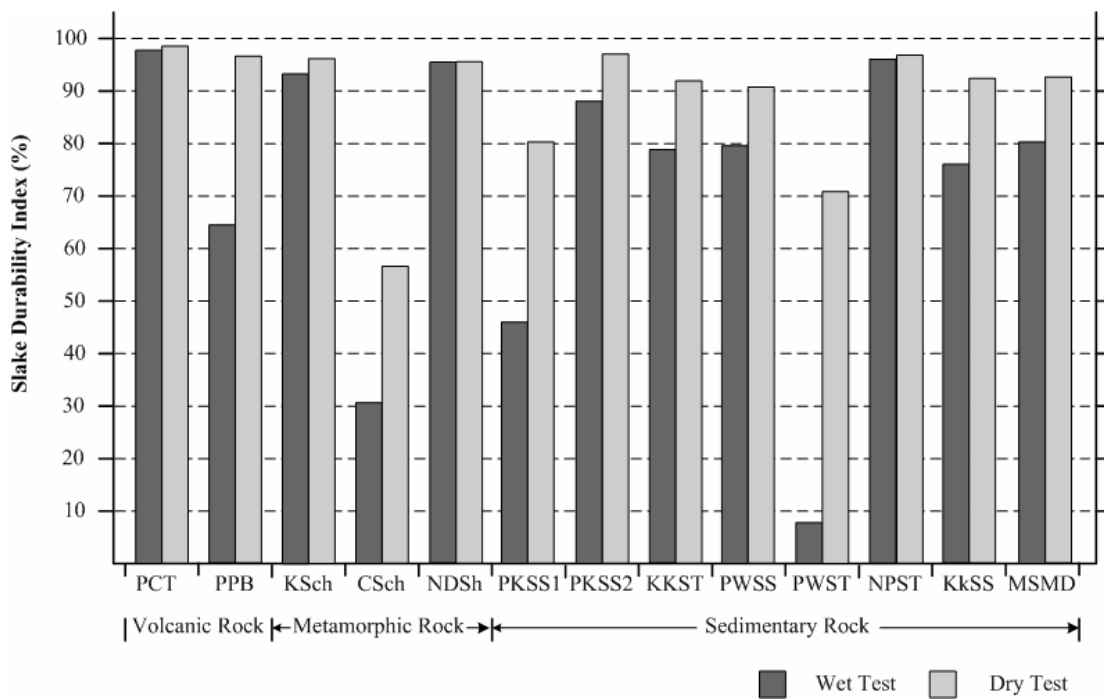


Figure 4.5 Comparison between SDI wet and dry test results at the sixth cycle.

the wet and dry testing are not much different, which implies that water has little impact on their degradation rates.

4.2.2 Implications of SDI for long-term durability

An attempt is made here to project the results of SDI testing toward the future conditions of the rocks. A hypothesis is proposed to describe the physical characteristics of the rock fragments used in the SDI test. It is assumed that all rock fragments inside the drum for each test are identical. Figure 4.6 shows two different types of the rates of degradation (weight loss) during SDI testing. The first type shows linear decreases of the SDI as the number of test cycles increases (Figure 4.6 – left). This implies that each rock fragment in the drum has relatively uniform texture (uniform degree of weathering, hardness or strength) from the inner matrix to the outer surface. The lower the strength of rock fragment, the higher the rate of degradation.

For the second type (Figure 4.6 – right) each rock fragment inside the drum has non-uniform texture. The outer surface is weaker (lower strength, higher degree of weathering or more sensitive to water) than the inner matrix. This is reflected by the decrease of the rate of degradation as the test cycles increase, the curves for samples D, E and F concave upward. Here the decrease of rock matrix strength from the outer surface to the inner part can be abrupt or grading, depending on rock type and weathering characteristics. The more abrupt the change, the more concave the SDI - N curve. It is believed that weathering characteristics of most rocks follow the second type, because the SDI - N curves obtained here and from elsewhere tend to be concave, more or less, upward.

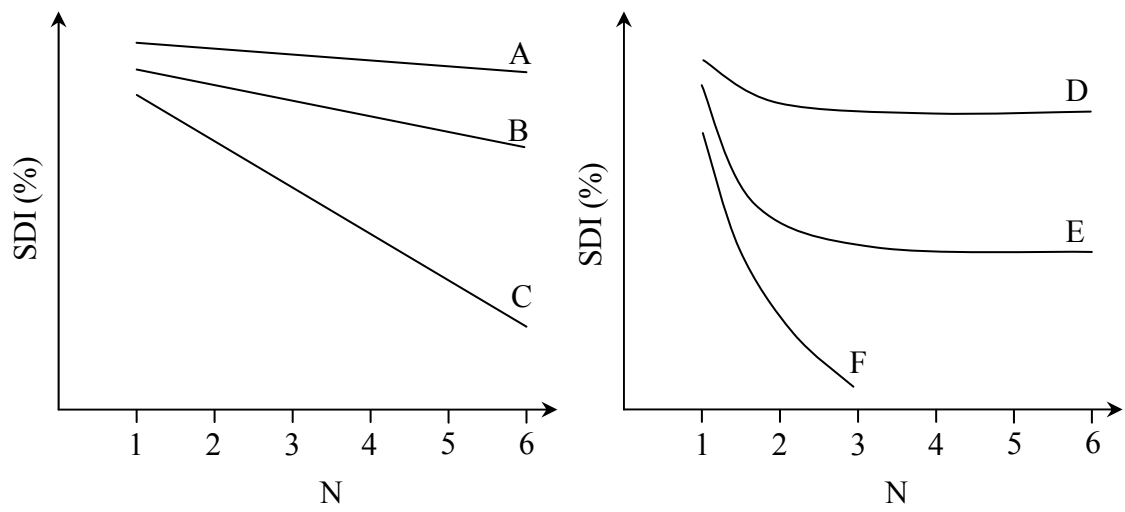


Figure 4.6 Proposed concept of rock degradation during SDI testing. Samples A, B and C (left) have uniform texture. Samples D, E and F (right) have rock matrix that is weaker outside and stronger inside.

4.2.3 Projection of rock durability

Let us assume here that the proposed hypothesis of the second type of weathering is valid. It can be postulated that rock fragments inside the drum tend to get stronger as they are subjected to a greater number of SDI test cycles. When the rock fragments become stronger, the difference of the SDI values between the adjacent cycles (hereafter called Δ SDI) will also get smaller. Δ SDI at any cycle can be represented by:

$$\Delta\text{SDI} = \text{SDI} (N) - \text{SDI} (N+1) \quad (4.1)$$

where SDI (N) is the slake durability index at cycle N, and SDI (N+1) is the slake durability index at cycle N+1.

In order to predict the rock durability in the future, the Δ SDI are calculated for the six cycles. Figure 4.7 plots Δ SDI of sedimentary rocks, volcanic rocks and metamorphic rocks as a function of number of cycles counted backward. This backward cycle is denoted by N^* , primarily to avoid confusing with the original forward cycles (N) defined earlier. This backward plotting is mainly for a convenience of analyzing the test results. For this new approach, while Δ SDI increases with N^* , the rock becomes weaker. This is similar to the actual rock degradation due to weathering process that has occurred in the in-situ condition. For the results obtained above the Δ SDI that represents the difference between the SDI of the first cycle and the conditions as collected (before subjecting to the first cycle) is plotted in cycle number, $N^* = 6$. Therefore the difference between the SDI values of the fifth and sixth cycles is plotted for $N^* = 1$.

The $\Delta\text{SDI} - N^*$ curves have a significant advantage over the conventional $\text{SDI} - N$ diagram. The new curves can show a future trend for the rock durability, as ΔSDI values can be statistically projected to a larger number of test cycles beyond those performed in the laboratory. As an example, the ΔSDI is projected to $N^* = 60$ cycles in Figure 4.7. Regression analyses on the 6 ΔSDI values indicate that an exponential equation can best describe the variation of ΔSDI with N^* . The implications of N^* and actual time or duration under which the rock is subject to actual in-situ conditions is very difficult to define, if at all possible. More discussions on this issue are given in the following chapter. Table 4.4 gives results of regression analysis on the empirical relation between ΔSDI and N^* for all rock types.

4.2.4 Classification of rock durability

A new classification system is proposed for rock durability based on ΔSDI and its projected values to any N^* , as shown in Table 4.5. The $\Delta\text{SDI} - N^*$ curves obtained from thirteen rock types tested here are compared against the new classification system (Figure 4.7). For example, at $N^* = 60$ or below, Pichit crystal tuff, Nam Phong sandy-siltstone, Nam Duk slaty-shale, and Kanchanaburi green schist are classified as high to very high durability rocks. Pichit pumice breccia, Chonburi quartz mica schist and Phra Wihan siltstone are classified as very low durability rock, because their ΔSDI values rapidly increase within few cycles of N^* . This agrees with the classification and conclusions drawn earlier from the results of wet and dry SDI test. It should be noted that the projection of $\Delta\text{SDI} - N^*$ curves relies heavily on the number of cycles actually tested. A larger the number of tested cycles will result in a higher reliability of the projected results.

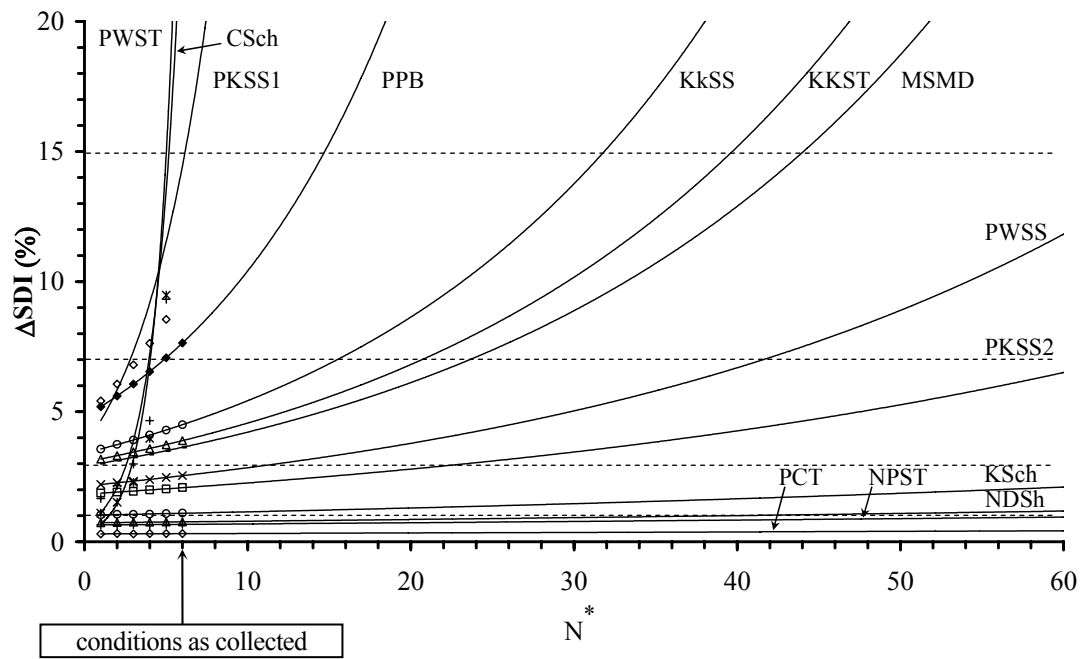


Figure 4.7 ΔSDI as a function of N^* . Rock conditions as collected are plotted at cycle no. 6.

Table 4.4 Empirical constants for an exponential relationship between Δ SDI and N^* .

Rock Types		Δ SDI = $\alpha \cdot \exp(\beta \cdot N^*)$		Correlation Coefficient
		α (%)	β (%/cycle)	
Volcanic Rocks	PCT	0.301	0.006	0.621
	PPB	4.801	0.077	0.999
Metamorphic Rocks	KSch	1.018	0.012	0.970
	CSch	0.607	0.620	0.934
	NDSch	0.728	0.008	0.959
Sedimentary Rocks	PKSS1	4.465	0.189	0.930
	PKSS2	1.828	0.021	0.999
	KKST	3.055	0.040	0.999
	PWSS	2.140	0.029	0.999
	PWST	0.315	0.770	0.935
	NPST	0.640	0.007	0.763
	KkSS	3.402	0.047	0.999
MSMD	2.902	0.037	0.999	

Table 4.5 Proposed classification system for durability of intact rocks.

Description	Δ SDI (%)
Very high durability	< 1
High durability	1-3
Moderate durability	3-7
Low durability	7-15
Very low durability	> 15

4.3 Simulation of rock degradation

4.3.1 Simulation methods

The objective of the simulation of rock degradation is to experimentally assess the degrees of rock weathering as it is subjected to the cyclic changes of temperatures and humidity. Fifteen rock cylindrical disks and five kilograms of rock fragments (1.5-3.0 inches) were prepared from thirteen rock types (Figures 4.8 and 4.9). The specimens were placed in an oven at 105 Celsius for 12 hours and rapidly submerged in a tank of water at 25 Celsius for 12 hours (Figure 4.10). This rapid heating and cooling process was repeated 140 times (140 days). After the rapid heating and cooling cycles, slake durability tests were performed on the rock fragment specimens. Weight loss, specific gravity, water absorption, and dynamic wave velocity of the specimens were monitored at every 14 cycles. The test procedures follow the ASTM (C127) standard practice. Point load strength test was performed at 1, 70 and 140 cycles. The test method follows the ASTM (D5731) standard practice. At every 28 cycles, tilt testing was performed on three pairs of cylindrical disk specimens with smooth saw-cut surface to determine the change of the basic friction angle. These physical and mechanical property parameters are used as indicators of rock degradation. Correlation between these parameters will also be carried out in an attempt to determine the mathematical relationship between the joint shear strengths and the rock degradation.

4.3.2 Slake durability index

The slake durability index test is performed on fragments of thirteen rock specimens after subjecting them to 140 cycles of heating and cooling.



Figure 4.8 Example of rock fragments of Phra Wihan sandstone prepared for slake durability index test.

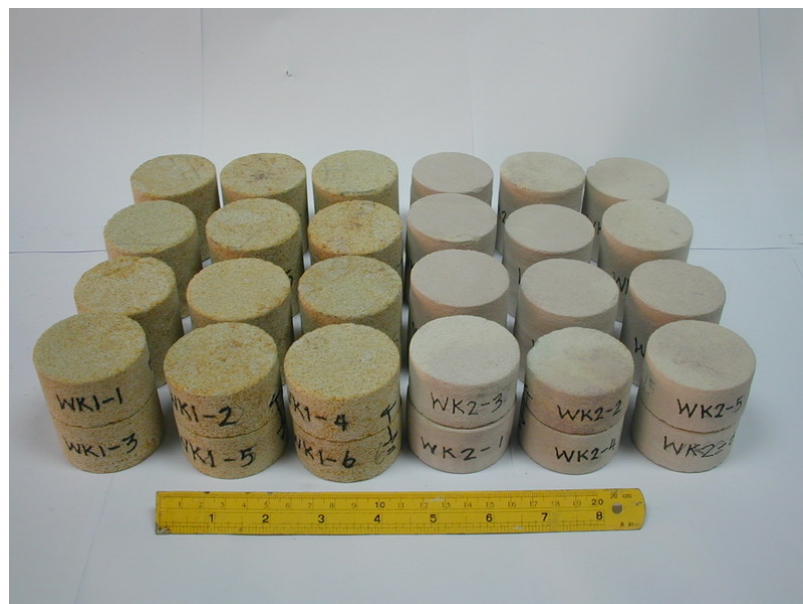


Figure 4.9 Example of rock disks of Phra Wihan sandstone and siltstone prepared for tilt tests and point load strength index tests.



Figure 4.10 Specimens of rock disks and fragments submerged under water tank at 25°C.

The SDI test procedure and data reduction were similar to that of the standard practice (wet-condition). Table 4.6 gives the results of SDI tests for all rock types. Figures 4.11 through 4.13 compare the SDI values of the sedimentary rocks, metamorphic rocks and volcanic rocks obtained before and after heating and cooling simulation. The durability of rock specimens that are subjected to 140 heating and cooling cycles are mostly lower than those not subjected to the heating and cooling cycles. This suggests that the 140 heating-cooling cycles have degraded the rock specimens. The reduction rate of SDI for these specimens is higher than that of the specimens not subjected to the heating-cooling cycles.

4.3.3 Point load strength index

The point load strength index test was performed on all rock types, using three sets of specimens. The first set is prepared from the samples as collected from the field site. The second set is from those subjected to 70 cycles of heating and cooling. The last set is from those subjected to 140 cycles of heating and cooling. The point load test is performed by using compression machine model SBEL PLT-75 which is capable of applying axial load up to 350 kN (Figure 4.14). Table 4.7 gives the results. The strength of Pichit crystal tuff (PCT), Phu Kradung red sandstone (PKSS2), Kaeng Krachan micaceous siltstone (KKST), Phra Wihan siltstone (PWST), and Nam Duk siltstone (NDST) decrease with increasing heating and cooling cycles. For the other rock types, the trend of the strength index is inconclusive. This is probably due to the intrinsic variability of the rock specimens.

Table 4.6 Results of SDI test for all rock types obtained after 140 cycles of heating and cooling simulation.

Rock Types	Code	Slake Durability Index, I_d (%)					
		Number of Cycles, N					
		1	2	3	4	5	6
Volcanic Rocks	PCT	98.71	98.00	97.39	96.87	96.63	96.37
	PPB	93.95	83.98	78.41	74.50	71.48	70.05
Metamorphic Rocks	KSch	98.41	96.81	95.67	94.62	93.86	93.45
	CSch	70.21	60.76	55.29	51.61	49.55	48.33
	NDSch	96.93	95.71	94.08	92.52	91.29	90.13
Sedimentary Rocks	PKSS1	81.95	73.56	65.28	59.10	54.83	50.03
	PKSS2	98.37	97.30	96.09	94.90	94.07	93.39
	KKST	94.86	89.77	85.51	81.44	78.11	75.18
	PWSS	96.08	93.75	91.78	90.66	89.51	88.49
	PWST	N/A	N/A	N/A	N/A	N/A	N/A
	NPST	97.42	96.27	95.52	94.76	94.22	93.81
	KkSS	89.02	76.63	70.66	66.52	61.39	58.66
	MSMD	N/A	N/A	N/A	N/A	N/A	N/A

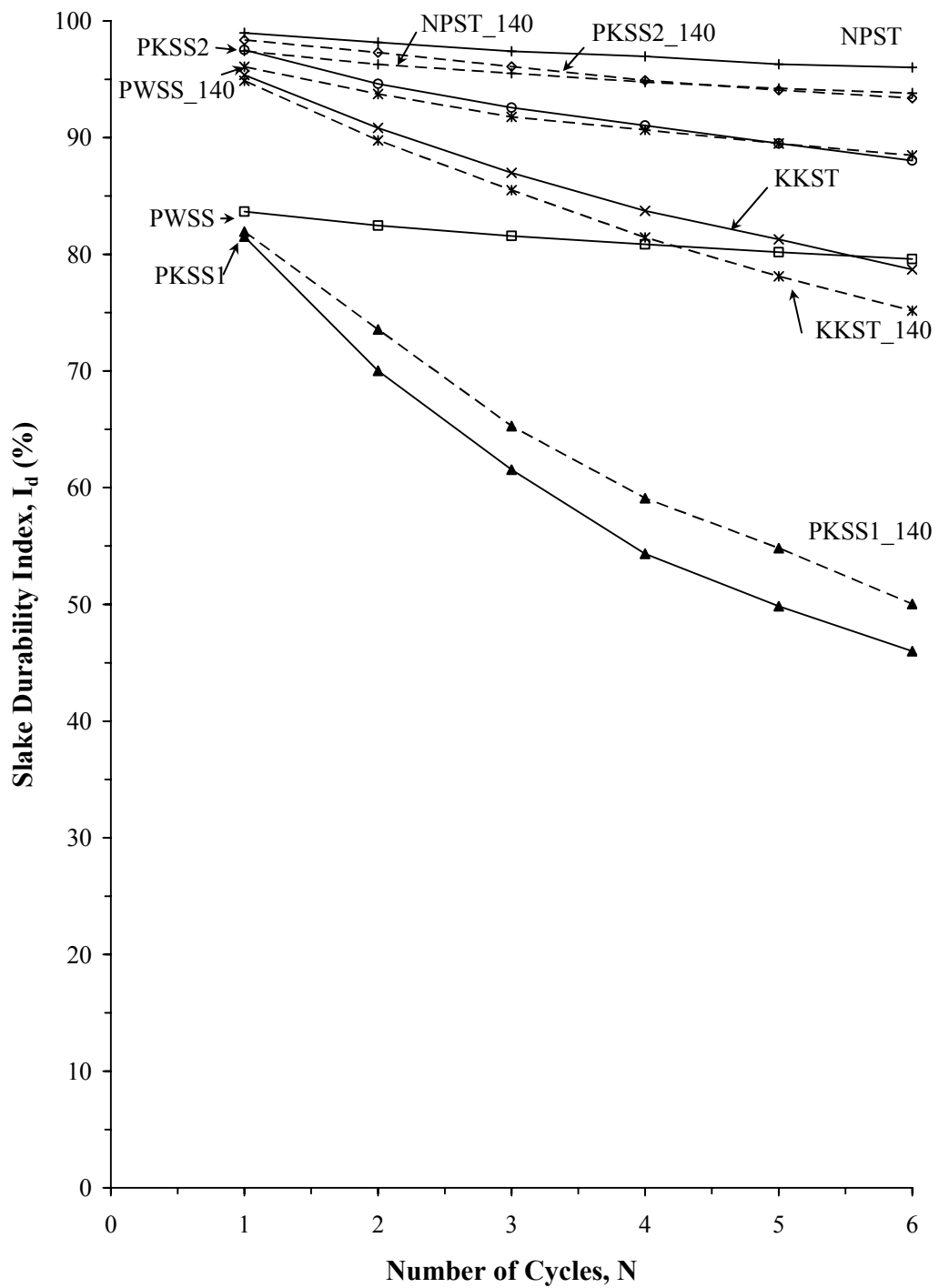


Figure 4.11 Comparison of SDI values of sedimentary rocks before (solid lines) and after (dash lines) 140 heating-cooling cycles.

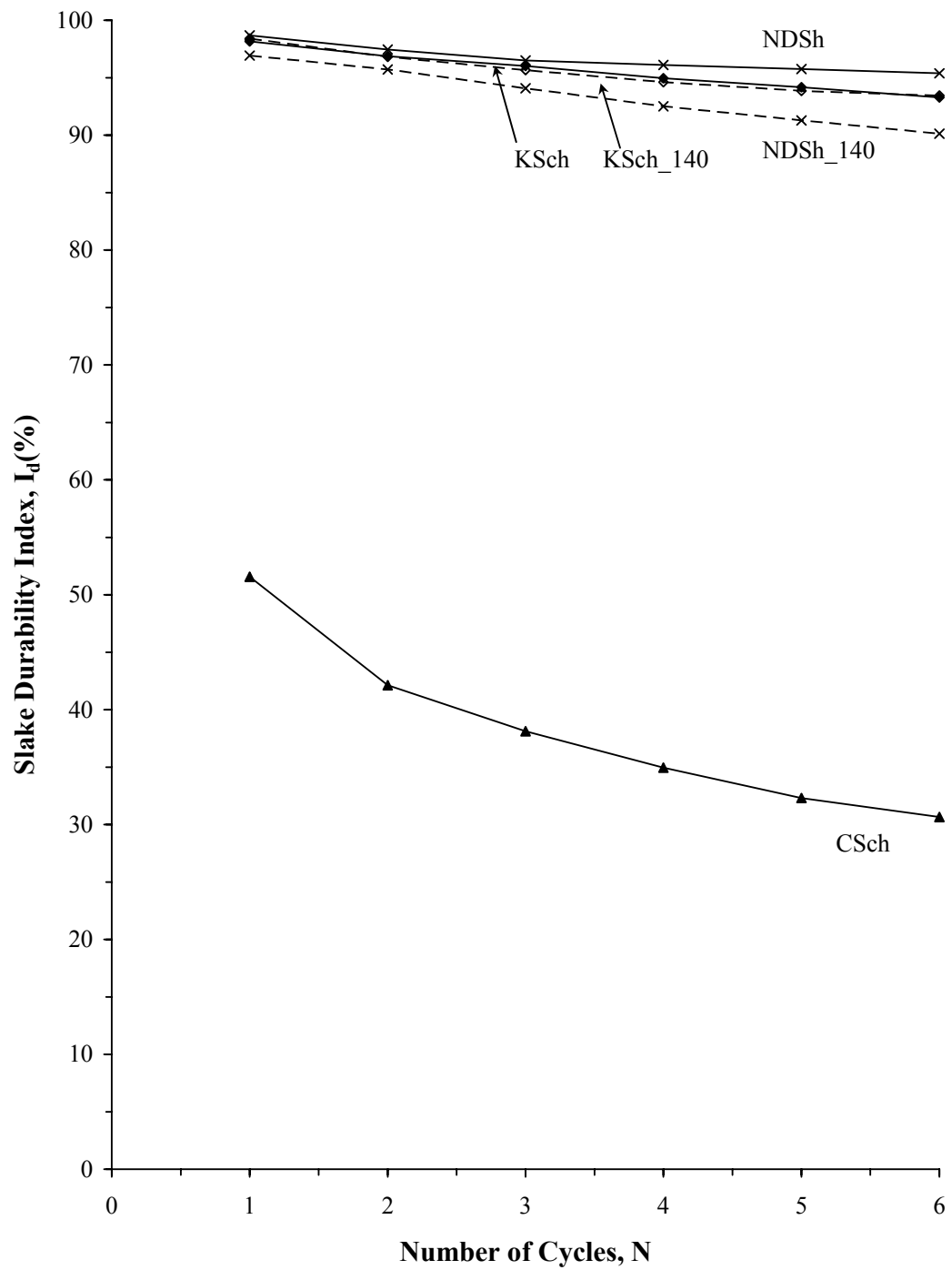


Figure 4.12 Comparison of SDI values of metamorphic rocks before (solid lines) and after (dash line) 140 heating-cooling cycles.

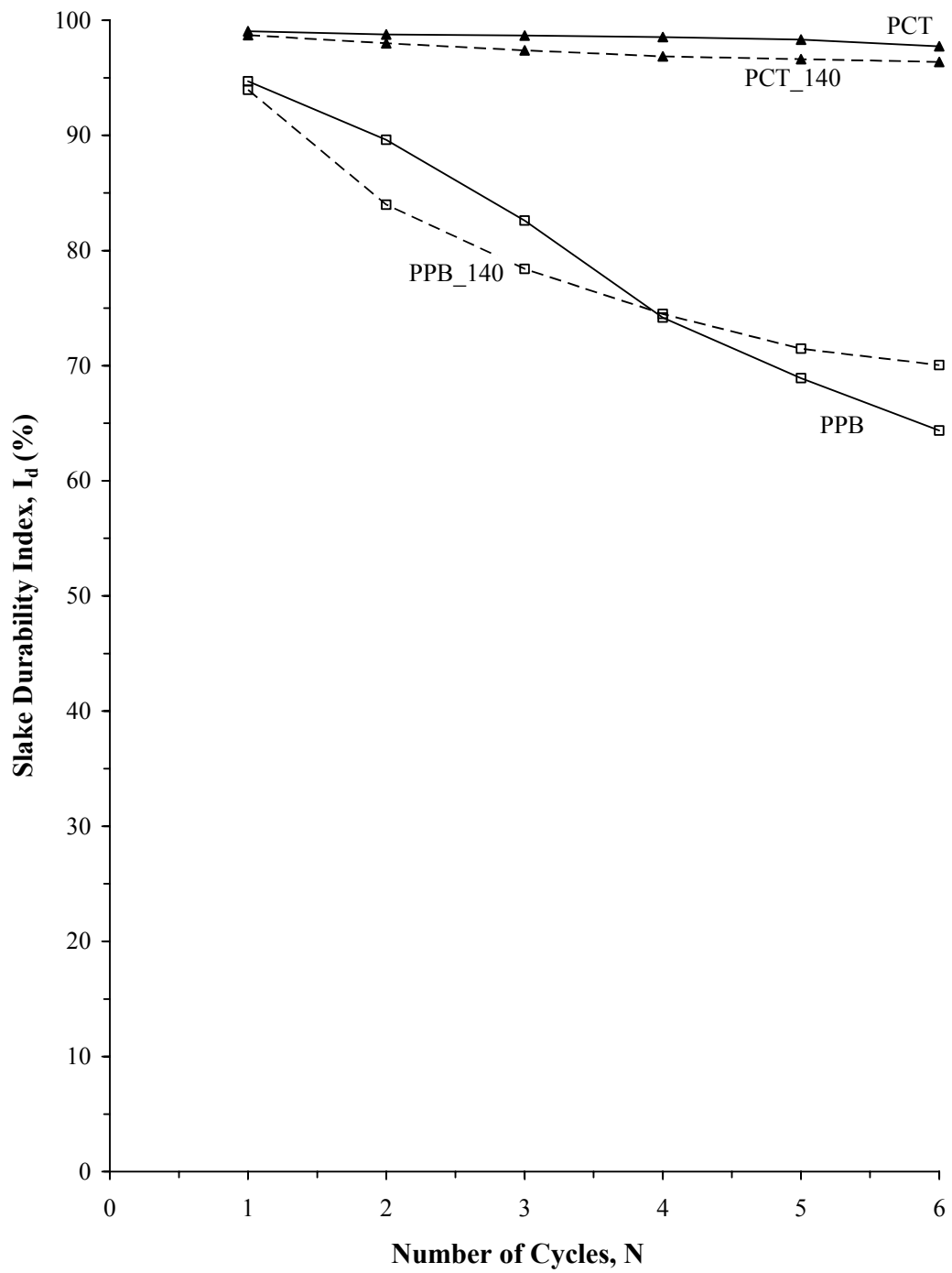


Figure 4.13 Comparison of SDI values of volcanic rocks before (solid lines) and after (dash lines) 140 heating-cooling cycles.

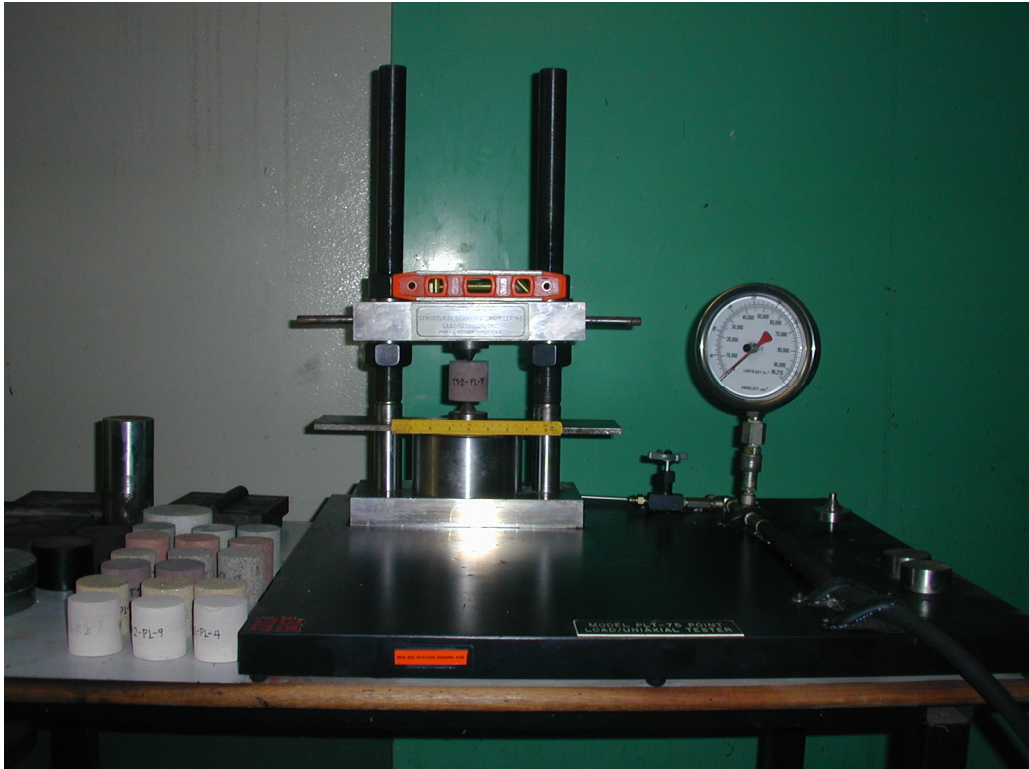


Figure 4.14 Test arrangement and apparatus for point load strength index test.

Table 4.7 Results of point load strength index test.

Rock Types	Code	Point Load Strength Index, $I_{s(50)}$ (MPa)		
		Cycle 1	Cycle 70	Cycle 140
Volcanic Rock	PCT	5.2	3.8	2.0
	PPB	3.5	N/A	N/A
Metamorphic Rock	KSch	2.7	2.1	4.0
	CSch	N/A	N/A	N/A
	NDSch	N/A	N/A	N/A
Sedimentary Rock	PKSS1	1.6	1.4	2.0
	PKSS2	6.8	6.4	5.1
	KKST	1.4	1.2	1.2
	PWSS	2.3	2.2	2.4
	PWST	1.0	0	N/A
	NPST	3.0	1.3	1.2
	KkSS	1.0	1.1	1.0
	MSMD	N/A	N/A	N/A

4.3.4 Weight loss monitoring

The results show that Phra Wihan siltstone (PWST), Chonburi quartz mica schist (CSch), and Pichit pumice breccia (PPB) have a higher rate of weight loss than the other rocks (Figure 4.15). This is probably due to the high percentage of kaolinite in the rock matrix. Nam Duk slaty-shale (NDSH) also has a high rate of weight loss under this simulation because the high amount of mica contents makes the rock disintegrate easily. Its fragments therefore become extremely brittle and weaker when they are subjected to rapid changing of temperatures. Pichit crystal tuff (PCT) and Kanchanaburi green schist (KSch) have the lowest rate of weight loss because those are crystallized forming rocks. This is the effect of chemical weathering rather than physical weathering. The other rocks do not show much weight loss under this simulation because they are composed of quartz grains and have grain contact texture.

4.3.5 Basic friction angles (Tilt test)

For all rock types the basic friction angles rapidly decrease during the first 28 cycles. After 28 cycles the decreasing rate becomes smaller (Figure 4.16). Variation of the friction angle with number of cycles can be best represented by a power equation. Table 4.8 lists the empirical constants in the power equation for each rock type.

4.3.6 Dynamic wave velocity

The test specimens have approximate length-to-diameter ratio of 0.5 (six specimens) and 1.0 (two specimens). There are eight specimens for each rock type. The dynamic wave velocity is measured using Sonic Viewer 170 Model 5228 (Figure

4.17). The detailed results are shown in Appendix A. Phra Wihan siltstone (PWST) shows that the P-wave velocity decreases with increasing numbers of heating and cooling cycles. This is probably due to the high percentage of weight loss in rock specimen, and therefore decreasing its density. Phu Kradung sandstone (PKSS), Kaeng Krachan micaceous siltstone (KKST), and Khok Kruat sandstone (KkSS) have a lower rate of wave velocity decrease. The wave velocity change for Pichit crystal tuff (PCT) and Kanchanaburi green schist (KSch) after 140 cycles of heating and cooling can not be detected by this testing. This is probably because the measurement technique of the P-wave velocity (both apparatus and method) is not sufficiently sensitive to detect the change of their rock characteristics.

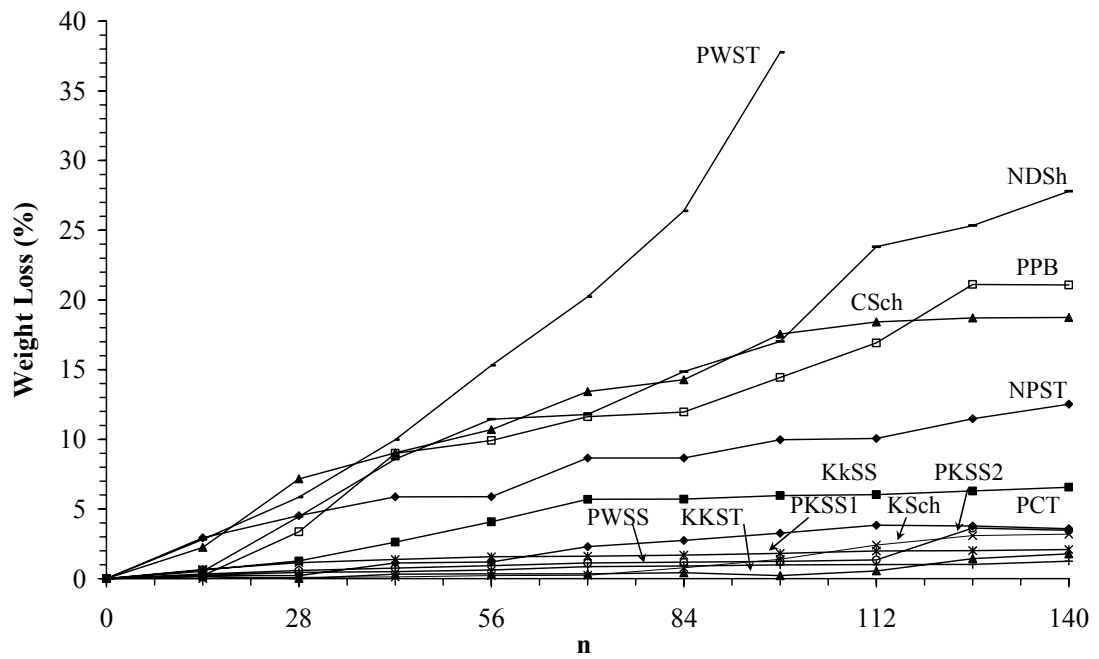


Figure 4.15 Weigh loss of rock specimens monitored every 14 cycles of heating and cooling cycles.

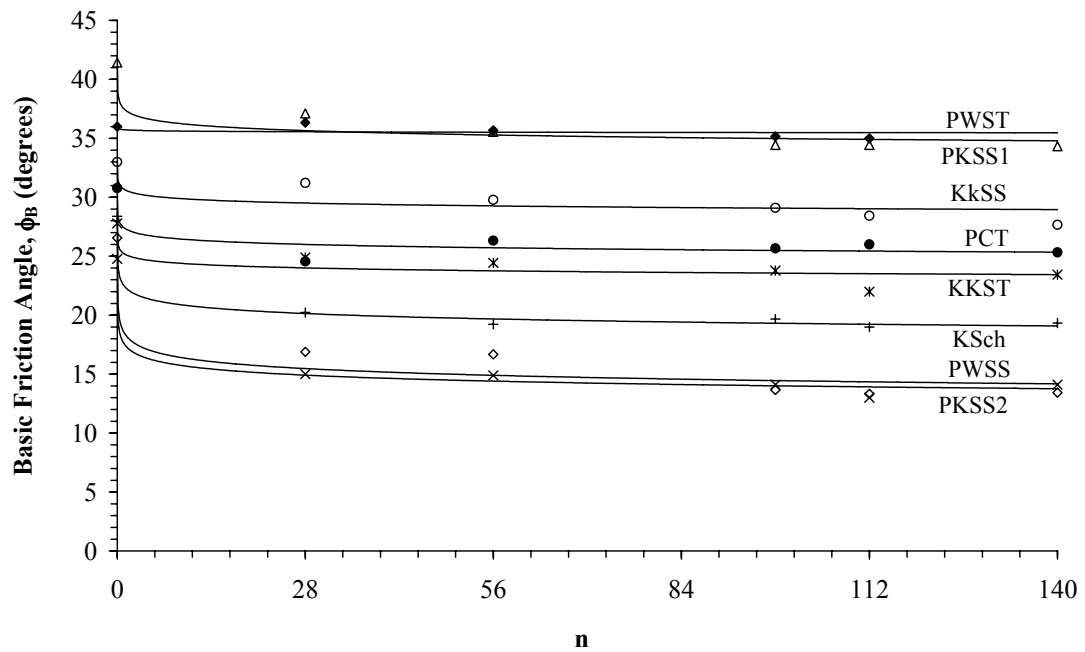


Figure 4.16 Basic friction angles of smooth (saw-cut) surface of rock specimens tested after various heating-cooling cycles (n)

Table 4.8 Empirical constants form power equation relating ϕ_B and n

Rock Types		$\phi_B = C \cdot n^{-\lambda}$		Correlation Coefficient
		C	λ	
Volcanic Rocks	PCT	27.42	0.016	0.928
Metamorphic Rocks	KSch	22.52	0.033	0.995
Sedimentary Rocks	PKSS1	37.51	0.015	0.956
	PKSS2	17.61	0.050	0.988
	KKST	25.23	0.015	0.883
	PWSS	18.55	0.055	0.953
	PWST	35.73	0.002	0.469
	KkSS	30.89	0.010	0.872

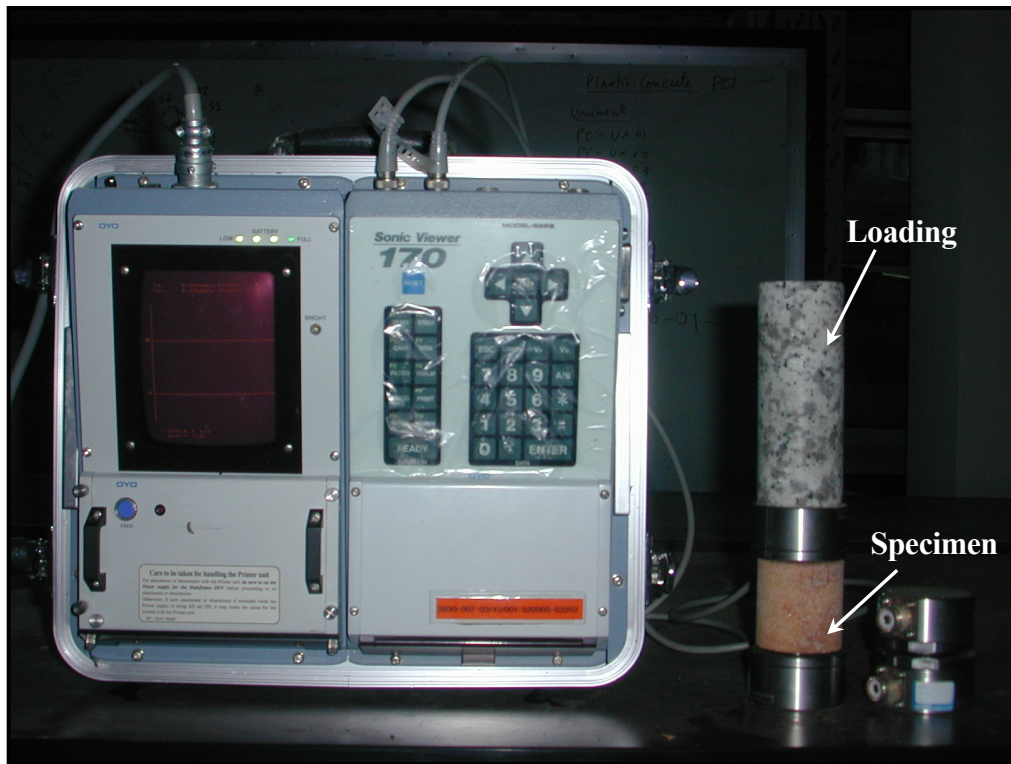


Figure 4.17 Sonic Viewer 170 Model 5228 used to measure P-wave velocity.

CHAPTER V

CORRELATION BETWEEN ROCK DURABILITY AND JOINT SHEAR STRENGTH

5.1 Introduction

The objective of this chapter is to correlate the weathering parameters (Δ SDI), rock strength (I_s) with the joint shear strength. Barton's joint shear strength is adopted here as it allows incorporating the rock strength parameter. A concept of heat energy absorption is used to compare the degradation simulation with the actual in-situ condition, in terms of time. The degradation of the joint shear strength can therefore be predicted as a function of time.

5.2 Relationship between rock strength and Δ SDI

The Δ SDI values obtained from both before and after subjecting to the degradation simulations are used to correlate with the corresponding point load strength index. Table 5.1 compares the strength index values obtained from the two sets of specimens of all rock types with the corresponding Δ SDI values. The point load strength results from both sets are plotted as a function of Δ SDI at $N^* = 6$ (or $N = 1$ - the first SDI test cycle) as shown in Figure 5.1. Variation of point load strength index with Δ SDI can be best represented by a power equation:

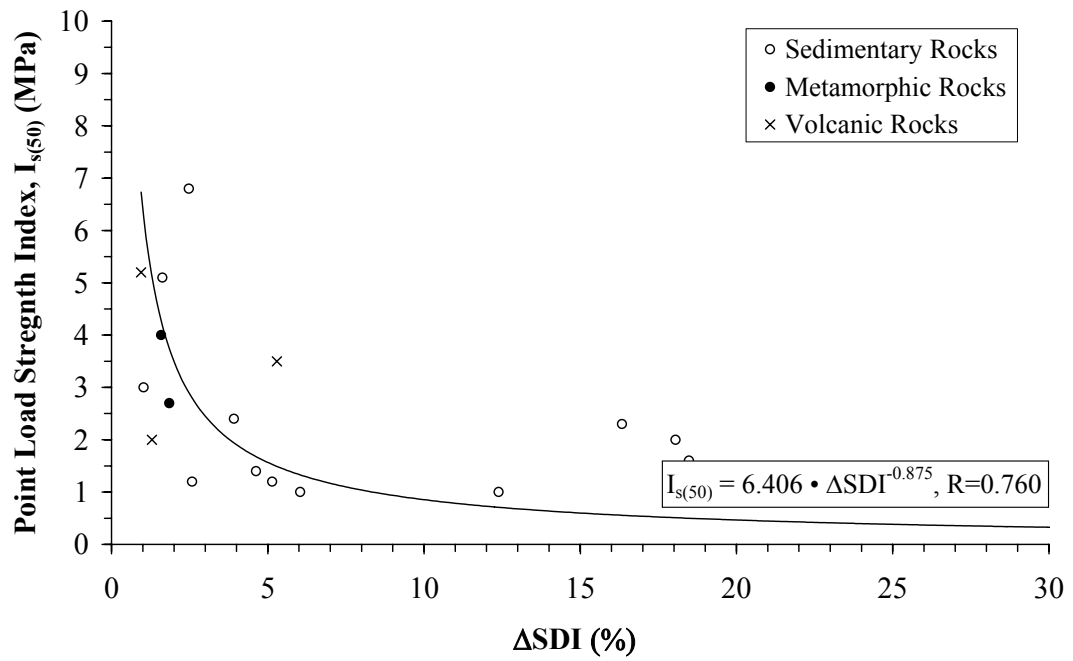


Figure 5.1 Point load strength index as a function of Δ SDI for all rock types tested.

Table 5.1 Point load strength index results and their corresponding Δ SDI at $N^* = 6$
(or $N=1$).

Rock Types	Code	Without heating-cooling cycle		With 140 cycles of heating-cooling	
		$I_{s(50)}$ (MPa)	Δ SDI (%)	$I_{s(50)}$ (MPa)	Δ SDI (%)
Volcanic Rocks	PCT	5.2	0.94	2.0	1.29
	PPB	3.5	5.29	-	-
Metamorphic Rocks	KSch	2.7	1.85	4.0	1.59
Sedimentary Rocks	PKSS1	1.6	18.48	2.0	18.05
	PKSS2	6.8	2.48	5.1	1.63
	KKST	1.4	4.63	1.2	5.14
	PWSS	2.3	16.33	2.4	3.92
	PWST	1.0	6.60	-	-
	KkSS	1.0	6.04	1.0	12.39
	NPST	1.02	3.00	1.2	2.58
	MSMD	1.0	48.82	-	-

$$I_{s(50)} = \delta \times \Delta SDI^{-\eta} \quad (5.1)$$

where $I_{s(50)}$ is point load strength index (MPa), δ is an empirical constant, and η is exponent of ΔSDI . Though widely scatted data are obtained, a general trend of the results shows that point load strength index decreases with increasing ΔSDI . The above equation suggests that if one can obtain or predict ΔSDI of the rock, the point load strength index can be estimated.

5.3 Correlation between simulation and actual in-situ condition

An attempt is made here to correlate the simulation cycles with the actual in-situ condition. An easy and relatively conservative approach is to use the concept of energy adsorption. The amount of heat energy that has been applied to the rock specimens during the degradation simulation is compared with that actually occurs in the field. Figure 5.2 shows the temperature change imposed on the rock during one cycle of degradation simulation. The Thai Meteorological Department (2004) has monitored the temperature change during the days throughout the year in the area of Nakhon Ratchsima province. Figure 5.3 shows the daily temperature changes averaged for the year 2004. The heat energy absorbed by the rock can be calculated by using an equation (Richard et al., 1998),

$$Q = \sum_{i=1}^n (m \cdot C_p \cdot \Delta T_i \cdot \Delta t_i) \quad (5.2)$$

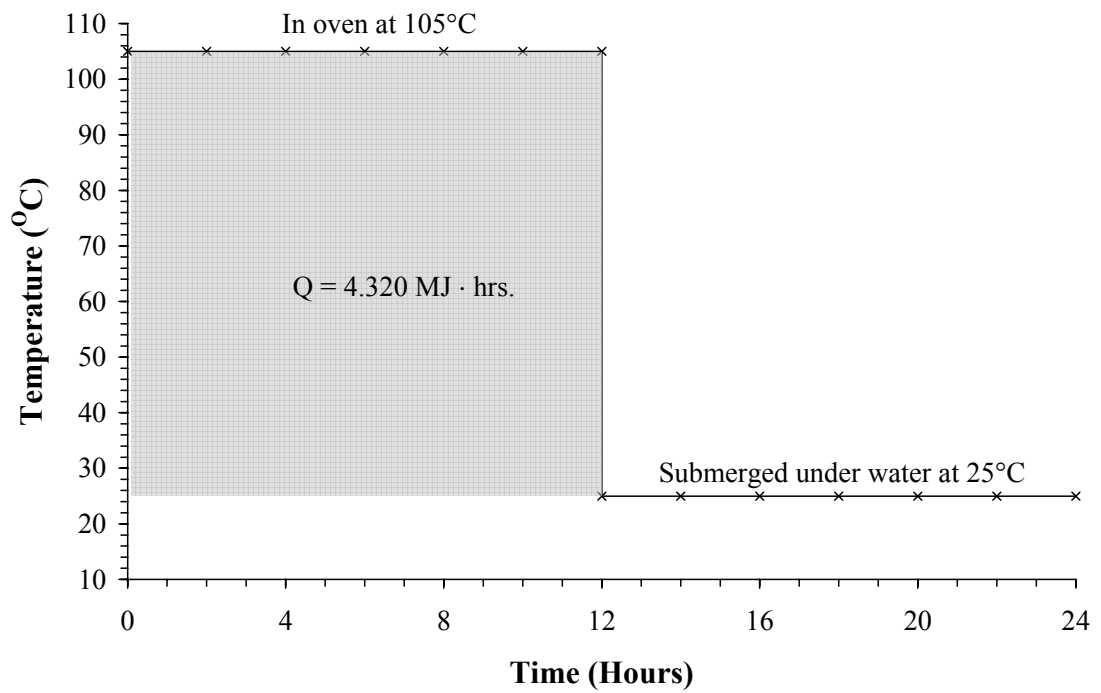


Figure 5.2 Variation of temperatures for one cycle of heating and cooling simulation in laboratory.

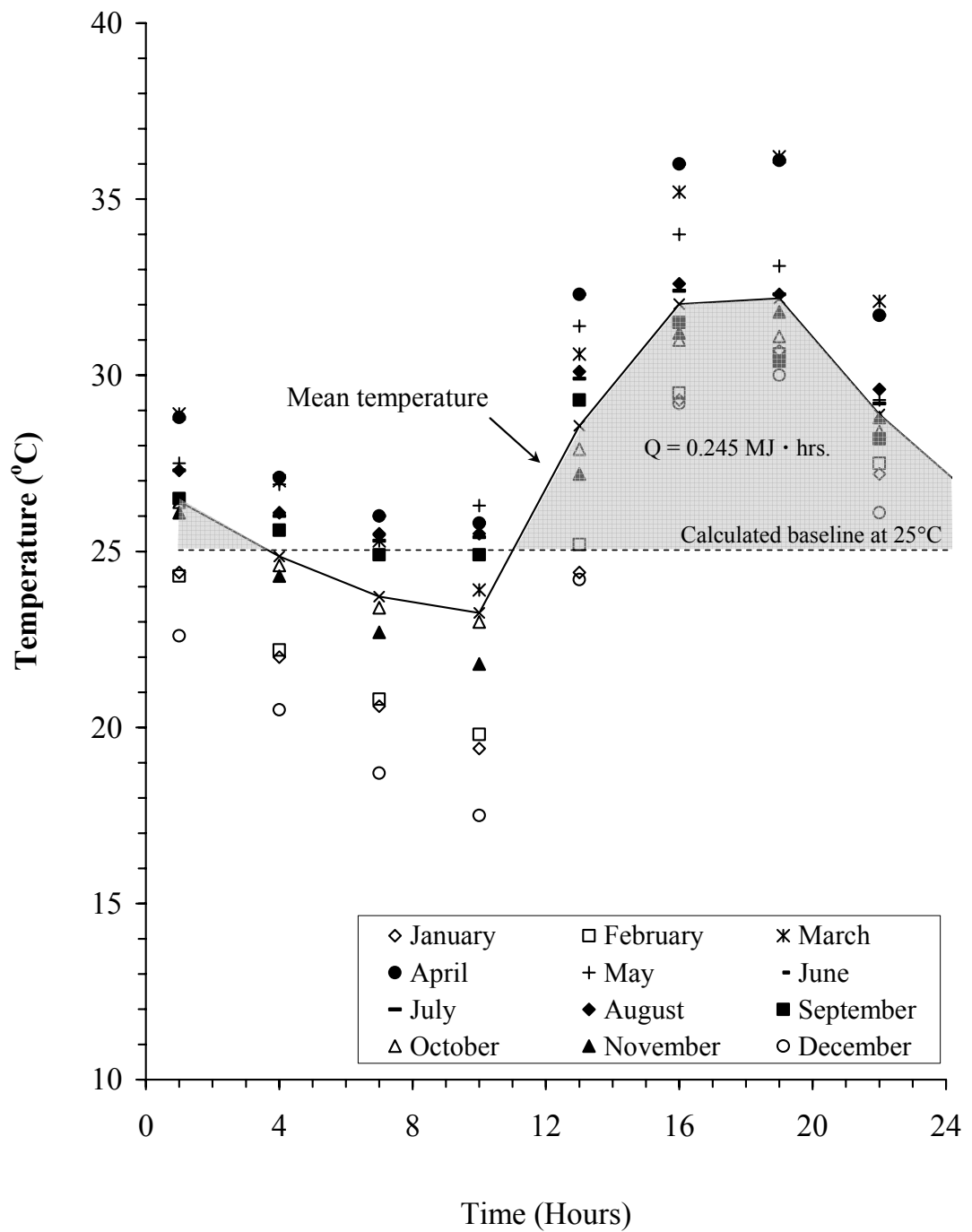


Figure 5.3 Variation of daily temperatures in the Nakhon Ratchasima province (Thai Meteorological Department, 2004). The line indicates average daily temperature change in the year 2004.

where Q is the absorbed energy of rock specimen (kJ), m is the weight of rock specimen (kg), C_p is the specific heat capacity (kJ/kg·K), ΔT_i is the temperature change in Kelvin, t_i is time interval of energy absorption (hours) and n is number of hours. The coefficient of heat capacity of most rocks varies between 0.6 and 1.2 kJ/kg·K with an average value of 0.90 kJ/kg·K (Figure 5.4).

From equation (5.2), the absorbed energy during heating simulation of most rocks is estimated as 4.320 MJ·hr (where $m = 5$ kg, $C_p = 0.90$ kJ/kg·K, $\Delta T = 80$ K, $t = 12$ hrs).

For the in-situ condition, the absorbed energy in one day is estimated as 0.245 MJ·hr (where $m = 5$ kg, $C_p = 0.90$ kJ/kg·K, ΔT is temperature change in each one hour as shown in Figure 5.2, $t = 16$ hrs.). Therefore, one simulation cycle of heating and cooling approximately equals to 18 days under in-situ condition ($\frac{4.320}{0.245} = 17.84$).

Therefore, n can be correlated with time.

$$n \approx 18 \text{ days} \quad (5.3)$$

where n is the cycle of heating and cooling simulation. The above correlation, equation (5.3), is considered extremely conservative because the temperature changes for the simulation are much more abrupt than those actually occurring under in-situ conditions. Since the applied energy in one day during the simulation is the same as that used in the SDI test, N^* can be related to time, as follows.

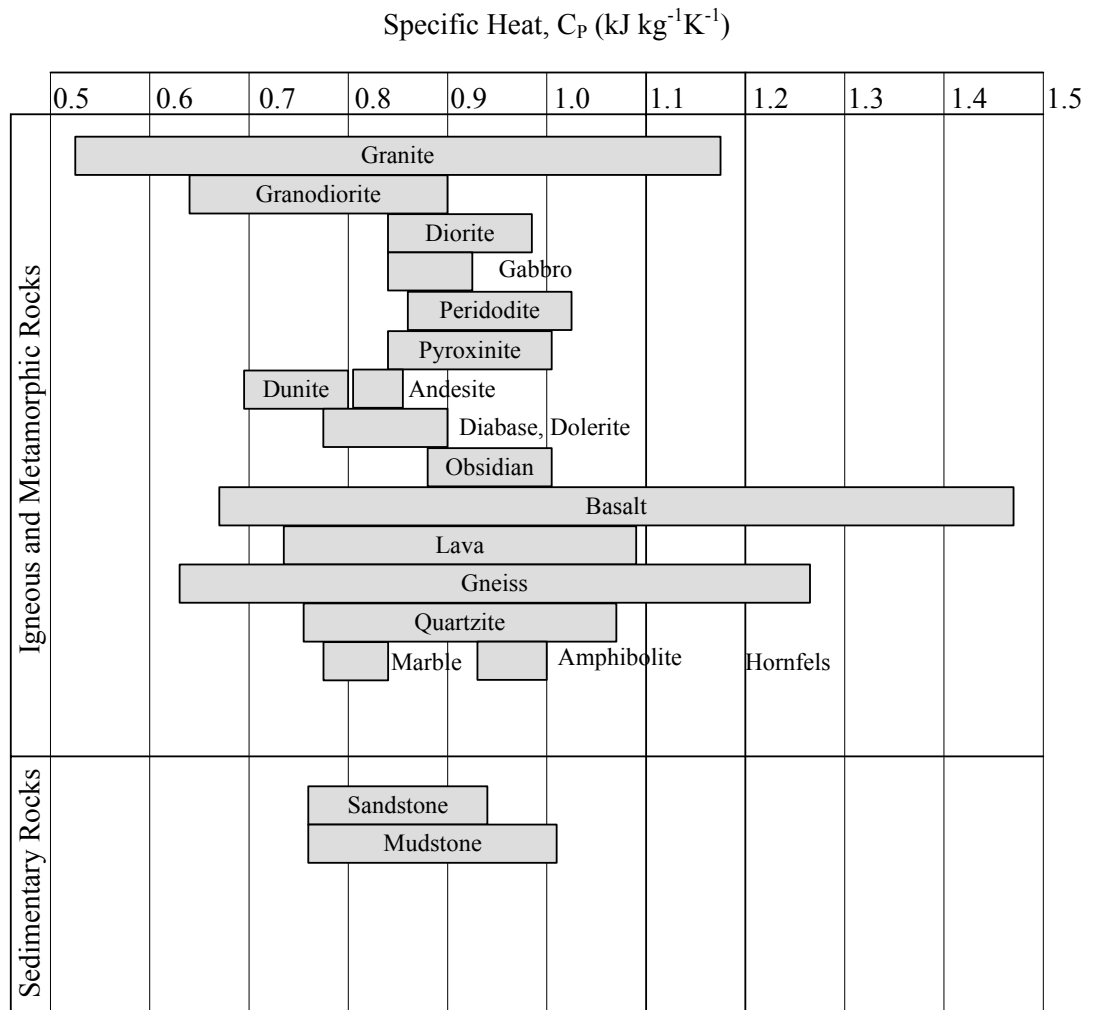


Figure 5.4 Comparison of coefficients of heat capacity of various rock types (Modified from Department Angewandte Geowissenschaften und Geophysik, 2006).

$$N^* \approx 18 \text{ days} \quad (5.4)$$

From equation (5.4) Δ SDI for each rock type can be plotted as a function of time (in days and years) in Figure 5.5.

5.4 Modified Barton's joint shear strength criterion

From Figures 5.1 and 5.5, the point load strength index of the rock can be correlated with time. The strength index can therefore be correlated to the uniaxial compressive strength of the rock by using the following relation.

$$\sigma_c = a \cdot I_{s(50)} \quad (5.5)$$

where σ_c is the uniaxial compressive strength and a is the multiplier factor. Numerous researches have proposed many criteria to define this multiplier factor. Different rock types have different “ a ” values. ASTM (D5731) standard practice also provides a guideline to define this value for different rock types. After σ_c value is estimated from $I_{s(50)}$, the rock strength can be correlated with time (Figures 5.1 and 5.2).

A joint shear strength criterion that is capable of incorporating rock strength (σ_c) has been proposed by Barton (1973):

$$\tau = \sigma_n \tan \left[\phi_B + JRC \cdot \log \left(\frac{\sigma_c}{\sigma_n} \right) \right] \quad (5.6)$$

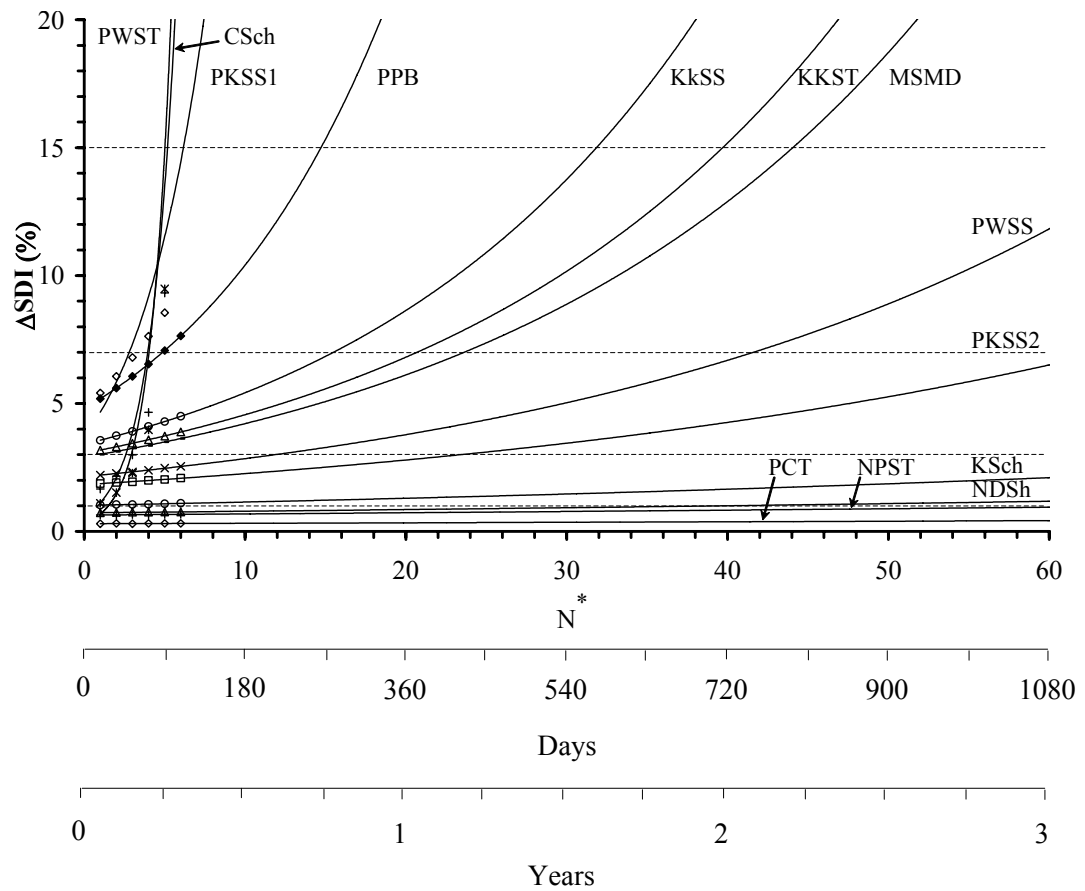


Figure 5.5 ΔSDI as a function of time under in-situ condition.

where σ_n is the normal stress, ϕ_B is the basic friction angle, JRC is the joint roughness coefficient (ranging from 0 to 20), and σ_c is the joint wall compressive strength or uniaxial compressive strength of rock.

The rock compressive strength in the Barton criterion can be defined in terms of Δ SDI, and number of days (D)

$$\sigma_c = \delta \cdot a \cdot [\alpha \cdot \exp(\beta \cdot D/18)]^{-\eta} \quad (5.7)$$

The above equation is obtained by substituting equation in Table 4.4 and equation (5.1) into equation (5.5). The Barton criterion can be rewritten as

$$\tau = \sigma_n \tan \left\{ \phi_B + \text{JRC} \cdot \log \left[\frac{\delta a \times \left(\alpha \times \exp \left(\frac{\beta D}{18} \right) \right)^{-\eta}}{\sigma_n} \right] \right\} \quad (5.8)$$

where a is multiplied factor from ASTM (5731) standard practice, D is the number of days, α and β are empirical constants for Δ SDI-N* curve. δ and η are empirical constants for the I_s - Δ SDI curve. The σ_c value in equation (5.7) must always be positive (≥ 0). Therefore the lower bound of equation (5.8) for the joint shear strength value is

$$\tau = \sigma_n \cdot \tan(\phi_B) \quad (5.9)$$

Strictly speaking the weathering or degradation of rock strength, as predicted here,

will affect only the roughness and wall strength of the joint. The equation (5.8) implies that as time goes by the joint shear strength will approach that of smooth surfaces which is controlled by its basic friction angle.

Table 5.2 gives parameters used in equation (5.8) to predict the joint shear strengths as a function of time for the thirteen rock types tested here. The basic friction angle for each rock type is obtained from the results of tilt testing. The JRC values are from field observations during sample collection.

Figures 5.6 through 5.8 plot the normalized joint shear strength (τ/σ_n) predicted as a function of time for the next 10 years, for volcanic, metamorphic and sedimentary rock groups, respectively. The shear strength of Pichit pumice breccia (PPB) degrades quickly and reaches the lower bound at about 3 years. At which point the predicted $\sigma_c = \sigma_n$ and $\tau_n/\sigma_n = \tan(\phi_B) = 0.554$ (Figure 5.6). The joint shear strength of Pichit crystal tuff (PCT) reduces by about 10% for the next 10 years. This tuff was classified as very high durability rock (in Chapter 4).

The joint shear strengths of Nam Duk slaty shale (NDSH) and Kanchanaburi green schist (KSch) decrease slightly for the next 10 years (Figure 5.7). The two rocks were classified by their Δ SDI values as high durability. For Chonburi quartz mica schist (CSch), the shear strength rapidly decreases and reaches the lower bound within six months. The schist is classified by Δ SDI as very low durability.

The shear strengths of the sedimentary rock specimens decrease with time at various rates. Phra Wihan siltstone (PWST), Phu Kradung white sandstone (PKSS1) and Maha Sarakham mudstone (MSMD) show relatively high joint shear strengths under the condition as collected from the field. Their strengths decrease with time and quickly reach the lower bound of the shear strengths which is controlled by their

Table 5.2 Parameters used to predict the joint shear strength of each rock type.

Rock Types	ϕ_B (degrees)	JRC	α	β	a
PCT	25	13	0.301	0.006	20 ^{**}
PPB	29	11	4.801	0.077	20 ^{**}
KSch	19	7	1.018	0.012	20 ^{**}
CSch	20	5	0.607	0.62	13 ^{**}
NDSch	27	2	0.728	0.008	13 ^{**}
PKSS1	34	7	4.465	0.189	11 [*]
PKSS2	14	7	1.828	0.021	11 [*]
KKST	23	7	3.055	0.04	13 ^{**}
PWSS	13	9	2.14	0.029	31 [*]
PWST	34	11	0.315	0.77	13 ^{**}
NPST	29	7	0.64	0.007	20 ^{**}
KkSS	28	7	3.402	0.047	13 ^{**}
MSMD	31	9	2.902	0.037	20 ^{**}

*Kemthong (2006). **Tsiabaos and Sabatakakis (2004).

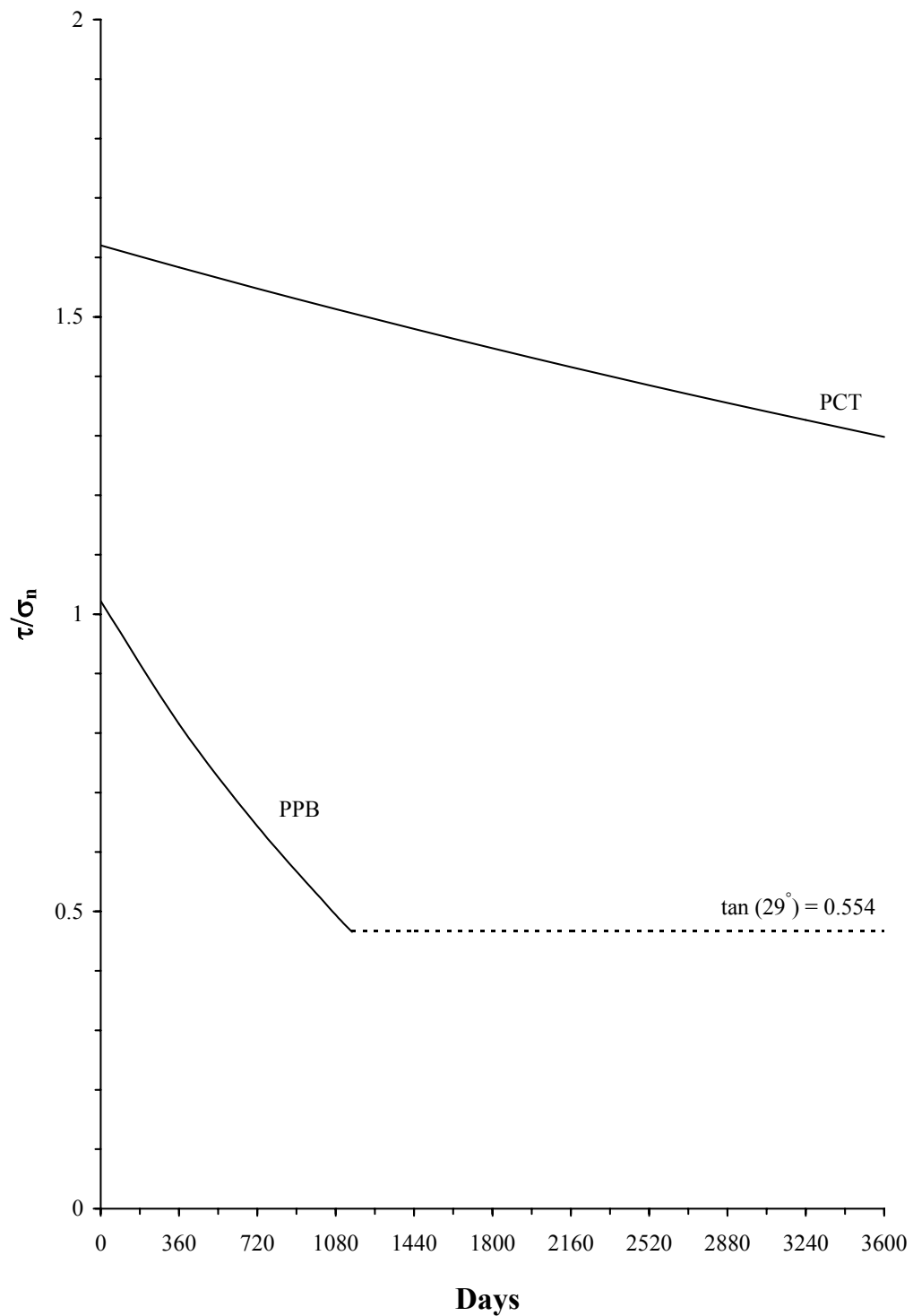


Figure 5.6 Normalized joint shear strength prediction for volcanic rocks. Dashed lines indicate the lower bound of normalized joint shear strength which is defined by the tangent of basic friction angle of each rock type.

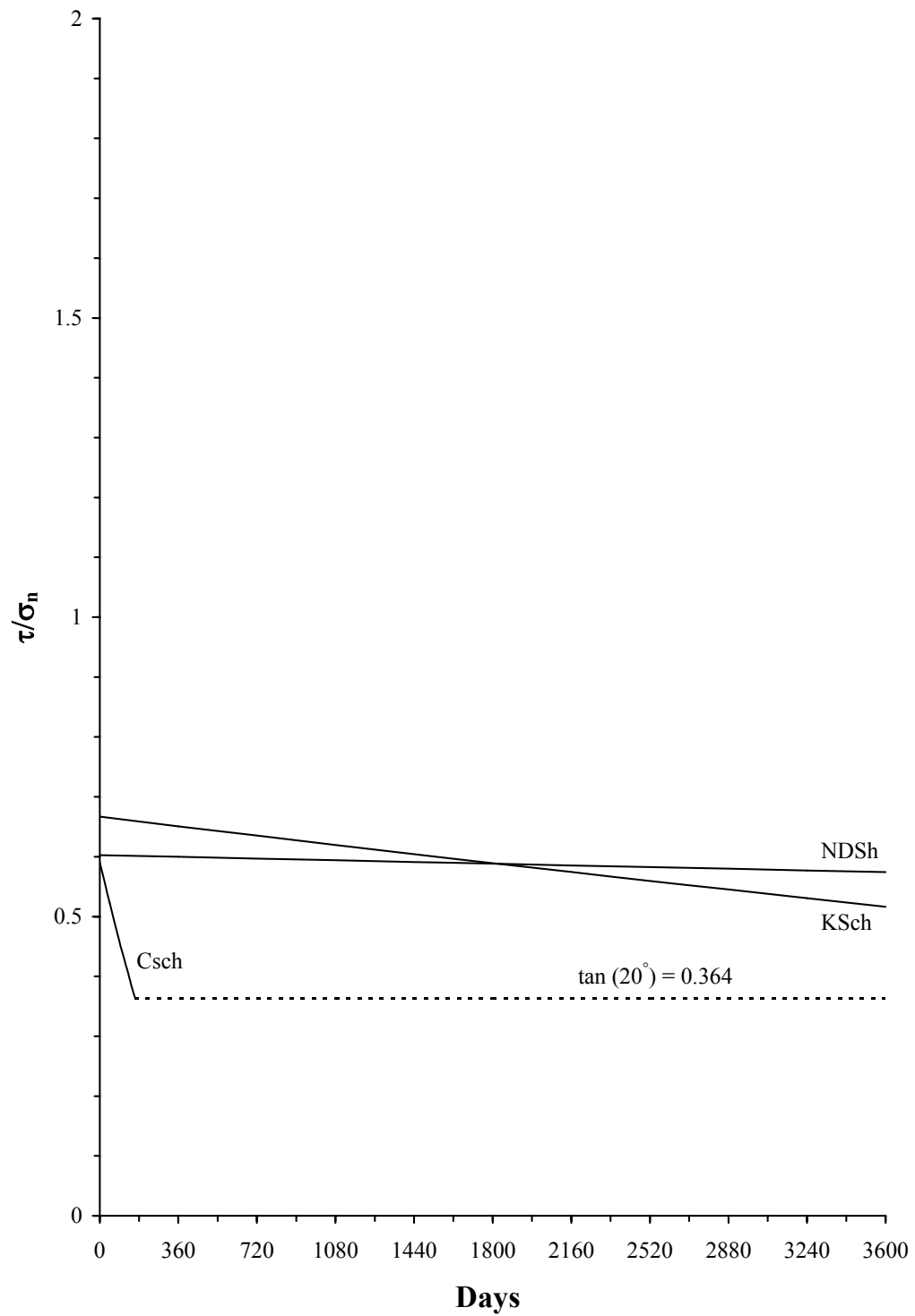


Figure 5.7 Normalized joint shear strength prediction for metamorphic rocks. Dashed lines indicate the lower bound of normalized joint shear strength which is defined by the tangent of basic friction angle of each rock type.

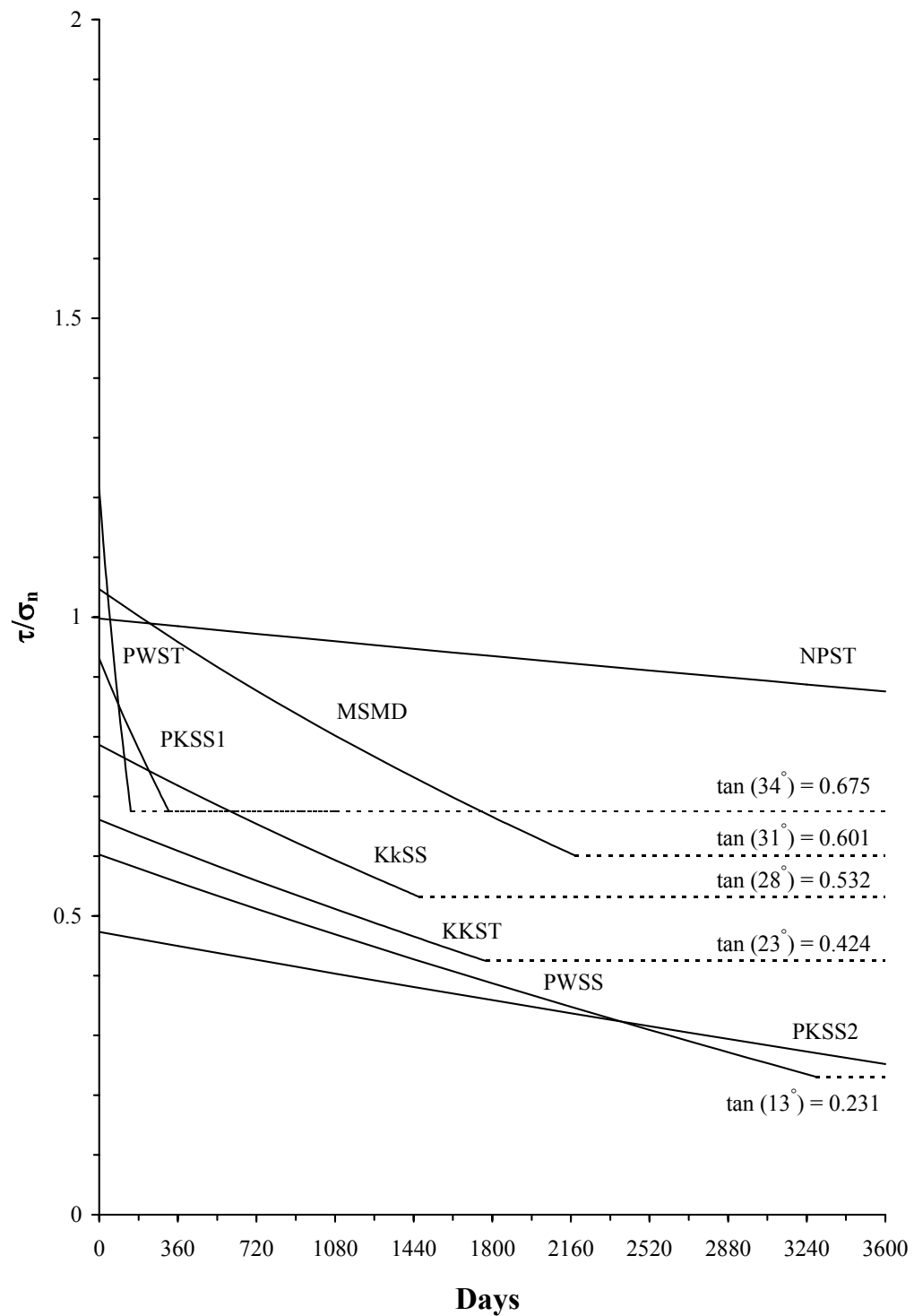


Figure 5.8 Normalized joint shear strength prediction for sedimentary rocks. Dashed lines indicate the lower bound of normalized joint shear strength which is defined by the tangent of basic friction angle of each rock type.

basic friction angles. The rest of the sedimentary rocks tested here show similar rate of joint shear strength reduction with time. It is interesting to note that the basic friction angle of Phu Kradung red sandstone (PKSS2) and its shear strength reduction rate are relatively low, therefore its joint shear strength does not reach the lower bound within the predicted period of 10 years.

The sensitivity of ϕ_B , JRC and σ_c to the degradation of the joint shear strength is investigated by calculating τ/σ_n of Khok Kruat sandstone under various assumed ϕ_B , JRC and σ_n values. Figures 5.9 through 5.11 plot the results. Variation of ϕ_B values does not affect the rate of joint shear strength reduction (Figure 5.9). The higher ϕ_B however results in a higher τ/σ_n . Figure 5.10 shows that as σ_n increases the normalized joint shear strength decreases. This suggests that rock joint under a higher σ_n may have a lower normalized shear strength. Variations of σ_n however do not affect the rate of joint shear strength reduction. As a result, shear strength of a joint under a higher σ_n will reach the lower bound strength quicker than that under a lower σ_n . A reduction of JRC values decreases the present τ/σ_n (at time = 0) and its degradation rate, but does not affect the time at which τ/σ_n reaches the lower bound (Figure 5.11). This implies that the roughness of a rock joint can not prolong the time at which the joint shear strength reaches its lower bound value.

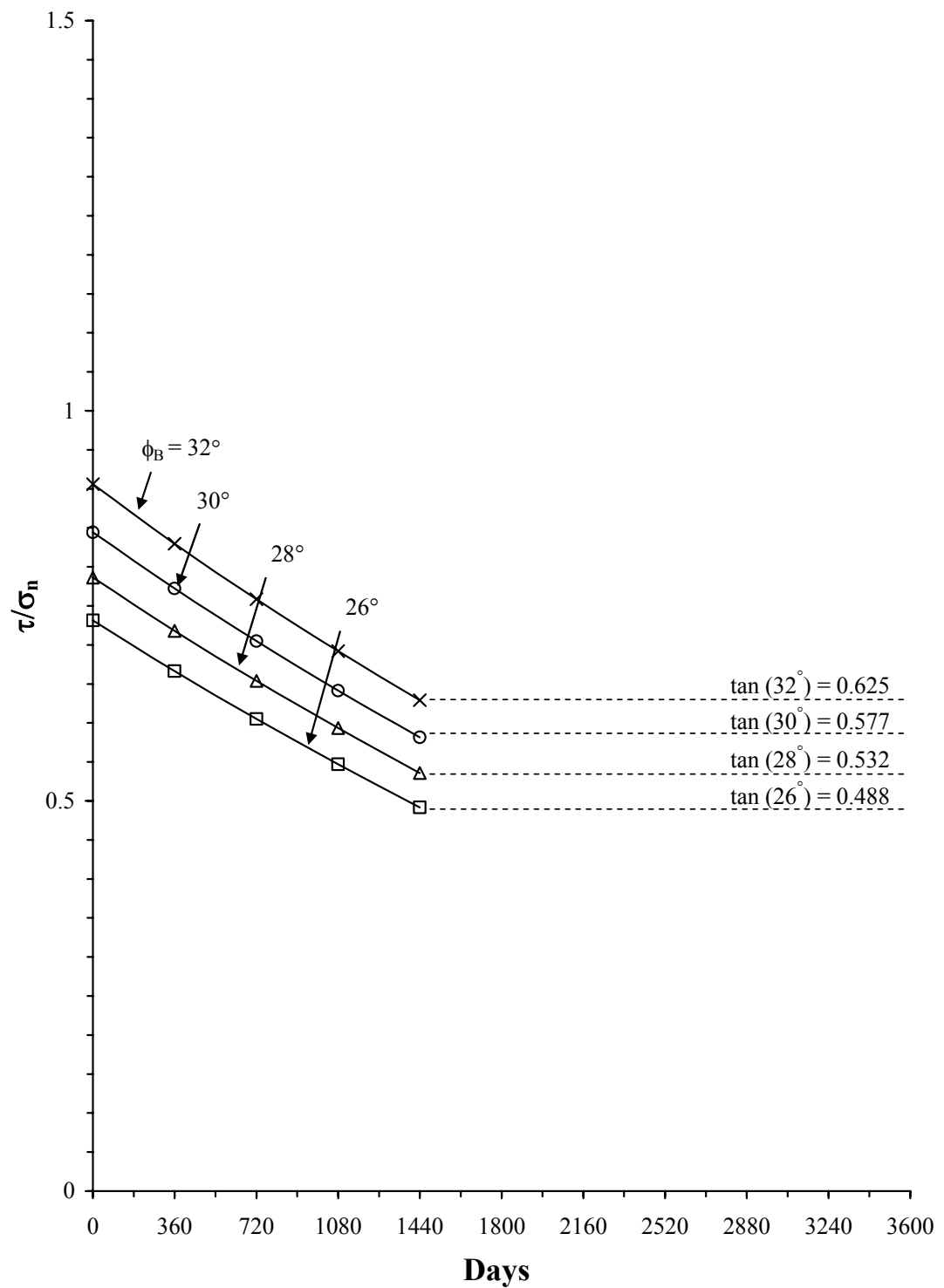


Figure 5.9 Normalized joint shear strength as a function of time for Khok Kruat sandstone for various assumed ϕ_B values.

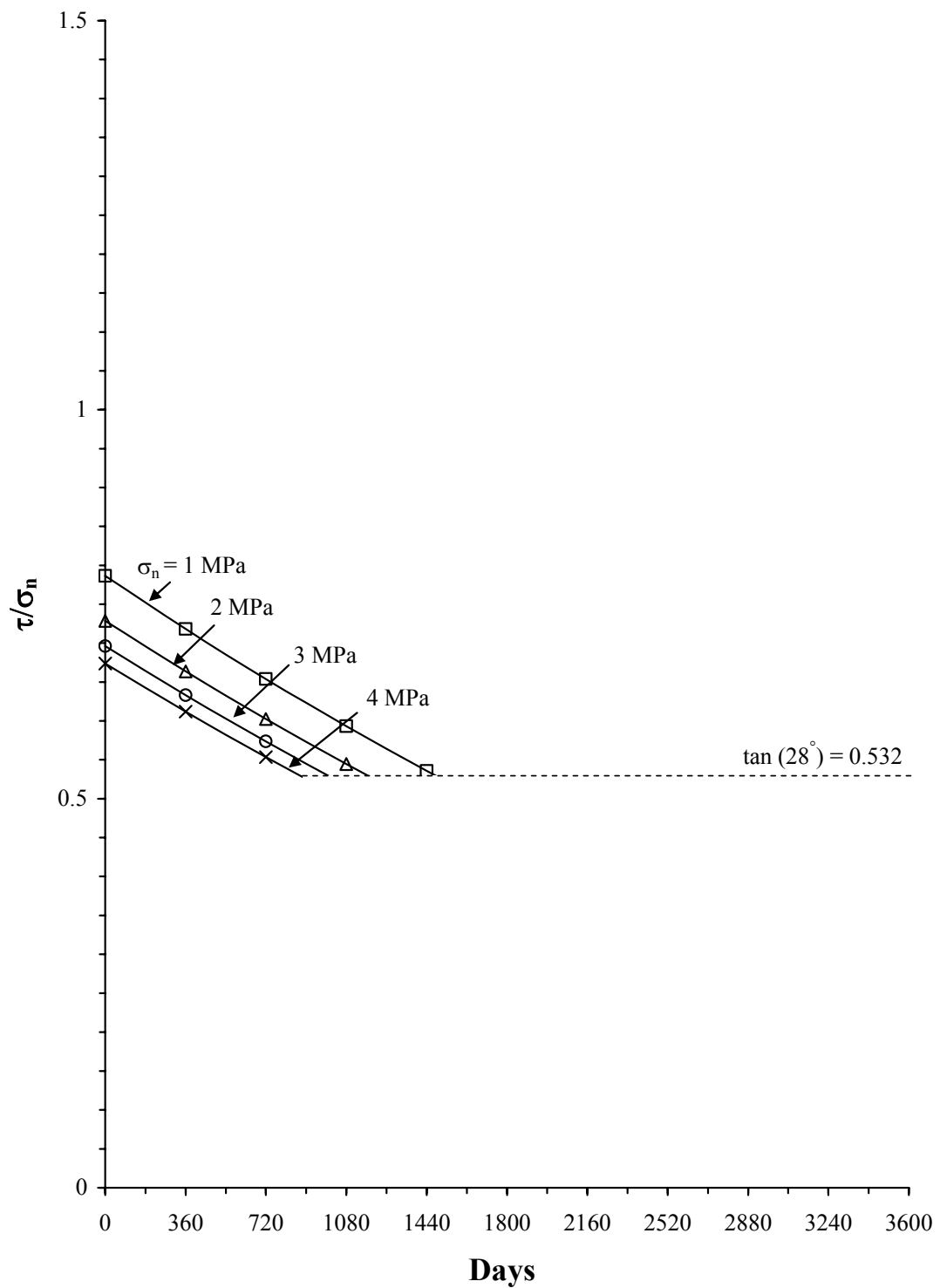


Figure 5.10 Normalized joint shear strength as a function of time for Khok Kruat sandstone for various normal stress (σ_n).

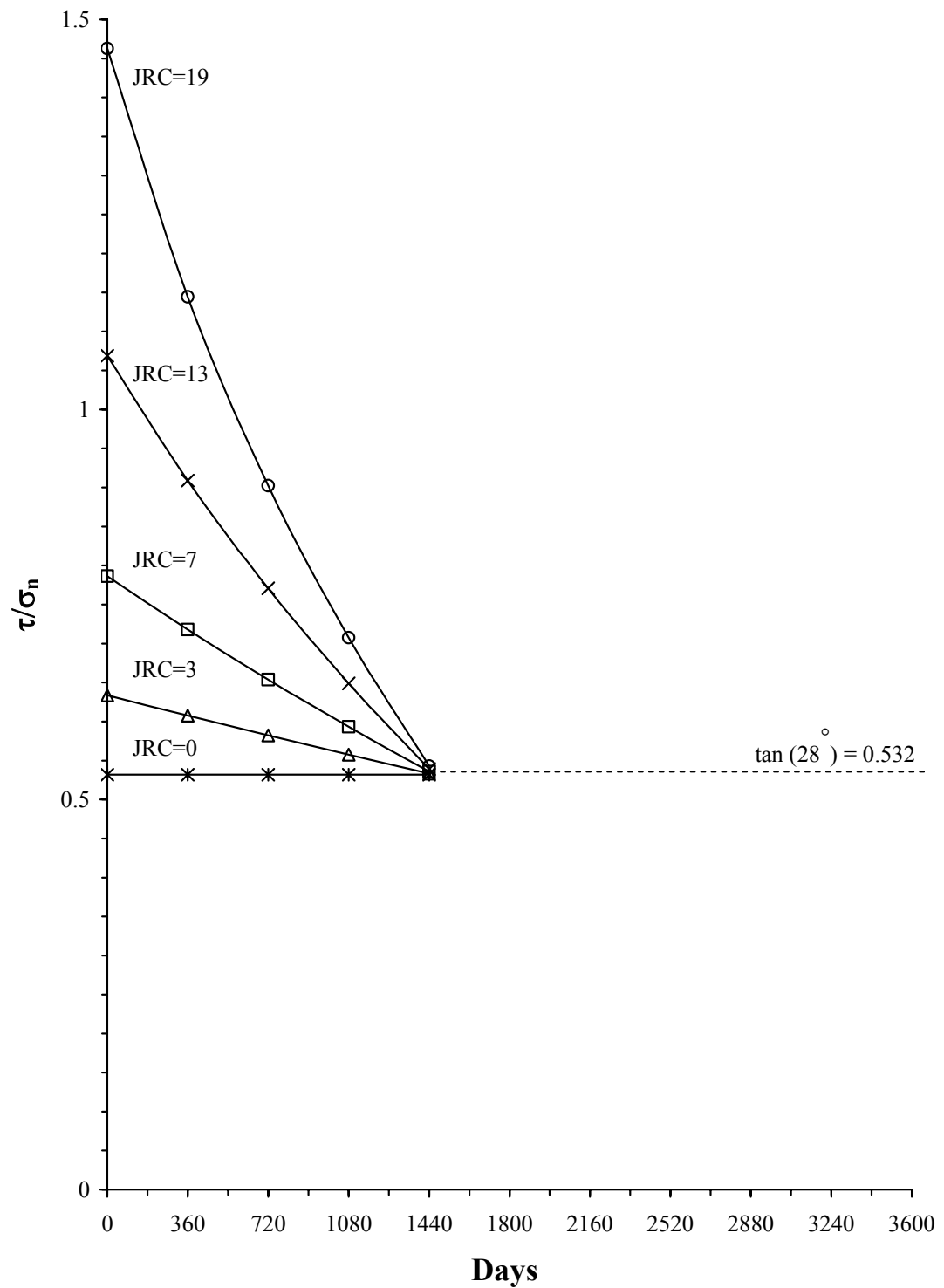


Figure 5.11 Normalized joint shear strength as a function of time for Khok Kruat sandstone for various assumed JRC values.

CHAPTER VI

DISCUSSIONS, CONCLUSIONS AND RECOMMENDATIONS FOR FUTURE STUDIES

6.1 Discussions

The factors affecting the degradation of the sedimentary rocks used in this research seem to be the packing density, grain contact characteristics and kaolinite content. Rocks with higher density and lower percentage of cementing materials (grain-to-grain contact) tend to degrade slower than those with lower density and higher amount of cementing materials. Kaolinite is highly sensitive to water which makes the rock disintegrated quickly. These observations agree reasonable well with those observed by Koncagul and Santi (1999). The effect of grain size can not be studied because all the sedimentary rocks tested in this research are fine grained rocks.

For the metamorphic and volcanic rocks, kaolinite content seems to be the most important factor affecting the rate of degradation, particularly when subjected to water. The pore spaces in volcanic rock also enhance the weathering process by allowing more water to penetrate into the inner matrix. The metamorphic rocks with distinct foliation planes formed by the alignment of flaky minerals (such as mica) can notably disintegrate under cyclic changes of surrounding temperatures even under dry condition. The governing mechanism probably involves the differential expansion of the rock forming minerals that have different thermal expansion coefficients. The cyclic changes of the temperature would induce repeated changes of shear stresses on the foliation planes and

eventually cause separation between them. This effect is probably enhanced if the foliation planes that separate two different types of minerals are well defined and planar, and hence the shear stresses are induced along one common direction. This is supported by the progressive separation of the Nam Duk slaty-shale foliations observed in the laboratory which agrees with that observed on-site during the field investigation.

The prediction of Δ SDI value as a function of N^* is obtained by extrapolation of the fitted curve to a higher number of N^* . The reliability of the prediction largely depends on the number of cycles during the SDI test. This issue is of concern particularly for the rock with high gradient of Δ SDI values which are normally obtained for low to very low durability rocks. A larger number of test cycles (probably 20 or more) would be required to provide a more reliable prediction. However, the Δ SDI values obtained for medium to very high durability rocks tend to have a linear relation with N^* . For these rocks, the number of SDI test cycles between 5 and 10 would be sufficient.

The relationship between $I_{s(50)}$ and Δ SDI is developed by assuming that these values are independent of rock types. This assumption is made here because the amount of $I_{s(50)}$ data is limited (two for each rock type). It is believed that $I_{s(50)}$ - Δ SDI relation is unique for each rock type or at least for rocks with comparable origin, composition and texture. This is because the failure mechanisms for each rock can not be directly related to the rock weathering under chemical and physical processes. Care should therefore be taken in applying this relation elsewhere as it may not be valid for other rocks with different physical and mineralogical characteristics from those tested here.

The approach to relate the simulation cycles with the actual time in the field by using the heat energy absorption concept is very conservative because it considers only the temperature difference and duration, not the rate change of temperatures. It is

believed that the rapid change of temperature during the simulation would impose more damage on the rock fabric than does the gradual change occurred under in-situ condition. During each cycle of SDI test the rock fragments are also subjected to scrubbing action in the rotating drum. This process is more severe than what the rock would be subject to under in-situ condition.

Incorporation of the Δ SDI and N^* into Barton's criterion as proposed here indicates that the predicted joint shear strength reduction is mainly governed by the degradation or the intact rock strength. The modified criterion is only valid where the predicted intact rock strength is equal to or greater than the applied normal stress. Below this limit the joint shear strength is governed by the rock basic friction angle. In reality the transition of the shear strengths across this limit would be smoother than what is predicted here. The abrupt transition is probably because the rock basic friction angle is assumed to remain constant with time. In reality the basic friction angle of the rock (mainly governed by cohesive bonding of mineral surfaces and/or by grain size and bonding – Kemthong, 2006) may change with time due to the mineral alterations or grain loosening, or both. Such processes are complicated and can either increase or decrease the basic friction angle, depending on the rock compositions.

6.2 Conclusions

The effect of weathering processes on the joint shear strength of some weak rocks has been experimentally investigated. The effort involves simulation of the weathering-induced degradation of rock specimens in the laboratory, determination of the physical and mechanical properties of the rocks at various stages of degradation, and development of a rock joint shear strength criterion that can incorporate the weathering-related

parameters. Thirteen rock types that were commonly encountered in the north and northeast of Thailand, have been used as rock samples. Petrographic analyses and x-ray diffraction method determine the texture and mineral compositions of the rocks.

Results from SDI tests indicate that factors controlling the degradation rate of the sedimentary rocks used here are primarily density, grain contact, and kaolinite content. For the metamorphic and volcanic rocks, grain size and mica and kaolinite contents are the primary factors controlling the rock degradation. Though not sensitive to water, rocks containing mica may disintegrate easily under cyclic changes of temperatures. The impacts of kaolinite and grain size on the rock degradation are more prominent when the rocks subjected to water than under dry condition.

Results from the degradation simulation suggest that the point load strength index decreases with increasing Δ SDI, which can be best represented by a power equation. The basic friction angles of the smooth (saw-cut) surfaces of the rocks also decrease as the number of heating-cooling cycle increases. The water absorption measurements show the increase of the apparent porosity of the rocks with increasing number of heating-cooling cycles. The water absorption results however can not be correlated with the rock mechanical properties. The cycles of the rock degradation simulation are correlated with the time (in days) under in-situ condition by using the concept of heat energy absorption. This conservative correlation suggests that one cycle used in the simulation approximately equals 18 days under in-situ condition. The Δ SDI and the decrease of the point load strength index can therefore be presented as a function of the actual time.

Barton's joint shear strength criterion is modified in this study to incorporate the weathering-related parameters into the rock wall strength variable. The joint wall strength for each rock type is determined from the point load index using the ASTM

calculation guideline. This allows predicting the decrease of joint shear strength as a function of time. It should be noted that this approach assumes that the rock degradation affects only the rock wall strength, therefore the lower bound of the joint shear strength will equal the strength of smooth saw-cut surfaces, which can be calculated using the rock basic friction angle. Since the relation of N^* - time is highly conservative, the time at which the joint shear strength will reach the lower bound value for each rock would be longer than what is predicted by this approach. The normalized joint shear strengths vs. time in Figures 5.6 through 5.8 can be used to conservatively predict the long-term stability of slope embankments of the rocks used in this study.

6.3 Recommendations for future studies

The uncertainties and adequacies of the research investigation and results discussed above lead to the recommendations for further studies, as follows.

A more diverse rock types, compositions and textures is required in order to truly assess all factors affecting the rock degradation. The sedimentary and weak volcanic rocks should have a wide range of grain (crystal) sizes, rock forming minerals, packing density (apparent porosity) and textures.

More SDI test cycles should be performed to obtain a more accurate projection of the $\Delta\text{SDI}-N^*$ curve, probably up to 10 cycles for strong rocks and over 20 cycles for weak rocks.

An attempt should be made to determine $I_{s(50)} - \Delta\text{SDI}$ relation for individual rock type. This requires a large number of rock fragments for the point load testing, or rock cylinders for the uniaxial testing at several periods of degradation simulation. Such relation would provide a more accurate estimation for the long-term rock strength.

A new or better approach should be sought to correlate the simulation cycles with the actual time. An alternative is to compare the results of rocks under simulated condition in the laboratory with those actually subjected to the in-situ environment. Such approach requires a long-term investigation program.

Experimental investigation of the effect of long-term degradation on the basic friction angle of rocks is also highly desirable.

REFERENCES

- Abramson, L.W., Lee, T.S., Sharma, S., and Boyce, G.M. (1995). **Slope Stability and Stabilization Methods**. New York: John Wiley & Sons.
- Alsaaran, N., and Olyphant, G.A. (1998). A model for simulating rock–water interactions in a weathering profile subjected to frequent alternations of wetting and drying. **Catena**. 32(3-4): 225-243.
- ASTM C127-04. Standard test method for determination of the specific gravity and water absorption of coarse aggregate. In **Annual Book of ASTM Standards** (Vol. 04.08). Philadelphia: American Society for Testing and Materials.
- ASTM D2216-98. Standard test method for laboratory determination of water (moisture) content of soil and rock by mass. In **Annual Book of ASTM Standards** (Vol. 04.08). Philadelphia: American Society for Testing and Materials.
- ASTM D2845-05. Standard test Method for laboratory determination of velocities and ultrasonic elastic constants of rock. In **Annual Book of ASTM Standards** (Vol. 04.08). Philadelphia: American Society for Testing and Materials.
- ASTM D4543-04. Standard practices for preparing rock core specimens and determining dimensional and shape tolerances. In **Annual Book of ASTM Standards** (Vol. 04.08). Philadelphia: American Society for Testing and Materials.

- ASTM D4644-07. Standard test method for slake durability of shale and similar weak rocks. In **Annual Book of ASTM Standards** (Vol. 04.08). Philadelphia: American Society for Testing and Materials.
- ASTM D5313-04. Standard test method for evaluation of durability of rock for erosion control under wetting and drying conditions. In **Annual Book of ASTM Standards** (Vol. 04.08). Philadelphia: American Society for Testing and Materials.
- ASTM D5731-02. Standard test method for determination of the point load strength index of rock. In **Annual Book of ASTM Standards** (Vol. 04.08). Philadelphia: American Society for Testing and Materials.
- Barton, N. (1973). Review of a new shear strength criterion for rock joints. **Engineering Geology**. 7: 287-332.
- Barton, N., and Choubey, V. (1977). The shear strength of rock joints in theory and practice. In **Proceeding of Mechanics** (Vol. 10, pp. 1-54). New York: Pergamon.
- Barton, N., Lien, R., and Lunde, J. (1974). Engineering classification of rock mass for the design of tunnel support. **Rock Mechanics**. 6(4): 189-236.
- Begonha, A., and Braga, M.A.S. (2002). Weathering of the Oporto granite: geotechnical and physical properties. **Catena**. 49: 57-76.
- Bell, F.G. (1992). **Engineering in Rock Masses**. London: Butterworth-Heinemann Ltd.
- Bell, F.G. (1978). The physical and mechanical properties of the fell sandstones, Northumberland, England. **Engineering Geology**. 12(1): 1-29.
- Bieniawski, Z.T. (1975). The point-load test in geotechnical practice. **Engineering Geology**. 9: 1-11.

- Brace, W.F. (1961). Dependence of fracture strength of rocks on grain size. **Proc. 4th Symp. Rock Mechanics** (pp. 99 - 103). University Park, Penn.
- Broch, E., and Franklin, J.A. (1972). The point-load test. **Int. J. Rock Mech. Min. Sci.** 9: 669-697.
- Brown, E.T. (1981). **Rock Characterization Testing and Monitoring: ISRM Suggested Methods**. New York: International Society for Rock Mechanics, Pergamon Press.
- Bye, A.R., and Bell, F.G. (2001). Stability assessment and slope design at Sandstone open pit, South Africa. **International Journal of Rock Mechanics and Mining Sciences**. 38: 449-466.
- Cai, F., and Ugai, K. (2002). Some aspects of finite analysis of rainfall effects on slope stability. Popescu, M (ed.). **Proceedings of the 3rd International Conference on Landslides, Slope Stability and the safety of Infra-Structures**. Singapore: CI-Premier Conference Organization.
- Chang, C.T., Hou, P.C., and Chang, C.Y. (1998). Case study on dip-slope hazards in sandstone and shale alternations. **Regional Symposium on Sedimentary Rock Engineering** (pp 191-195). Taipei, Taiwan: Pssre.
- Chigira, M., and Oyama, T. (1999). Mechanism and effect of chemical weathering of sedimentary rocks. **Engineering Geology**. 55(1-2): 3-14.
- Chonglakmani, C., and Sattayarak, N. (1978). Stratigraphy of the Huai Hin Lat Formation (Upper Triassic) in Northeastern Thailand. **Third Regional conference on Geology and Mineral Resources of Southeast Asia**. pp. 739-762.

- D'Appolonia Consulting Engineers (1980). **Environmental Effects of Slaking of Surface Mine Spoils Eastern and Central United States**. Final Report, J0285024. Prepared for: U.S.D.I. Bureau of Mines, 232 p.
- Dearman, W.R. (1995). Description and classification of weathered rocks for engineering purposes. **Quarterly Journal of Engineering Geology**. 28(3): 267-276.
- Dearman, W.R., Baynes, E.J., and Irfan, T.Y. (1978). Engineering grading of weathered granite. **Engineering Geology**. 12(4): 345-374.
- Deere, D.U., and Miller, R.P. (1966). **Engineering Classification and Index Properties for Intact Rock**. Department of Civil Engineering, University of Illinois, Urbana, IL , pp. 90-101.
- Department Angewandte Geowissenschaften und Geophysik. (2006). Chapter 8: Thermal Properties of Rocks [On-line]. Available: <http://www.unileoben.ac.at/~geophwww/neu/data/chapter8thermal.pdf>
- Dhakal, G., Yoneda, T., Kata, Y., and Kaneko, K. (2002). Slake durability and mineralogical properties of some pyroclastic and sedimentary rocks. **Engineering Geology**. 65(1): 31-45.
- Dobereniér, L., and DeFreitas, M.H. (1986). Geotechnical properties of weak sandstones. **Geotechnique**. 36(1): 79-94.
- Domenico, P.A., and Schwartz, F.W. (1990). **Physical and Chemical Hydrogeology**. John Wiley and Sons, New York, 824 p.
- Dube, A.K., and Singh, B. (1972). Effect of humidity on tensile strength of sandstone. **Journal of Mines Metals and Fuel**. 20(1): 8-10.

- Fahy, M.P., and Guccione, M.J. (1979). Estimating strength of sandstone using petrographic thin-section data. **Engineering Geology**. 16(4): 467-85.
- Fang, Z., and Harrison, J.P. (2001). A mechanical degradation index for rock. **International Journal of Rock Mechanics and Mining Sciences**. 38(8): 1193-1199.
- Fuenkajorn, K., and Kamutchat, S. (2001). Rock slope design using expert system: ROSES program. **Sixth Mining, Metallurgical, and Petroleum Engineering Conference**. Chulalongkorn University: Bangkok, Thailand.
- Fuenkajorn, K., and Kamutchat, S. (2003). Neural network for rock slope stability evaluation. In **Proceedings of the Fourth Regional Symposium on Infrastructure Development in Civil Engineering** (pp. 655-664). Bangkok, Thailand.
- Fujita, T. (1999). Geological characteristics of landslides of the soft rock type, Central Japan. In **Proceeding of the international symposium on slope stability engineering** (Vol. 1, pp 169-174). Shikoku, Japan., Rotterdam, Netherlands: Balkema.
- Ghosh, A., and Daemen, J.K.K. (1993). Fractal characteristics of rock discontinuities. **Engineering Geology**. 34(1): 1-9.
- Goodman, R.E. (1989). **Introduction to Rock Mechanics**. John Wiley & Son, New York, 562 p.
- Goudie, A.S., Allison, R.J., and McLaren, S.J. (1993). Relations between modulus of elasticity and temperature in the context of the experimental simulation of rock weathering by fire. **International Journal of Rock Mechanics and Mining Science & Geomechanics Abstracts**. 30(2): A77.

- Greminger, M. (1982). Experimental studies of the influence of rock anisotropy on size and shape effects in point-load testing. **Int. J. Rock Mech. Min. Sci.** 19: 241-246.
- Gunsallus, K.L., and Kulhawy, F.H. (1984). A comparative evaluation of rock strength measures. **Int. J. Rock Mech. Min. Sci. & Geomech. Abstr.** 21: 233-248.
- Gupta, A.S., and Seshagiri, K.R. (2000). Weathering effect on the strength and deformational behavior of crystalline rocks under uniaxial compression state. **Engineering Geology.** 56(3-4): 257-274.
- Gurgenli, H. (2006). **Geomechanical and weathering properties of weak roof shales in coal mines.** Master of Science Dissertation
- Hachinohe, S., Hiraki, N., and Suzuki, T. (1999). Rates of weathering and temporal changes in strength of bedrock of marine terraces in Boso Peninsula, Japan. **Engineering Geology.** 55(1-2): 29-43.
- Handlin, J., and Hager, R.V. (1957). Experimental deformation of sedimentary rock under a confining pressure. **Journal American Association of Petroleum Geologists.** 41: 1-50.
- Hantz, D. (1986). Pit slope design in French surface coal mines. In Singhal, R.K. (ed.). **International Symposium on Geotechnical Stability in Surface Mining** (pp 107-111). Netherlands: A.A. Balkema.
- Hayashi, Y., Higaki, D., and Ishizuka, M. (1994). Structure of slip surface formed by rock block slide. **International Journal of Rock Mechanics and Mining Science & Geomechanics Abstracts.** 31(1): A10.
- Hoek, E., and Bray, J.W. (1981). **Rock Slope Engineering** (Revised third edition). Institution of Mining and Metallurgy, London.

- Hoek, E., and Brown, J.W. (1980). Empirical strength criterion for rock masses. **Geotechnical Engineering Div., A.S.C.E.** 106(GT9): 1013-1035.
- Hoek, E. (1965). **Rock Fracture Under Static Stress Conditions.** CSIR Report, MEG 383.South Africa.
- Horn, H.M., and Deere, D.U. (1962). Frictional characteristics of minerals. **Geotechnique.** 12(4): 319-35.
- Howarth, D.F., and Rowlands, J.C. (1986). Development of an index to quantify rock texture for qualitative assessment of intact rock properties. **J. C. Geotechnical Testing Journal.** 9(4):169-179.
- Hudson, J.A., and Harrison, J.P. (1997). **Engineering Rock Mechanics An Introduction to the Principles.** UK : Pergamon.
- ISRM, (1985). Suggested method for determining point load strength. **Int. J. Rock Mech. Min. Sci. & Geomech. Abstr.** 22: 53-60.
- ISRM, (1978). Suggested method for determining sound velocity. **Int. J. Rock Mech. Min. Sci. & Geomech. Abstr.** 15(2): 53-58.
- Jaeger, J.C., and Cook, N.G.W. (1979). **Fundamentals of Rock Mechanics.** London: Chapman and Hall.
- Kasim, M., and Shakoor, A. (1996). An investigation of the relationship between uniaxial compressive strength and degradation for selected rock type. **Engineering Geology.** 44(1-4): 213-227.
- Kawamura, K., and Ogawa, S. (1997). Slope failure in major tertiary mudstone zone. **Deformation and progressive failure in geomechanics** (pp 701-706). Japan.
- Kemthong, R. (2006). **Determination of rock joint shear strength based on rock physical properties.** M.S. thesis, Suranaree University of Technology, Thailand.

- Kjaernsli, B., and Sande, A. (1966). Compressibility of some coarse grained material. **Norwegian Geotechnical Institute Report** (pp. 245-251).
- Koncagul, E.C., and Santi, P.M. (1999). Predicting the unconfined compressive strength of the Breathitt shale using slake durability, Shore hardness and rock structural properties. **International Journal of Rock Mechanics and Mining Sciences**. 36(2):139-153.
- Lan, H.X., Hu, R.L., Yue, Z.Q., Lee, C.F., and Wang, S.J. (2002). Engineering and geological characteristics of granite weathering profiles in south China. **Journal of Asia Earth Sciences**. 01: 1-2.
- Ladanyi, B., and Archambault, G. (1970). Simulation of shear behavior of a jointed rock mass. **Proc. 11th Symposium on Rock Mechanics**, Published by AIME, New York, pp. 105-125.
- Leung, C.F., and Lo, K.W. (1993). Stability Analysis of Multiple-Block Sliding Surfaces. **International Journal of Rock Mechanics and Mining Sciences & Geomech. Abstr.** 30(7): 1579-1584.
- Lo, H.B., and Cardott, B.J. (1995). Detection of natural weathering of Upper McAlester coal and Woodford Shale, Oklahoma, U.S.A. **Organic Geochemistry**. 22(1): 73-83.
- Made, B., and Fritz, B. (1990). The composition of weathering solutions on granitic rocks: Comparison between field observations and water-rock interaction simulations based on thermodynamic and kinetic laws. **Chemical Geology**. 84(1-4): 100-104.

- Maharaj, R.J. (1999). Site investigation of weathered expansive mud rock slopes: Implications for slope instability and slope stabilization. **In Proceedings of the International Symposium on Slope Stability Engineering, Shikoku, Japan** (Vol. 1, pp. 115-120). Rotterdam, Netherlands: Balkema.
- Mitchell, J.K. (1993). **Fundamentals of Soil Behavior**. John Wiley and Sons, New York 1993, p. 437.
- Moon, V., and Jayawardane, J. (2004). Geomechanical and geochemical changes during early stages of weathering of Karamu basalt, New Zealand. **Engineering Geology**. 74(1): 57-72.
- Moon, V. (1993). Microstructural controls on geomechanical behavior of ignimbrite. **Engineering Geology**. 35(1-2): 19-31.
- Moriwaki, Y., and Mitchell, J.K. (1977). The role of dispersion in the slaking of intact clay. In *Dispersive Clays, Related Piping and Erosion in Geotechnical Projects*, ASTM STP 623, eds. **American Society for Testing and Materials** (pp. 287-302).
- Mules, G.J.(1991). Landslide features reflecting valley-wall rebound, Kaiya River, Porgera, Papua New Guinea. Bell (ed.). **Landslides**. Balkema, Rotterdam: 1311-1316.
- Nahon D.B. (1991). *Introduction to the Petrology of Soils and Chemical Weathering*. John Wiley & Sons, Inc., New York
- Nishiyama, T., and Kusuda, H. (1996). Application of a fluorescent technique to the study of the weathering process. **Engineering Geology**. 43(4): 247-253.
- O'Brien, N.R., and Slatt, M. (1990). **Argillaceous rock atlas**. Springer-Verlag, New York, pp.124-125.

- Oguchi, C. T., and Matsukura, Y. (1999). Effect of porosity on the increase in weathering-rind thickness of andesite gravel. **Engineering Geology**. 55(1-2): 77-89.
- Okura, Y., Kitahara, H., and Sammori, T. (2000). Fluidization in dry landslides. **Engineering Geology**. 56(3-4): 347-360.
- Oyama, T., and Chigira, M., (1999). Weathering rate of mudstone and tuff on old unlined tunnel walls. **Engineering Geology**. 5(1-2): 15-27.
- Oztekin, B., Topal, T., and Kolat, C. (2006). Assessment of degradation and stability of a cut slope in limestone, Ankara-Turkey. **Engineering Geology**. 84(1): 12-30.
- Pattin, F.D. (1966). Multiple modes of shear failure in rock. **Proc. 1th International Congress of Rock Mechanics**. Lisbon, Vol. 1, pp. 509-513.
- Petsch, S.T., Berner, R.A., and Eglinton, T.I. (2000). A field study of the chemical weathering of ancient sedimentary organic matter. **Organic Geochemistry**. 31(5): 475-487.
- Phienwej, N., and Singh, V.K., 2005. Engineering Properties of Rocks of Phu Kadung and Phra Wihan Formations in Northeast Thailand. **Proc.of the International Symposium-GEOINDO**. Khon Kaen, Thailand, pp.199-204.
- Ramamurthy, T., Rao, K.S., Goel, S., and Mohi-ud-din, A.G. (1992). Stability analysis of some slides in Garhwal Himalayas. **Regional Symp. on rock Slopes** (pp 219-224). India.
- Reid, G., and Stewart, D. (1986). A large scale toppling failure at Afton. In Singhal, R.K. (ed.). **International Symposium on Geotechnical Stability in Surface Mining** (pp 215-223). Netherlands: A.A. Balkema.

- Richard, E.S., Claus, B. and Gordon J.V.W. (1998). **Fundamentals of Thermodynamics**. John Wiley & Son, Singapore.
- Robert, J.B. and Jerome, D.V. (1988). **Principles of Engineering Geology**. John Wiley & Son, Singapore.
- Robinson D.A., and Williams R.B.G. (1994). Rock Weathering and Landform Evolution. John Wiley & Sons, Inc., New York.
- Sam Boggs, J.R. (1995). **Principles of sedimentology and stratigraphy**. Prentice-Hall, Inc. A Simon & Schuster Company. Englewood Cliffs, New Jersey. p 773.
- Santi, P.M., and Koncagul, E.C. (1996). **Predicting the mode, susceptibility, and rate of weathering of shales**. In Design with Residual Materials in Geotechnical and Construction Considerations, ASCE Special Publication 63, ed., pp. 12-27.
- Shakoor, A., and Bonelli, R.E. (1991). Relationship between petrographic characteristics, engineering index properties and mechanical properties of selected sandstones. Bull. Assoc. **Engineering Geology**. 28(1): 55-71.
- Singh, B., and Goel, R.K. (2001). **Rock Mass Classification: A Practical Approach in Civil Engineering**. Netherland: Elsevier Science Ltd.
- Sirat, M., and Talbot, C.J. (2001). Application of artificial neural networks to fracture analysis at the Aspö HRL, Sweden: fracture sets classification. **International Journal of Rock Mechanics & Mining Sciences**. 38(5): 621-639.
- Sousa, L.M.O., Suarez del Rio, L.M., and Calleja, L. (2005). Influence of microfractures and porosity on the physico-mechanical properties and weathering of ornamental granites. **Engineering Geology**. 77(1-2): 153-168.

- Stacey, T.R., and Page, C.H. (1986). **Practical handbook for underground rock mechanics**. Series on rock and soil mechanics (Vol. 12). Germany: TRANSTECH.
- Stewart, D.P., Coulthard, M.A., and Swindells, C.F. (1996). Studies into the influence of underground workings on open-pit slope stability. **Rock Mechanics**. (pp 515-522). Balkema, Rotterdam.
- Thongthiangdee, P. (2003). **Slope failure along lomsak-chumpae highway Phetchabun province, Thailand**. Mh. D. Dissertation, Suranaree University of Technology, Thailand.
- Tocher, R.J., and Fishel, W.K. (1986). Design of the development pit highwalls at the An Tai Bao mine. In Singhal, R.K. (ed.). **International Symposium on Geotechnical Stability in Surface Mining** (pp 31-38). Netherlands: A.A. Balkema.
- Touloukian, Y.S., Judd, W.R., and Roy, R.F. (1981). **Physical Properties of Rocks and Minerals, Circlas Data Series on Material Properties**. Vol. 2. McGraw Hill, pp. 85-91.
- Thapa, B.B., Cassel, D.K., and Garrity, D.P. (1999). Assessment of tillage erosion rates on stepland Oxisols in the humid tropics using granite rocks. **Soil and Tillage Research**. 51(3-4): 233-243.
- Thai Meteorological Department (2004). Climate Information Services, CD.
- Tsiambaos, G., and Sabatakakis, N. (2004). Considerations on strength of intact sedimentary rocks. **Engineering Geology**. 72(3-4): 261-273.

- Tugrul, A. (2004). The effect of weathering on pore geometry and compressive strength of selected rock types from Turkey. **Engineering Geology**. 75(3-4): 215-227.
- Ulusay, R., Tureli, K., and Ider, M.H. (1994). Prediction of engineering properties of a selected litharenite sandstone from its petrographic characteristics using correlation and multivariate statistical techniques. **Engineering Geology**. 38(1-2): 135-57.
- Vallejo, L.E., Robinson, M.K., Stewart, M., and Ann, C. (1994). Role of shale pores in settlement. In **Proceedings of the Conference on Vertical and Horizontal Deformations of Foundations and Embankments, Part 2** (pp. 1425-1434). University of Pittsburgh, PA,
- Vutukuri, V.S., Lama, R.D., and Saluja S. S. (1974). **Handbook on Mechanical Properties of Rocks**. Vol. 1. Trans Tech Publications, Clausthal, Germany, p. 280.
- Wannakao, L., Archwichai, L., Buaphan, C., Wannakao, P., and Muangnoicharoen, N. (1985). **The Study of Rock Slope Stability at km 18-24 along Lomsak-Chumpae highway**. Department of Geotechnology, Khon Kaen University, Thailand.
- Warke, P.A., and Smith, B.J. (1998). Effects of direct and indirect heating on the validity of rock weathering simulation studies and durability tests. **Geomorphology**. 22(3-4): 347-357.
- Wines, D.R., and Lilly, P.A. (2003). Estimates of rock joint shear strength in part of the Fimiston open pit operation in Western Australia. **International Journal of Rock Mechanics & Mining Sciences**. 40(6): 929-937.

- Wyrwoll, K.H. (1986). Characteristics of a planar rock slide: Hamersley Range, Western Australia. **Engineering Geology**. 22(3-4): 335-348.
- Yokota, S., and Iwamatsu, A. (1999). Weathering distribution in a steep slope of soft pyroclastic rock as an indicator of slope instability. **Engineering Geology**. 55(1-2): 57-68.
- Zhu, W., and Zhang, Y. (1998). Effect of Reinforcing the High Jointed Slopes of Three Gorges Flight Lock. **Rock Mechanics and Rock Engineering**. 33(1): 63-77.

APPENDIX

LABORATORY TEST RESULTS

Table A.1 Result of slake durability index test for 6 cycles with water in trough.

Rock Types	Code	Initial Dry Weight (g)	Weight of Oven-Dry Specimens (g)					
			Number of Cycles					
			1	2	3	4	5	6
Volcanic Rocks	PCT	528.10	523.11	521.58	521.06	520.42	519.21	516.22
	PPB	508.70	481.78	455.84	420.19	377.31	350.56	327.47
Metamorphic Rocks	KSch	508.60	499.20	492.70	488.30	482.90	479.00	474.40
	CSch	490.20	252.80	206.50	186.90	171.30	158.40	150.30
	NDSH	510.10	503.40	497.10	492.20	490.20	488.40	486.50
Sedimentary Rocks	PKSS1	533.00	434.50	373.20	328.00	289.60	265.70	245.10
	PKSS2	517.00	504.20	489.10	478.60	470.70	462.70	455.20
	KKST	510.20	486.60	463.40	443.80	427.20	414.70	401.60
	PWSS	526.50	440.50	434.20	429.50	425.70	422.20	419.10
	PWST	415.60	138.80	78.80	64.70	52.30	43.00	32.40
	NPST	497.60	492.50	488.50	484.70	482.50	479.20	477.80
	KkSS	612.90	575.90	547.90	521.20	495.90	475.30	465.70
	MSMD	568.40	547.64	531.30	500.50	487.50	473.20	456.40

Table A.2 Result of slake durability index test for 6 cycles without water in trough.

Rock Types	Code	Initial Dry Weight (g)	Weight of Oven-Dry Specimens (g)					
			Number of Cycles					
			1	2	3	4	5	6
Volcanic Rocks	PCT	566.50	564.40	562.50	560.80	560.20	558.60	557.60
	PPB	581.50	575.80	572.10	568.70	566.40	563.80	561.10
Metamorphic Rocks	KSch	542.60	536.60	532.60	529.40	526.30	524.00	521.70
	CSch	531.40	431.50	384.40	354.20	328.60	311.20	300.50
	NDSch	524.00	518.70	512.70	507.90	504.70	502.00	500.30
Sedimentary Rocks	PKSS1	509.90	483.00	462.80	447.80	435.20	421.40	409.20
	PKSS2	522.10	516.60	514.00	512.00	510.10	508.30	506.40
	KKST	583.90	567.30	559.50	551.10	545.70	540.70	536.20
	PWSS	494.30	475.60	468.20	462.80	458.10	452.80	448.40
	PWST	470.50	429.80	401.60	380.80	362.00	347.50	333.50
	NPST	529.60	524.00	520.60	518.30	516.40	514.50	512.50
	KkSS	598.60	587.60	580.30	573.20	566.20	559.40	552.60
	MSMD	539.20	523.40	515.40	503.80	502.10	500.40	498.80

Table A.3 Effective porosity of rock specimens.

Rock Types	Code	Effective Porosity of Specimens (%)
Volcanic Rock	PCT	0.53
	PPB	8.65
Metamorphic Rock	KSch	5.47
	CSch	15.95
	NDSH	13.4
Sedimentary Rock	PKSS1	11.90
	PKSS2	4.81
	KKST	13.89
	PWSS	10.01
	PWST	21.77
	NPST	8.70
	KkSS	7.99
	MSMD	N/A

Table A.4 Basic friction angles of smooth saw-cut surfaces of specimens during heating and cooling simulation.

Rock Types	Code	Basic Friction Angle, ϕ_B (degrees)					
		Cycle 1	Cycle 28	Cycle 56	Cycle 84	Cycle 112	Cycle 140
Volcanic Rock	PCT	30.8	24.6	26.3	25.7	26.0	25.3
	PPB	29.3	N/A	N/A	N/A	N/A	N/A
Metamorphic Rock	KSch	28.4	20.2	19.2	19.7	19.0	19.3
	CSch	N/A	N/A	N/A	N/A	N/A	N/A
	NDSch	N/A	N/A	N/A	N/A	N/A	N/A
Sedimentary Rock	PKSS1	41.4	37.1	35.6	34.4	34.4	34.3
	PKSS2	24.8	15	14.9	14.1	13.0	14.1
	KKST	27.8	24.9	24.4	23.8	22.0	23.4
	PWSS	26.6	16.9	16.7	13.7	13.3	13.4
	PWST	36.0	36.0	35.7	35.2	35.0	N/A
	NPST	N/A	N/A	N/A	N/A	N/A	N/A
	KkSS	33.0	31.2	29.8	29.1	28.4	27.7
	MSMD	N/A	N/A	N/A	N/A	N/A	N/A

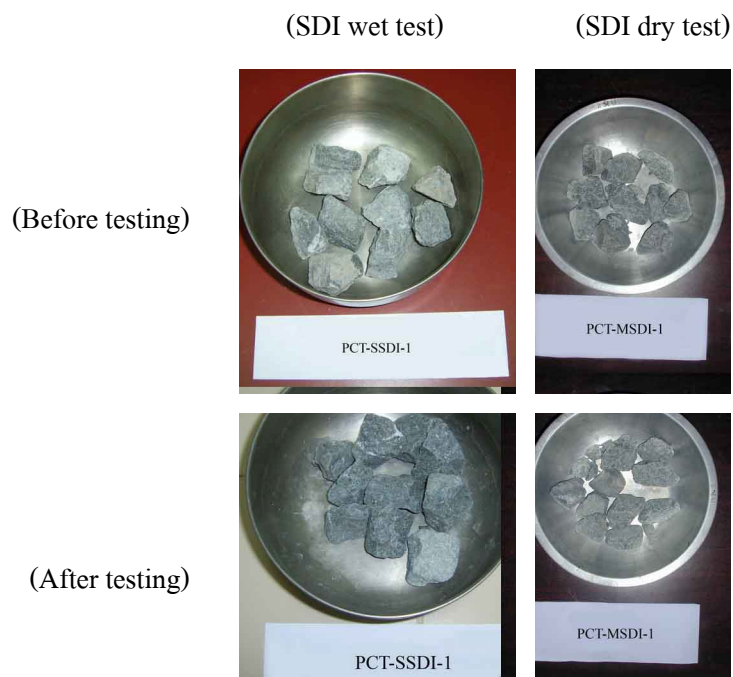


Figure A.1 Pichit crystal tuff before (top) and after (bottom) the slake durability test.

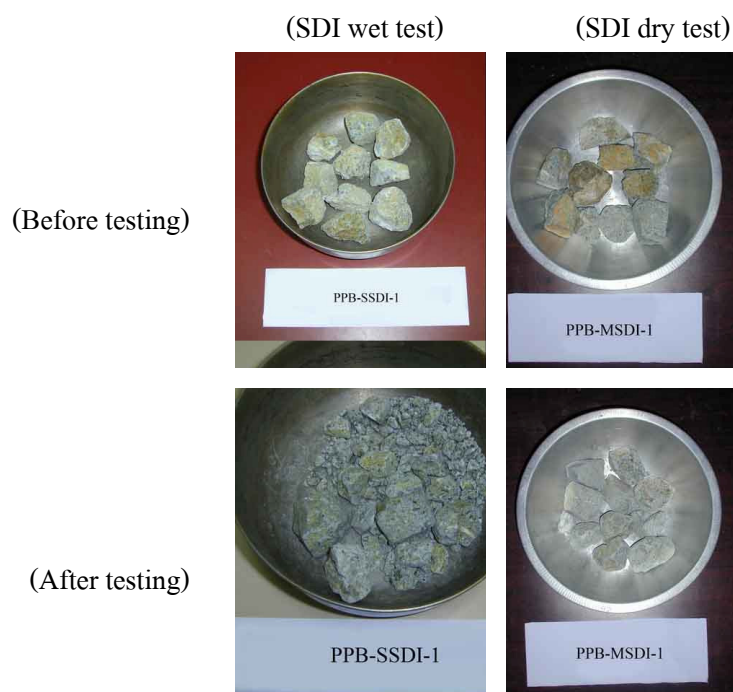


Figure A.2 Pichit pumice breccia before (top) and after (bottom) the slake durability test.

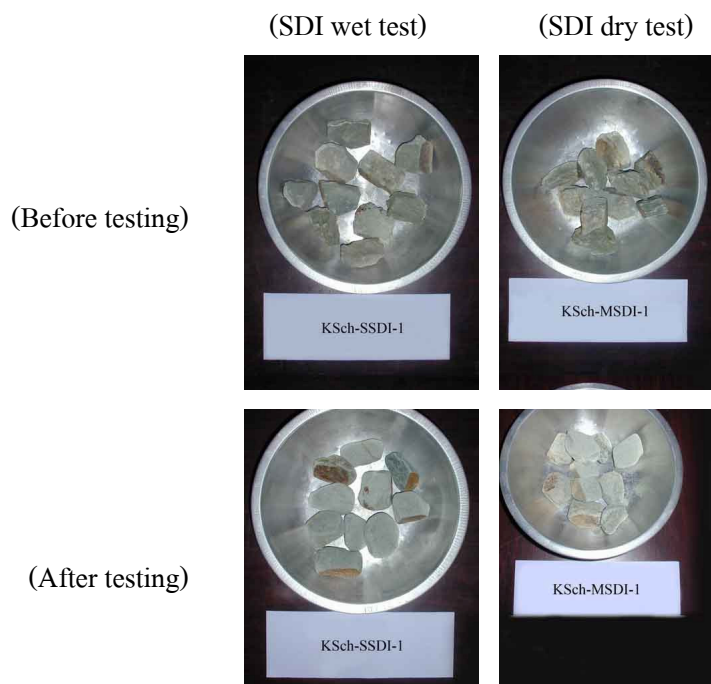


Figure A.3 Kanchanaburi green schist before (top) and after (bottom) the slake durability test.

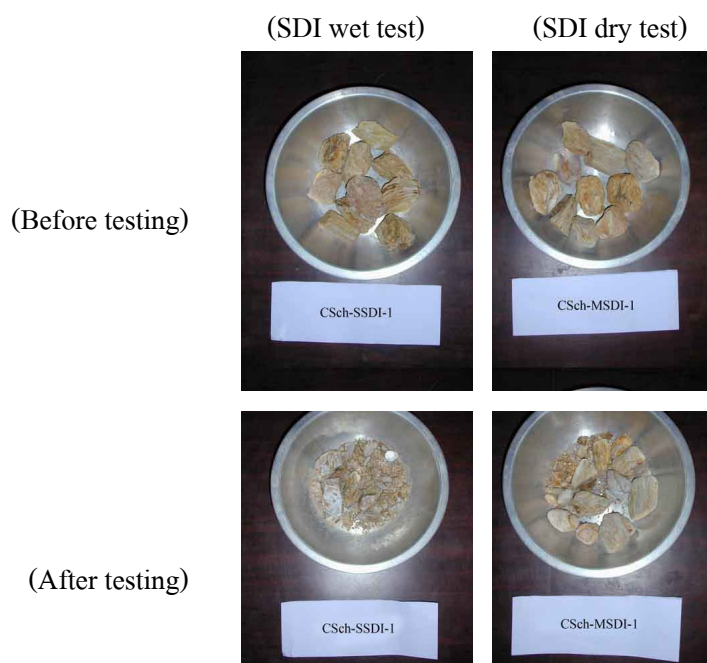


Figure A.4 Chonburi quartz mica schist before (top) and after (bottom) the slake durability test.

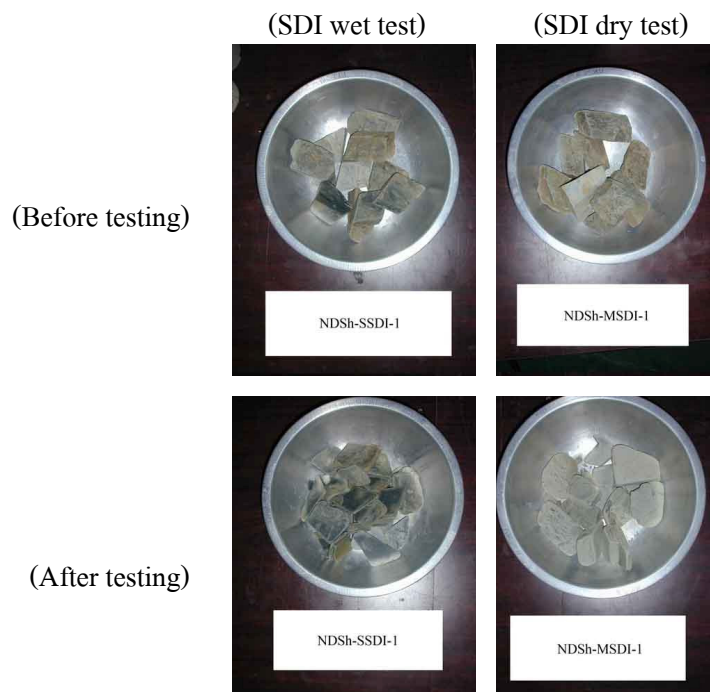


Figure A.5 Nam Duk slaty shale before (top) and after (bottom) the slake durability test.

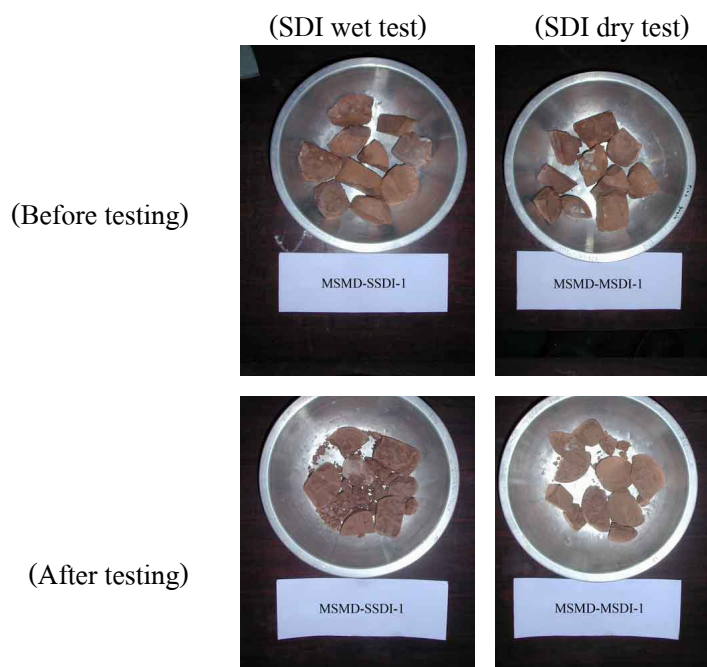


Figure A.6 Maha Sarakham mudstone before (top) and after (bottom) the slake durability test.

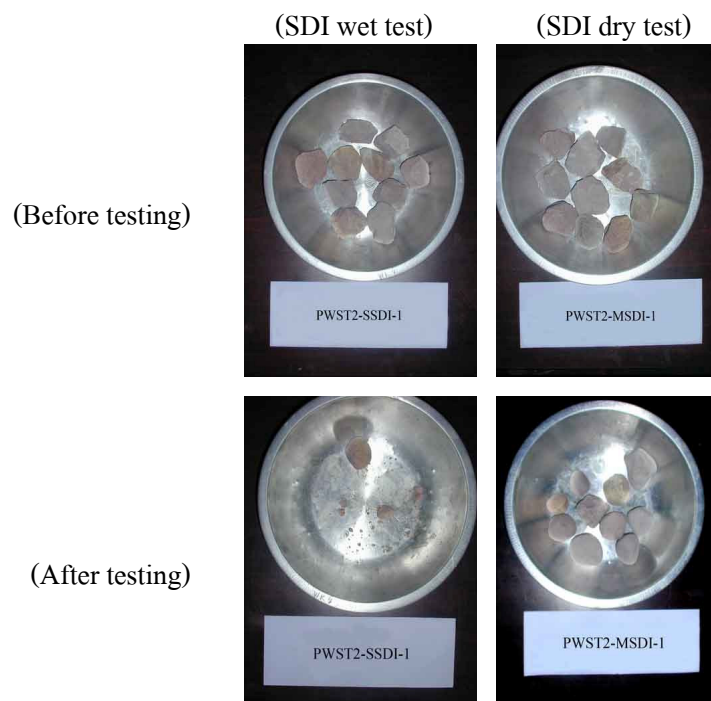


Figure A.7 Phra Wihan siltstone before (top) and after (bottom) the slake durability test.

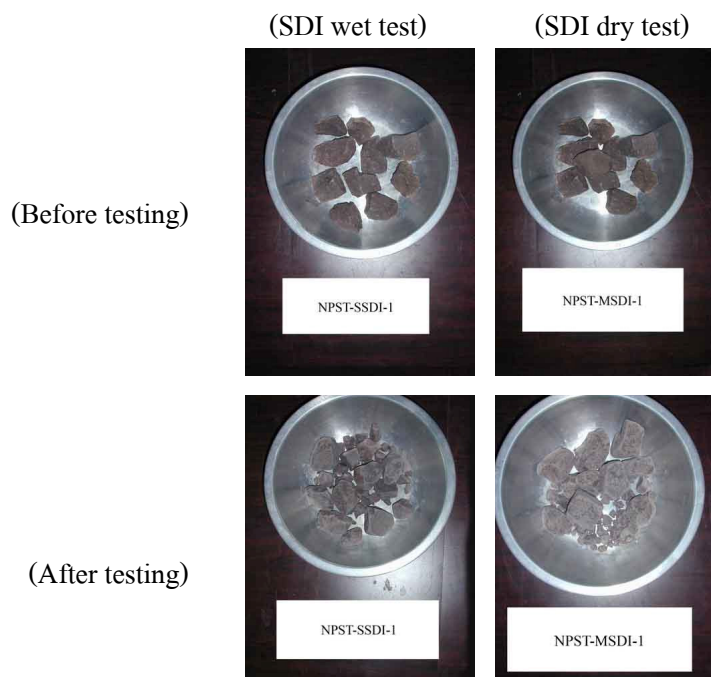


Figure A.8 Nam Phong sandstone before (top) and after (bottom) the slake durability test.

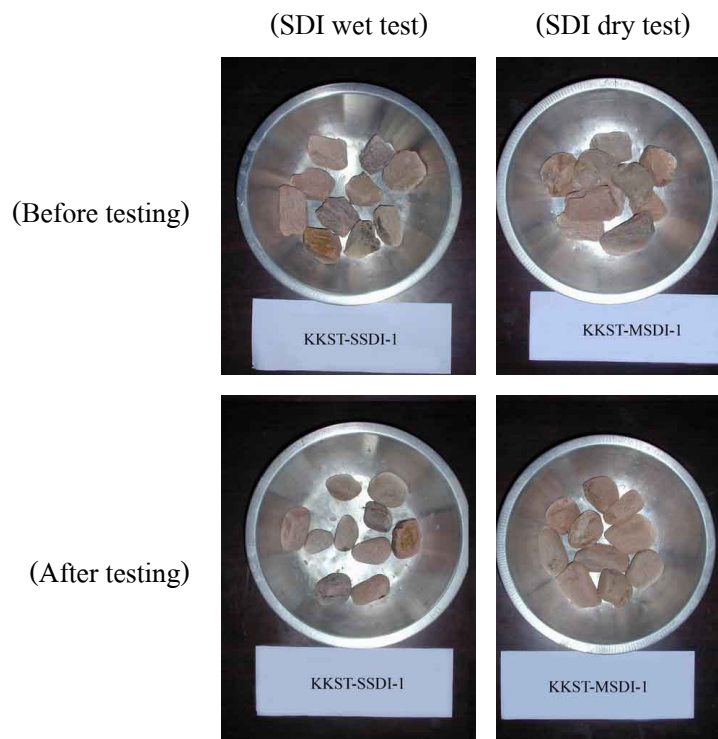


Figure A.9 Kaeng Krachan micaceous siltstone before (top) and after (bottom) the slake durability test.

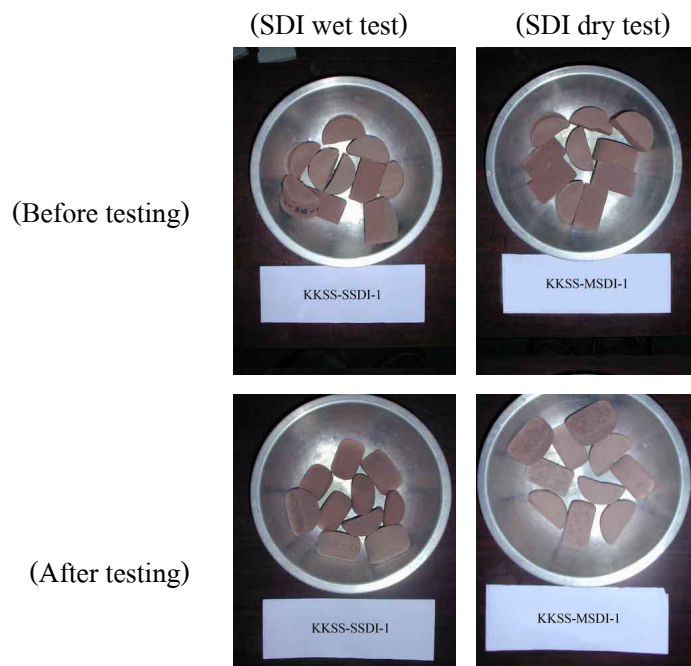


Figure A.10 Khok Kruat sandstone before (top) and after (bottom) the slake durability test.

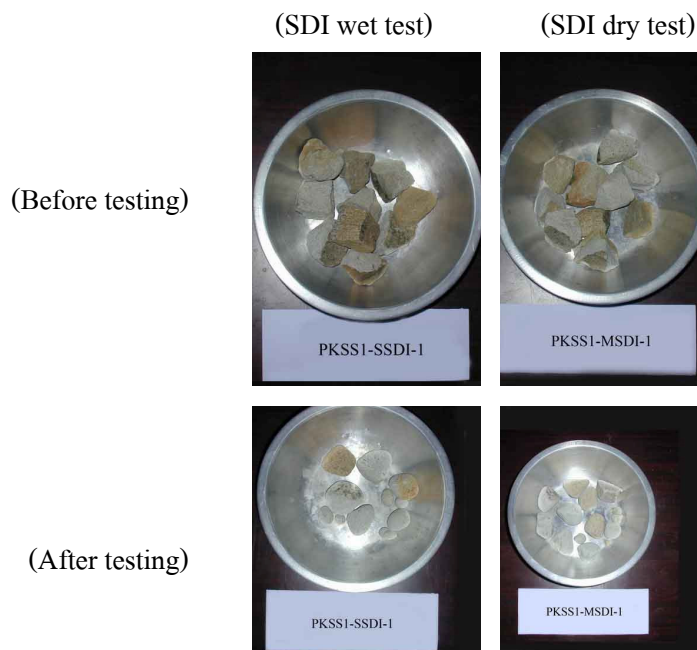


Figure A.11 Phu Kradung white sandstone before (top) and after (bottom) the slake durability test.

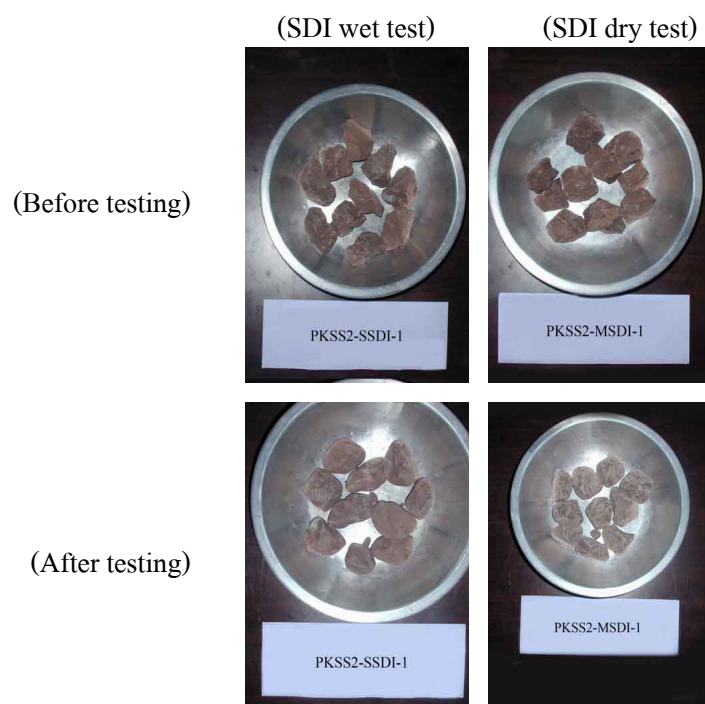


Figure A.12 Phu Kradung red sandstone before (top) and after (bottom) the slake durability test.

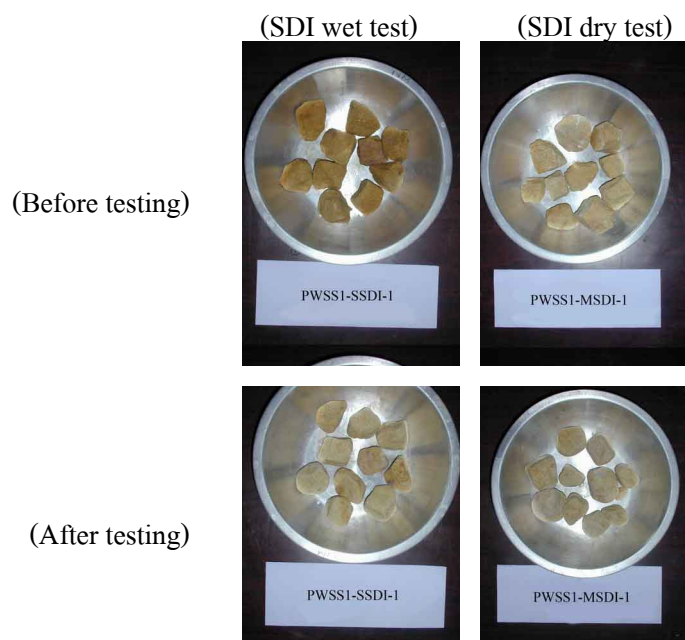


Figure A.13 Phra Wihan sandstone before (top) and after (bottom) the slake durability test.

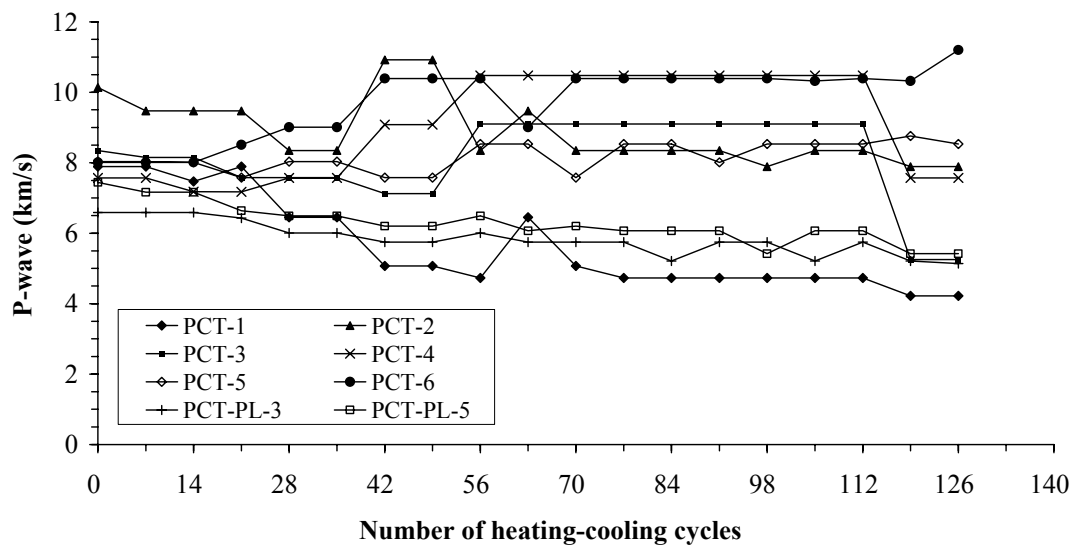


Figure 4.14 Dynamic wave velocity of Phichit crystal tuff specimens

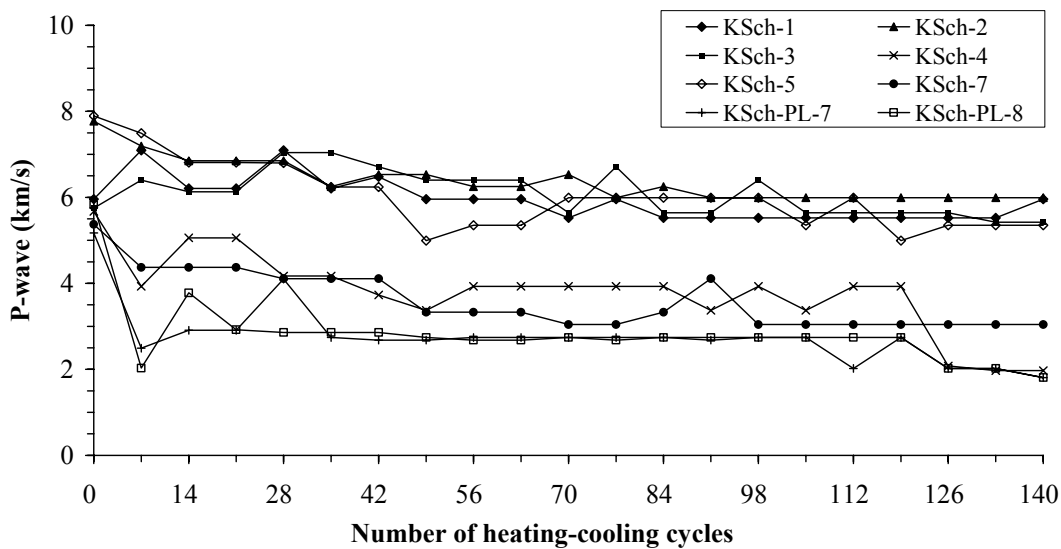


Figure 4.15 Dynamic wave velocity of Kanchanaburi green schist Pichit crystal tuff specimens.

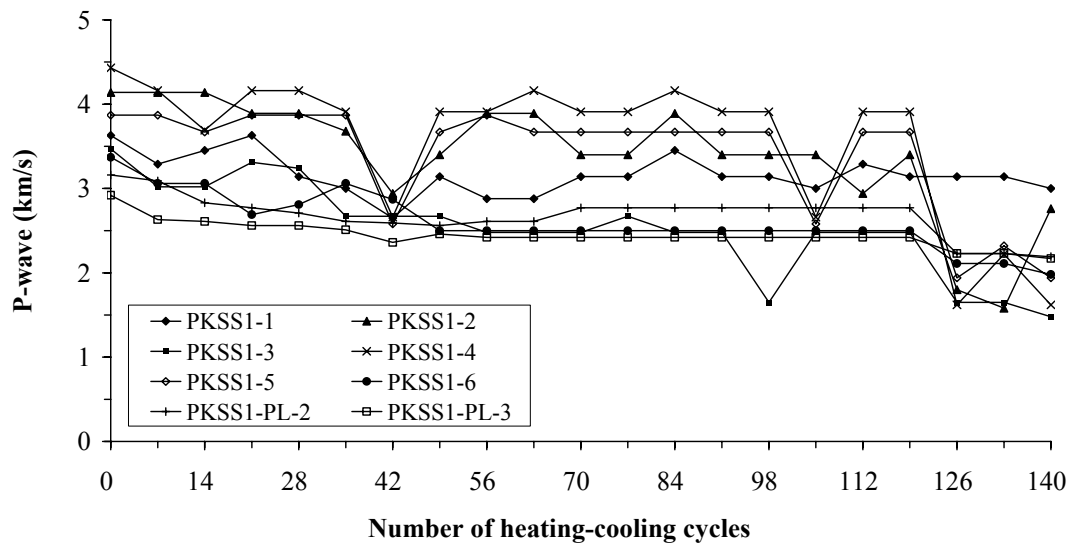


Figure 4.16 Dynamic wave velocity of Phu Kradung white sandstone specimens.

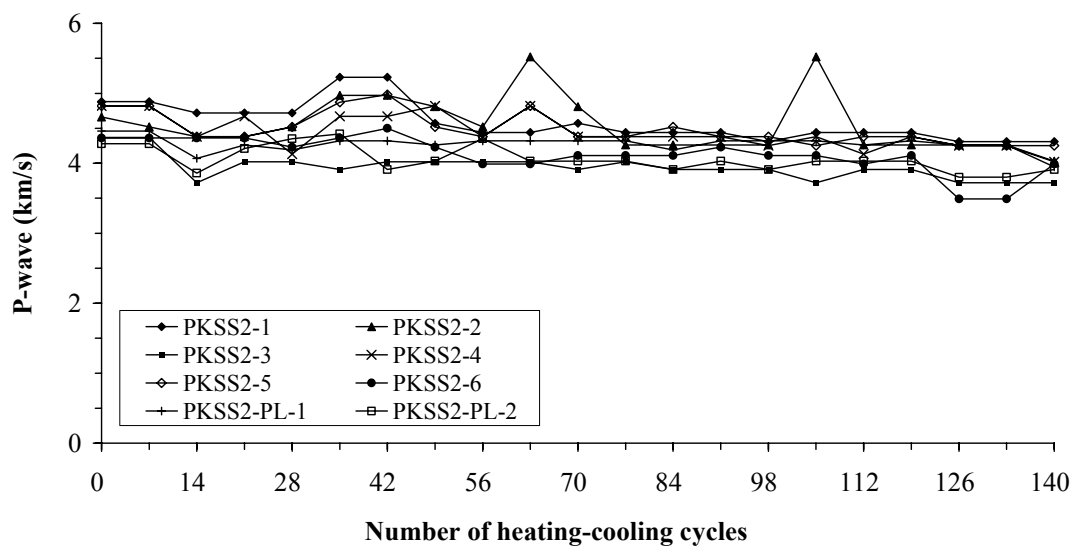


Figure 4.17 Dynamic wave velocity of Phu Kradung red sandstone specimens.

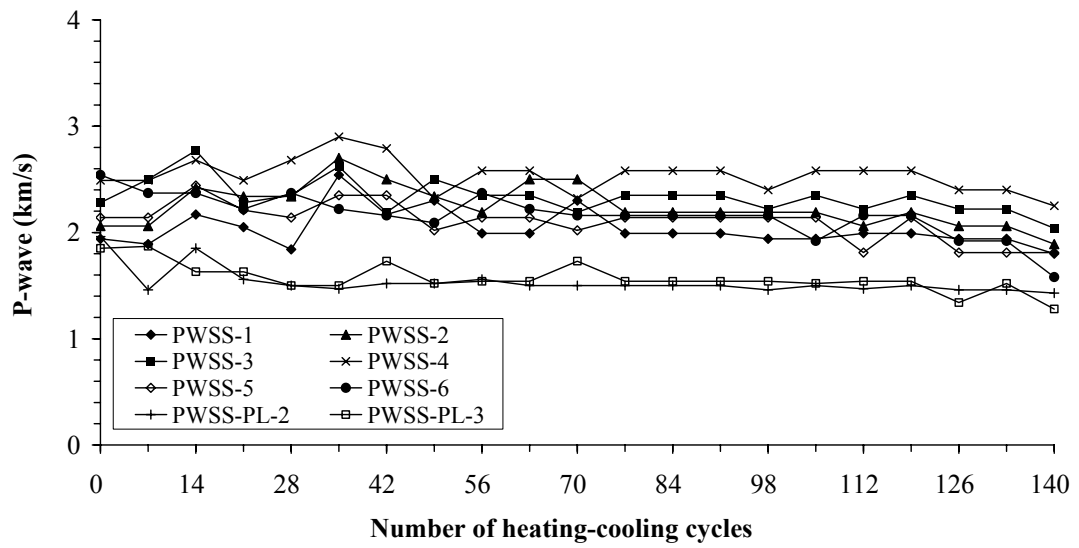


Figure 4.18 Dynamic wave velocity of Phra Wihan sandstone specimens.

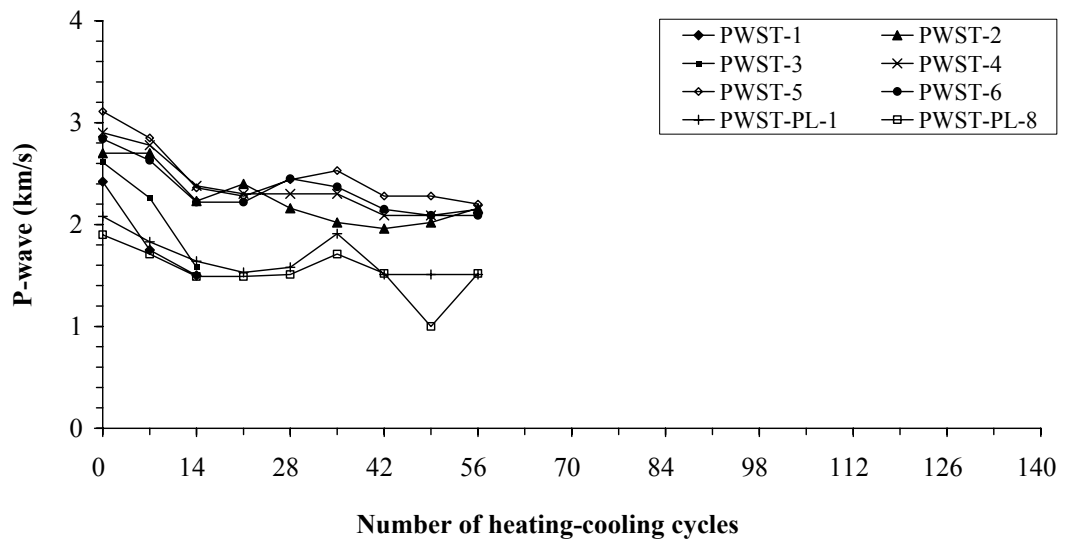


Figure 4.19 Dynamic wave velocity of Phra Wihan siltstone specimens.

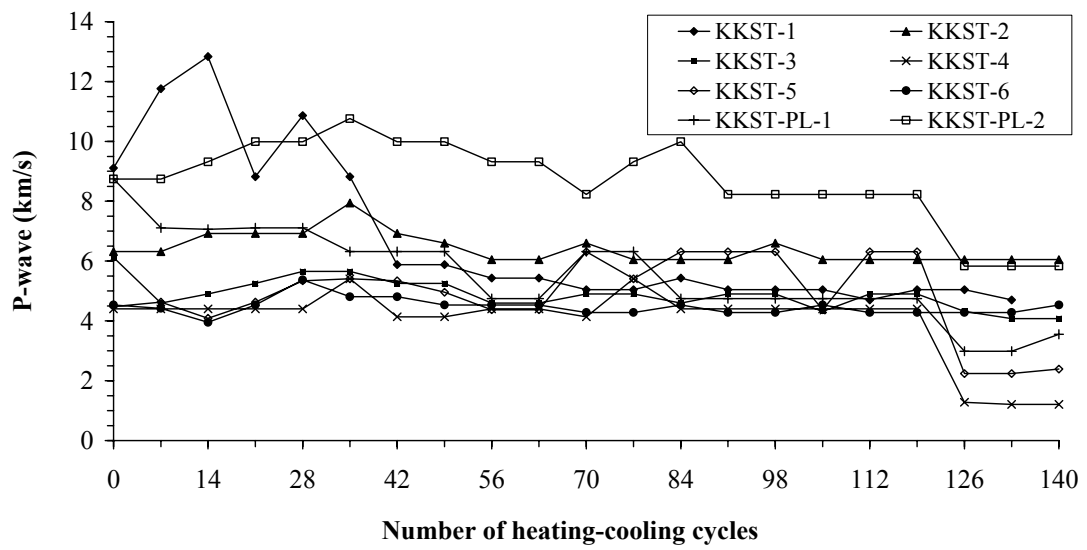


Figure 4.20 Dynamic wave velocity of Kaeng Krachan micaceous siltstone specimens.

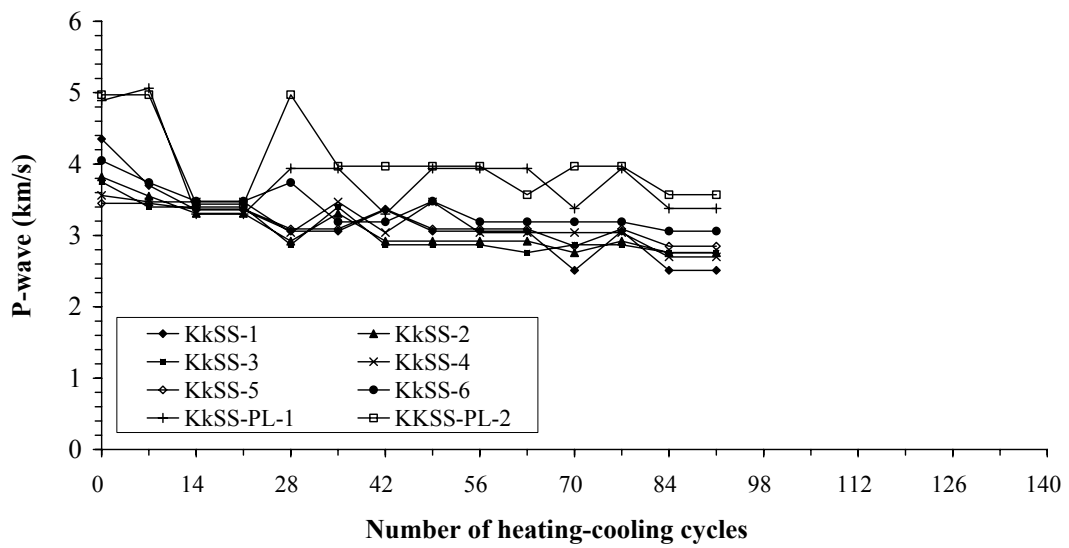


Figure 4.21 Dynamic wave velocity of Khok Kruat sandstone specimens.

BIOGRAPHY

Mr. Teepawit Sri-in was born on December 30, 1980 in Trang province, Thailand. He received his Bachelor's Degree in Engineering (Geological Engineering Program) from Suranaree University of Technology in 2004. For his post-graduate, he continued to study with a Master's Degree in the Geological Engineering Program, Institute of Engineering, Suranaree University of Technology. During graduation, 2004-2007, he was a part time worker in position of research assistant at the Geomechanics Research Unit, Institute of Engineering, Suranaree University of Technology. In 2007, he has published three technical papers related to rock mechanics at the proceeding of the First Thailand Symposium on Rock Mechanics, Nakhon Ratchasima, Thailand, September 13-14; 1) Slake durability index and strength testing of some rocks in Thailand, 2) End effect on strength and stiffness of Maha Sarakham siltstone specimens, and 3) Verifications of rock slope rating (RSR) and slope mass rating (SMR) systems. For his work, he is a good knowledge in geomechanics theory and practice.